Hovedprosjekt

for

Michal Malisz og Mathias Scholze

Skipsdesign

Vårsemester 2019

Tittel:

Bølgemodellering i kystområder

I forbindelse med beregning av bølgekrefter på offshore konstruksjoner, baserer man seg gjerne på bølgespektrum som gir en god beskrivelse av irregulære bølger til havs. Et bølgespektrum vil være uniformt og gyldig over et relativt stort område til havs, men etter hvert som bølgene når inn til kysten der det er et komplisert landskap av fjorder, øyer, holmer og skjær vil disse overordnede modellene bli for enkle. For å kunne gi gode estimat på bølgene i kystområder må man kunne modellere påvirkningen fra landområder (øyer, nes og bukter), fra varierende dybder og fra lokale strømforhold for å nevne noe. Et dataprogram som tar hensyn til mange av disse påvirkningene er SWAN (Simulating Waves Nearshore).

I denne oppgaven skal vi bruke SWAN til å modellere bølgesituasjonen i Sulafjorden. I Sulafjorden har Statens Vegvesen et omfattende måleprogram av bølger, vind og strøm, som gjør det hensiktsmessig å kunne sammenligne simuleringer fra SWAN med målte data for å se hvor bra dette dataprogrammet er til å estimere bølgeforhold i kystområder. Resultatene fra simuleringer med SWAN kan brukes til å bestemme hvilke bølger man skal legge til grunn for å beregne bølgekrefter på konstruksjoner som t.d. bruer, havner eller fiskeoppdrettsanlegg.

I denne oppgaven skal vi gjøre oss kjent med begrensningene i SWAN ved å gjennomføre noen enkle case som fokuserer på fundamentale effekter for bølger i kystområder og til slutt studere hvor bra vi kan gjenskape bølgesituasjonen i Sulafjorden slik vi ser den gjennom bølgemålingene fra Statens Vegvesen.

Oppgavens omfang kan deles inn i følgende deler:

- Sette seg inn i bakgrunnen for metodene som er brukt til å modellere bølger i SWAN
- Gjennomføre noen enkle case i SWAN som fokuserer på
    - Refraksjon
    - Diffraksjon
    - Shoaling
    - Brytende bølger
- Gjennomføre bølgesimulering i Sulafjorden og sammenligne resultatene med målte data fra Statens Vegvesen sitt måleprogram i Sulafjorden/Breisundet.

Veileder ved NTNU i Ålesund er Karl Henning Halse og Henry Piehl. Arbeidet er støttet av Runde Miljøsenter og Rolls-Royce Marine og kontaktpersoner er Jenny Ullgren (Runde Miljøsenter) og Leif Vartdal (Rolls-Royce Marine).

BACHELOROPPGAVE

Institutt for havromsoperasjoner og byggteknikk

NTNU
Ålesund

Besvarelsen redigeres som en teknisk rapport, med et sammendrag både på norsk og engelsk, konklusjon, litteraturliste, innholdsfortegnelse etc. Ved utarbeidelsen av teksten skal kandidaten legge vekt på å gjøre teksten oversiktlig og velskrevet. Med henblikk på lesning av besvarelsen er det viktig at de nødvendige henvisninger for korresponderende steder i tekst, tabeller og figurer anføres på begge steder. Ved bedømmelsen legges det stor vekt på at resultatene er grundig bearbeidet, at de oppstilles tabellarisk og/eller grafisk på en oversiktlig måte og diskuteres utførlig.

Kandidatene skal i arbeidet med hovedprosjektet lage en tydelig fremdriftsplan med kritiske milepeler, samt presentere oppgaven og redegjøre for hvordan de tenker å gå fram for å løse den, samt status på presentasjonstidspunktet.

Presentasjon av milepelene foregår på følgende datoer:

Milepel-1
Tidspunkt ... : **onsdag 30. januar 2019, kl.12.15 - 14.00**
Sted ..... : **auditorium *Kaupangen***

Ved denne presentasjonen leveres også inn et A3 ark som illustrerer oppgavens utfordringer. En mal for dette finnes på *Blackboard Hovedprosjekt*. Arket skal oppdateres ved sluttinnlevering av hovedprosjektet.

Milepel-2
Tidspunkt ... : **onsdag 20. mars 2019, kl.12.15 - 14.00**
Sted ..... : **auditorium *Kaupangen***

Sluttpresentasjon

Ved semesterslutt skal det endelige resultatet presenteres.
Tidspunkt ... : **onsdag 22. mai 2019, kl.08.15 - 15.00**
Sted ..... : **auditorium *Kaupangen***

Samtlige presentasjoner er obligatoriske. Omfanget og arbeidsbelastingen av 20 studiepoeng er i følge departementet angitt som 540 studentarbeidstimer pr. student.

For innlevering av avsluttende oppgaver til bachelorstudiet ved NTNU i Ålesund vises det til detaljer på *Innsida*. Avdelingen skal også ha prosjektrapport, statusrapport, tegninger og lignende levert på en CD, som legges ved hovedprosjektrapporten. **Innleveringsdato er mandag 20. mai 2019.**

Ålesund 5. januar 2019

Arne Jan Sollied

Studieprogramansvarlig
Skipsdesign

Mottatt:

Dato: 20/05 - 2019

Signatur: _____

Signatur: M. Scholze

Wave modelling in coastal areas
IP305012

Candidates: 10009 and 10020

A thesis presented for the degree of
Bachelor of Science

Department of Civil and Environmental Engineering
Norwegian University of Science and Technology (NTNU)
Ålesund, Norway
May 19, 2019

Summary

SWAN is a wave modelling program that is used to simulate wave propagation in coastal areas. The aim of this paper is to determine the accuracy of the results from SWAN. For this reason, Sulafjorden is a perfect match, since it got easily available buoy data gathered from statens vegvesen.

This thesis covers the fundamental theory of waves in coastal regions as a way to make an introduction to wave modelling in SWAN. The modelling of the few simple cases are regarded as a extension of the fundamental theory and is expected to cover the groundwork when diving into Sulafjorden.

To establish if SWAN returns satisfactional values when simulating waves in Sulafjorden, the results will be compared with buoy data at the respected coordinates. The simulations and therefore the comparisons has been done at four different times. All of them have been modelled without any wind and currents, and with all relevant physical effects present. The results for all of these simulations are documented in this paper, but not extensively analyzed. This has been done for one case, but the conclusions can be applied to all of them.

The absent of wind and currents was expected to give some errors in the results. What was surprising to find out is that the significant wave height seemed to be satisfactional for all buoys except buoy A. Nevertheless, the lack of wind and currents caused for the directional spreading to miss severely for almost all cases. We were not happy with few other parameters, but that can be blamed on our input.

SWAN is believed to give good results, but it is required to simulate more models, with the inclusion of wind and currents.

Abstract

SWAN is a third-generation numerical wave model that solves spectral action balance equations for waves in coastal regions with shallow water and ambient currents. SWAN is developed by Delft University of Technology in Netherlands.

The purpose of this thesis is to find out how well does SWAN (Simulating WAves Nearshore) simulate wave propagation in general and at Sulafjorden, based on the input we give it.

For this purpose we need to verify the validity of SWAN. This will be done by creating few simple cases that represent the basic theories behind waves in coastal waters. These cases will be modelled in a text format that SWAN can read, simulated in SWAN and furthermore post processed in MATLAB.

There had been plans and attempts at including wind and currents into this document, where we cover the effects they have for few simple cases and for Sulafjord.

It was planned to create a layered model, starting with a single effect, adding one at a time and ending with all of them combined. This was unfortunately cut due to time constraints.

It needs to be noted that this report will not explain the wave behaviour at nearshore in greater detail. For this purpose we strongly recommend the book "Waves in oceanic and coastal waters" by Leo H. Holthuijsen, which was used extensively throughout this semester. This report will also not explain the use of SWAN to create these models, for this please read through the SWAN user manual (hopefully we will deliver a complete guide about how to model with SWAN, with many examples).

This report will help you understand the purpose of SWAN and give insight as to how it can be used to model and simulate simple cases for research purposes.

This report is dedicated to my friends, which helped me extensively in my time of need and bothered to listen to all of my wild ideas. You motivated me to continue with my research and lifted few burdens of my chest.

We want to thank our supervisors, Karl Henning Halse and Henry Piehl. Their guidance helped us extensively and we only hope that the offices hours where as much fun for them as they were for us.

I declare that this report ate away my entire life for its duration, which concludes a semester worth of intensive work which closes this chapter of my life here at this university, god gave mercy to whoever reads this.

List of Abbreviations

T	Period $[s]$
T_p	Peak period $[s]$
ω	Wave period (absolute radial period) $[rad/s]$
f	Frequency $[Hz]$
f_p	Peak frequency $[Hz]$
f_{PM}	Peak frequency value for PM
Δf	Frequency resolution $[Hz]$
$\Delta\theta$	Directional resolution $[Deg]$
Δx	Element size in x-direction $[m]$
Δy	Element size in y-direction $[m]$
λ	Wave length $[m]$
λ_a	Average wave length $[m]$
λ_p	Peak wave length $[m]$
λ_∞	Wave length at deep water $[m]$
k	Wave number $[rad/m]$
$\vec{k}$	Wave number vector $[rad/m]$
d	Depth $[m]$
d_l	Local depth $[m]$
H_∞	Wave height at deep water $[m]$
H_b	Breaking wave height $[m]$
H_s	Significant wave height $[m]$
θ	Wave propagation direction $[Deg]$
θ_p	Peak wave direction $[Deg]$
θ_m	Mean wave direction $[Deg]$
J	Wave energy density $[J/m^2]$
J_{tot}	Total wave energy density $[J/m^2]$
$E(f)$	One-dimensional spectral wave energy density $[m^2/Hz]$

$E(f,\theta)$	The two-dimensional spectral wave energy density, in f- domain $[m^2/Hz]$
$E(\omega,\theta)$	Directional spectral wave energy density, in ω- domain $[m^2/Hz]$
$E(\sigma,\theta)$	Directional spectral wave energy density, in σ- domain $[m^2/Hz]$
$D(\theta)$	The directional distribution $[-]$
σ	Relative radian frequency, defined as $\sigma = \omega - \vec{k} \cdot \vec{u}$ $[rad/s]$
σ_θ	The directional width (directional spreading) $[Deg]$
σ_θ^2	The directional standard variance
σ_j	Peak-width parameter
σ_{fr}	Width of the Gaussian frequency spectrum (Standard deviation) $[Hz]$
$\overline{\eta^2}$	Variance of the sea surface $[m^2]$
η	Sea surface elevation $[m]$
ξ_∞	Iribarren number for deep water $[-]$
ξ_{br}	Iribarren number at breaking $[-]$
c_p	Phase velocity $[m/s]$
c_{pD}	Phase speed for deep water$[m/s]$
c_{pS}	Phase speed for shallow water$[m/s]$
c_g	Forward speed (Group velocity) $[m/s]$
$c_{g,x}$	Propagation velocity in x-space $[m/s]$
$c_{g,y}$	Propagation velocity in y-space $[m/s]$
$c_{g,\sigma}$	Propagation velocity in σ-space $[m/s]$
$c_{g,\theta}$	Propagation velocity in θ-space $[m/s]$
α	Bottom angle $[Deg]$
α_{PM}	Energy scale value for PM
$N(\sigma,\theta)$	Spectral action balance density, described as $E(\sigma,\theta)/\sigma$ $[m^2 s]$
S_{tot}	Sum of all source terms $[m^2 s/Hz]$
S_{in}	Wind input source term $[m^2 s/Hz]$
S_{nl3}	Triad wave-wave interaction source term $[m^2 s/Hz]$
S_{nl4}	Quadruplet wave-wave interaction source term $[m^2 s/Hz]$
$S_{ds,w}$	White-capping source term $[m^2 s/Hz]$
$S_{ds,b}$	Bottom friction source term $[m^2 s/Hz]$
$S_{ds,br}$	Depth-induced wave breaking source term $[m^2 s/Hz]$
m_0	Zero-th moment of the energy density spectrum $[m^2]$
ρ_w	Sea water density $[kg/m^2]$
γ	Peak-enhancement factor (JONSWAP)

g	Gravitational acceleration $[m/s^2]$
u_x	Particle velocity $[m/s]$
$\vec{u}$	Ambient current velocity vectors $[m/s]$
a	Wave amplitude $[m]$

Contents

Chapter 1

Introduction

The modelling of wind waves in shallow water is important for many coastal engineering applications in the nearshore zone. To conduct an marine construction or operation, it is important to determine how the waves will propagate and what does the wave energy transform to.

Coastal areas experience more complex processes that affect the evolution of waves, than what occurs at oceanic waters. This makes it much harder to predict the wave propagation and wave transformation detail [1]. In addition, the wave spectrum, which is used to determine the irregular sea becomes mostly irrelevant for waves at fjords or rivers.

Statens vegvesen are working on a challenging engineering project called ferry-free E39. This project involves the removal of seven ferry paths between Trondheim and Kristiansand. They will do so by constructing bridges or tunnels across fjords. Sulafjorden is one of these challenging areas where constructions will be conducted.

As of now Sulafjorden is under the design phase, where information about the waves and wind are being gathered with buoys (currently 4 in this area). This makes it possible to compare numerical simulations with field measurements.

There exist various ways to simulate wave behaviour in nearshore zones. The most advanced and precise method is simulated with CFD (Computational Fluid Dynamics), but it is also the most time and computational demanding. A good computational friendly alternative is to use a wave model like SWAN.

The SWAN wave model is a third-generation wave model that computes random, short-crested wind generated waves with ambient currents in coastal regions and inland waters. It does so by computing the spectral action balance equation, where it requires no prior restrictions of the spectrum for the evolution of the wave growth.

The purpose of this thesis is to determine how well do SWAN estimate the propagation of waves and if it returns values that corresponds well to the real wave data. This will be done by processing the buoy data for the month of January 2019, creating a wave model of Sulafjord based on these buoy data and comparing the results from the simulation with the respected buoy.

Before diving into Sulafjord, we need to understand how to use SWAN and what are its limitations. For this purpose we can create few simple cases that explains the main physics of waves in coastal areas.

This report is divided into 5 chapters. Introduction (the one you are reading), general theory, modelling of coastal waves, sulafjord and the conclusion, with appendices at the end.

In the general theory chapter, we roughly explained the wave theory in oceanic and coastal waters, with a simple explanation of what phenomenons occur where.

In the chapter called "modelling of coastal waves", we cover the basic explanation of SWAN, the spectral action balance equation and few clarifications about the boundary conditions. This chapter also covers the representation of the wave spectrum in SWAN and wave models of few fundamental effects for coastal areas.

The entire fourth chapter is dedicated to Sulafjord. The explanations for this chapter and how it is build can be read in its own introduction.

The last chapter is the conclusion, and afterwards the appendices, where the most tables and figures for Sulafjord can be found and the plots of the wave and wind data from buoys.

Chapter 2

General theory

2.1 Wave theory

The first step in describing ocean waves is to consider the vertical motion of the sea surface at one horizontal position, for instance along a vertical pole at sea as addressed in the previous chapter. The ocean waves then manifest themselves as a surface moving up and down in time at that one location.

It is normal to classify ocean waves by their wavelength or period and "disturbing force", the force that originally created the waves. This information alone will tell a lot about how the wave will behave out on the ocean and how it will propagate towards land. Short wind generated waves will normally be easy to notice and predict, while longer waves like tsunamis can be hard to notice at first because of their long wavelength but can suddenly build up to really huge waves once they hit shallow water near shore.

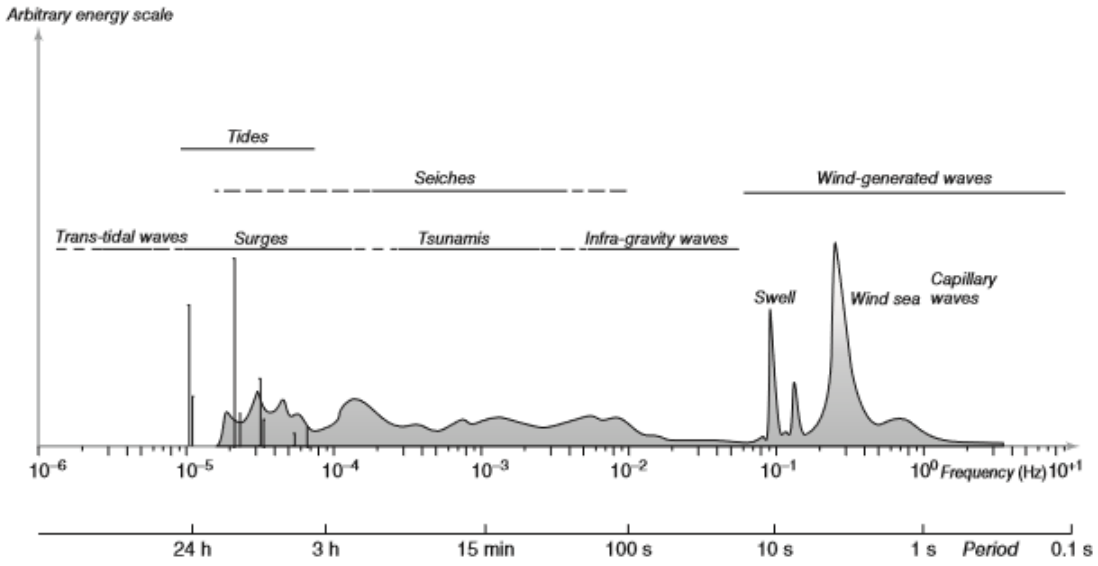

Figure 2.1: The frequencies and period of the vertical motions of the ocean surface [2]

With the definition of wave as "vertical motions of the ocean surface", the longest waves are trans-tidal waves and tides generated by low-frequency fluctuations in the Earth's crust, the rotation of the earth and the gravitational attraction of the moon and

the sun. Their wavelength can vary from a few hundred kilometers to half the circumference of the earth, with periods ranging from few hours to little more than a day at the most.

Next is waves generated by sudden changes to the seafloor, like earthquakes, landslides and volcanic eruptions under water. These are therefor called seismic sea wave or tsunamis. Like mentioned earlier tsunamis can be really dangerous and hard to predict. They normally have a period around 15-20 minutes and corresponding wavelength of about 200km.

Seiches waves are standing waves generated in enclosed or partially enclosed bodies of water like harbor, lakes, but can also happen at sea like the Adriatic Sea where the sea is partially enclosed by Italy. Seiches is often the result of distant waves, storm surges, seismic activity or change in atmospheric pressure that makes the body of water oscillate back and forth within the basin. Wavelength vary as a function of the basin size as the frequency is equal to the resonance frequency of the basin in which they occur. Seiches can be really hard to notice because of their really long wavelengths, and with periods up to several hours they are often mistaken for tides.

"Wind generated waves" can be split into 3 different groups, Capillary Waves, Wind waves and Swell. They are all generated by the effect of wind over water transferring wind energy into the water. The smallest of these waves are called Capillary waves with periods shorter than ¼ of a second which gives a wavelength of about 10 centimeters. Unlike wind waves and swells that are restored to equilibrium by gravity the restoring force of the smaller capillary waves are mainly the surface tension.

Wind generated waves with a period longer than 1/4 of a second, but shorter than 30 seconds are called wind sea/wind waves. These waves are irregular and short crested while they are in the wind affected area called the "fetch", where they are being generated by local winds.

In deep water, longer waves travel faster than shorter waves and leave the generating area faster. Once out of the wind affected zone these waves take on a regular and long-crested appearance and are called "swells". [2]. Swells travel huge distances and are unlike "Wind Sea" hardly affected by local winds.

"Infra Gravity waves" are generated when swells and shorter periods wind waves mix together and are most noticeable in shallow water where they can build up to huge and irregular waves.

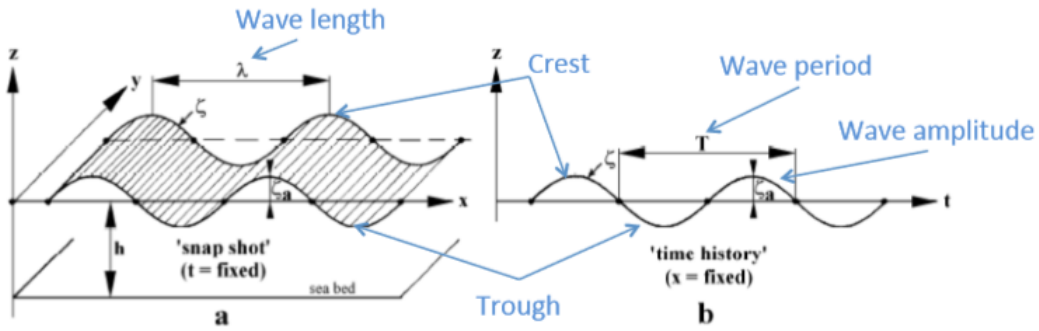

Figure 2.2: Linear ocean surface wave [3]

- Wave crest: Highest point of a wave.
- Wave trough: Lowest point of a wave.
- Wave height [H]: Distance between the through and the crest.
- Wave length [λ]: Distance between one crest and the next.
- Wave period [T]: The time required for the wave to travel one wave length.
- Wave frequency [f]: Number of waves over one unit time. Labeled as $f = 1/T$.
- Phase velocity: The propagation velocity of the wave form. Labeled as $c_p = \frac{\lambda}{T}$ for infinite depth.
- Group velocity: The velocity of multiple waves combined. Which is also the speed of the energy transfer.
- Significant wave height [H_s]: The mean of the highest one-third of waves in the wave record.

2.2 Shallow water vs. deep water

It is considered deep water if the depth is bigger than 1/2 the wavelength. In deep water the waves are not affected by the bottom and are normally only affected by winds and currents etc. As soon the depth is less than 1/2 wavelength it is called intermediate depth and the waves starts to "feel" the bottom.

The wave speed C and wavelength L decreases while wave height increases. When the depth is less than 1/20 of the wavelength it is called shallow water. In shallow waters the wavelength and wave speed is depth-dependent and decreases utterly while the period does not change. This results in increased wave height and eventually breaking of wave if the wave becomes too steep.

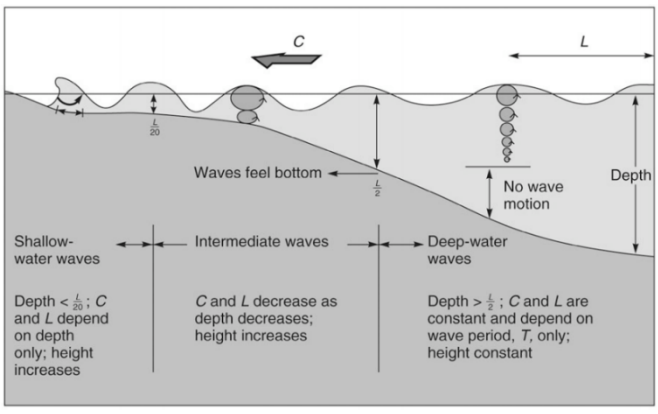

Figure 2.3: The influence of the depth on the particle motion [4]

Process	Oceanic waters	Coastal waters		
		Shelf seas	Nearshore	Harbour
Wind generation	●●●	●●●	●	○
Quadruplet wave–wave interactions	●●●	●●●	●	○
White-capping	●●●	●●●	●	○
Bottom friction	○	●●	●●	○
Current refraction / energy bunching	○/●	●	●●	○
Bottom refraction / shoaling	○	●●	●●●	●●
Breaking (depth-induced; surf)	○	●	●●●	○
Triad wave–wave interactions	○	○	●●	●
Reflection	○	○	●/●●	●●●
Diffraction	○	○	●	●●●

●●● = dominant, ●● = significant but not dominant, ● = of minor importance, ○ = negligible.

Figure 2.4: The relative importance of the various processes affecting the evolution of waves in oceanic and coastal waters (after Battjes, 1994)[2]

2.3 Effects in shallow water

2.3.1 Shoaling

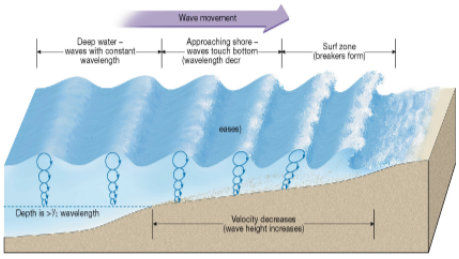

Figure 2.5: Changes that occur when a wave shoals (moves into shallow water).[5]

Wave shoaling is the effect by which sea surface waves entering shallower water change in wave height. This is caused due to the decrease in the group velocity.

We can consider a condition where the wave propagates along an even slope and perpendicularly towards the beach. The incoming wave energy needs to be conserved when it depart from the inlet. Since the group velocity (which is the energy transport velocity) is decreasing, the wave amplitude needs to compensate for these loses by increasing. This increase in the wave amplitude can be called as 'energy bunching' or shoaling.

What also can be mentioned is that shoaling waves will exhibit a reduction in wavelength while its frequency remains the same. This allows for the dispersion relationship for arbitrary depth to be retained, which simplifies a already complex field [2].

$$\omega^2 = gk\tanh(kd) \tag{2.1}$$

Where ω is the radial frequency, g is the gravitational acceleration, k is the wave number and d is the water depth.

2.3.2 Refraction

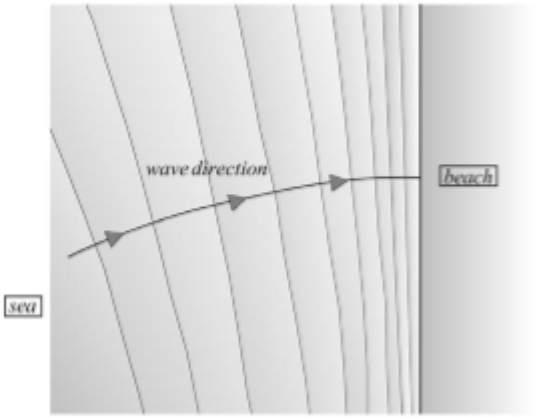

Figure 2.6: Refraction [2]

When waves propagate towards a shore at an angle they tend to bend and become aligned parallel with the shoreline. This effect is called refraction and is caused by the fact that the waves propagate more slowly in shallow water than in deep water. In a given time interval, the crest moves over a larger distance in deeper water than it does in shallower water (see figure 2.7) [2].

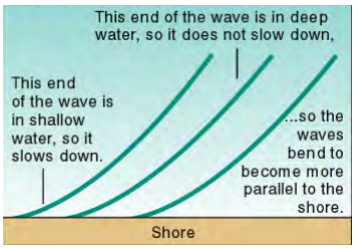

Figure 2.7: The change of wave [6]

As mentioned in the chapter about wave theory, once we are in shallow water the wave speed is dependent of the water depth. The result is that the waves bend towards the region with shallower water, i.e., towards the coast. This is a universal characteristic of waves: a wave always turns towards the region with lower propagation speed [2].

Normally the coastline is not straight and regular, but vary in both depth contours and outline, like bays, headlands and beaches.

Below, figure 2.8 showing wave refraction around headlands.

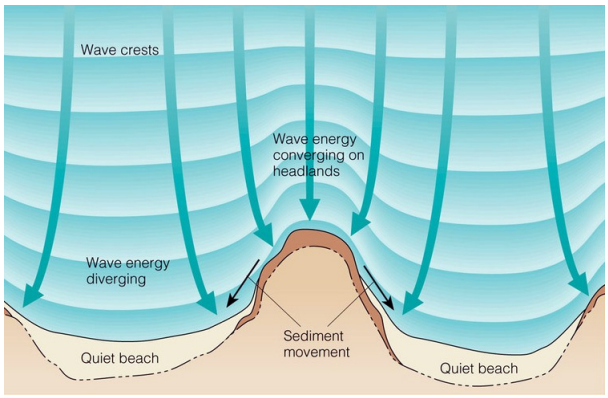

Figure 2.8: Refraction around headlands [7]

An interesting phenomenon happens when waves propagate towards a irregular coastline with headlands, as in figure 2.8. The waves will then converge on the headland, focusing the wave energy in a smaller area creating a bigger wave at this location. This is called Concave refraction.

The opposite happens when the wave propagates towards a larger, shallow water area like bays and such, again see figure 2.8. Here we get defocusing of the waves, and the wave energy diverges, making a quite zone since the energy gets spread out over a larger area. This is called Convex refraction [8].

Wave refraction can also be caused by currents, which can reduce or increase parts of waves phase speed.

Wave refraction can also have a small impact on the amplitude of the wave [9].

2.3.3 Diffraction

Wave diffraction happens when a wave tries to bend around an obstacle like headland or breakwater into the shadow of these objects.

The intensity of diffraction dependant on the size of the aperture. The lower the aperture the higher the diffraction.

What happens it that the wave will try to fill the lee side of the obstacle by spreading its amplitude in a circular pattern towards areas with lower amplitude. The highest amplitude remains at the direction of the propagation, where it will steadily decrease [11] [2].

Figure 2.9: Circular waves generated by diffraction from the narrow entrance of a flooded coastal quarry [10].

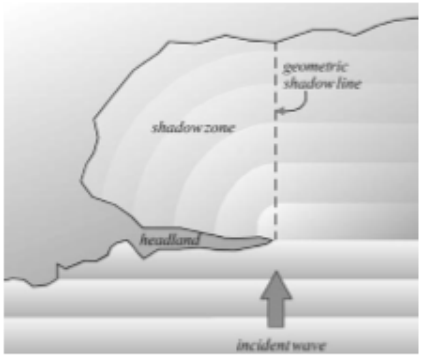

(a) Diffraction around a headland.

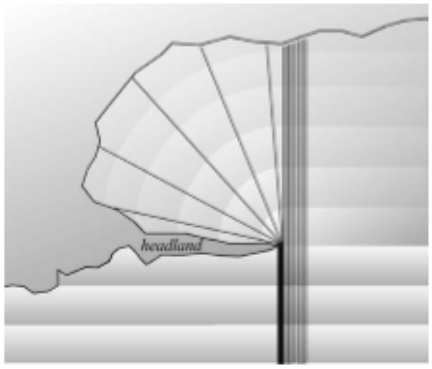

(b) Diffraction represented with wave rays.

Figure 2.10: Diffraction [2]

2.3.4 Wave Breaking

Wave breaking occurs when a wave becomes progressively steeper, until it reaches a critical point.
When that point is reached the wave front overturnes and eventually breaks. This is usually determined by the fact that the particle velocity u_x in the crest cannot be larger than the forward speed of the wave ($u_x \leq c_g$)[2].

Wave breaking in coastal regions is affected by multiple parameters (Wave amplitude, wave length, depth, etc.).

For deep waters, where the wave particle motion is unaffected by the depth, the wave breaks when the wave steepness (H_∞/λ_∞) becomes 0.141[1] [12].

The dominant dissipative mechanism for deep waters is due to white-capping [13]. This is not a strong dissipative mechanism, which means that the waves needs to be frequent for it to break in deep waters. This is characterized by the white foam in the sea.

We can consider an example.

[1] This is usually used as the upper breaking limit for deep water waves.

For deep water the dispersion relationship is defined as $\omega^2 = kg$. When we consider a low frequency wave of $f = 1/8Hz$ ($\omega = 2\pi \cdot f$), we can then calculate the wave height.

$$\omega^2 = kg \Rightarrow \lambda_\infty = \frac{2\pi g}{\omega^2} \approx 100.0m \tag{2.2}$$

By using the breaking criterion for deep water we get that the wave height needs to be 14.0 meters (wave amplitude 7.0 meters) in order to break. This is impossible to occur at deep waters.

For shallow waters the water particle motion is severely obscured by the water depth. This influence causes the wave to deform as it propagates into the decreasing water depth.

For a wave to break in shallow waters, the wave steepness needs also to exceed a specific steepness. For shallow waters although, it is more dynamic. The wave breaking limit is defined as, $\frac{H_b}{\lambda} = 0.142 \cdot \tanh\left(\frac{2\pi d}{\lambda}\right)$.

Where H_b is the wave height at breaking, λ is the wave length and d is the depth.

The dissipative mechanism for shallow water are mainly caused due to the depth variation and bottom friction, but also due to the same effects as in deep water, but enhanced [2]. Examples of shallow water breaking will be shown in later sections.

White-capping

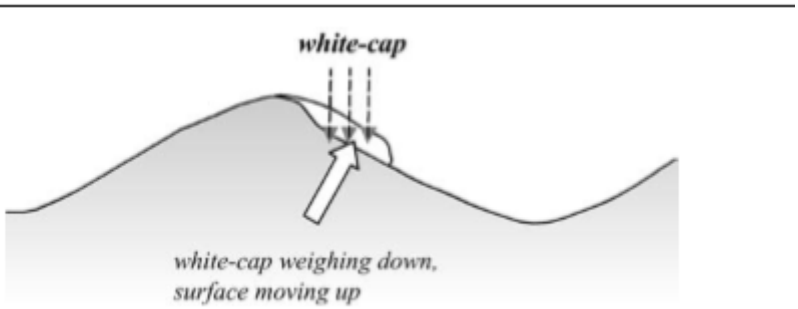

Figure 2.11: The white-cap as pressure pulse at the lee-wind side of the crest of a breaking wave [2].

Water waves are mainly wind generated. When the wind blows with a certain strength over a large fetch distance, large wind-waves will develop.

When the waves are small enough and the wind is strong, the waves will break due to white-capping. This phenomenon is very complicated, thus will not be well explained here.

White-capping is the white foam occurring at the surface of the wave crests. When the wind is strong enough, it blows away the water particles at the crest. This water mass falls down at the lee-wind side of the crest and slightly slowing it down, but stops further development (figure 2.11)[2].

Depth-induced breaking

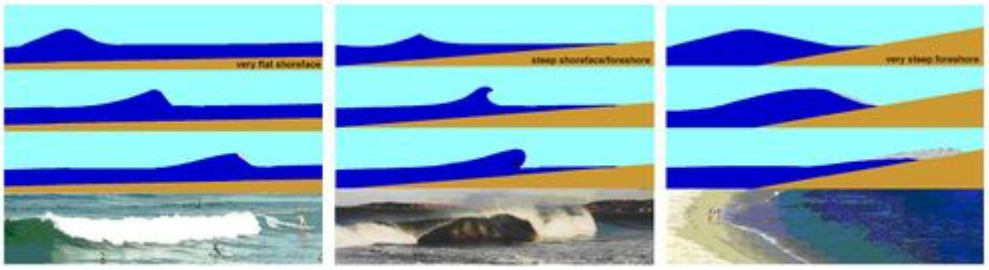

Figure 2.12: Depth-induced wave-breaking: spilling, plunging and surging [14]

Depth-induced breaking is the leading way that waves break in shallow water. Waves will eventually approach the shore, where the total remaining energy is dissipated at the shoaling zone or to land. This dissipation is dependent on the slope of the seabed and the steepness of the incoming wave.

At shallow waters, it has been documented four possible ways that a wave can break. It can break by spilling, plunging, surging and collapsing [15]. These breaker types can be identified based on the surf similarity parameter. Surf similarity parameter (Or Iribarren number) is defined like this $\xi_\infty = \frac{\tan\alpha}{\sqrt{H_\infty/\lambda_\infty}}$ or at the point of incipient breaking $\xi_{br} = \frac{\tan\alpha}{\sqrt{H_{br}/\lambda_\infty}}$, where ξ_∞ is the iribarren number for deep water, ξ_{br} is the iribarren number at breaking, α is the seabed angle, H_∞ is the wave height at the deep water, H_{br} is the wave height at breaking and λ_∞ is the wave length at the deep water.[2].

The iribarren values ranges for defining different types for depth-induced breaking can be seen on the next page.

spilling:	if $\xi_\infty < 0.5$	or $\xi_{br} < 0.4$
plunging:	if $0.5 < \xi_\infty < 3.3$	or $0.4 < \xi_{br} < 2.0$
collapsing or *surging*:	if $\xi_\infty > 3.3$	or $\xi_{br} > 2.0$

Figure 2.13: Surf similarity parameter ranges [2]

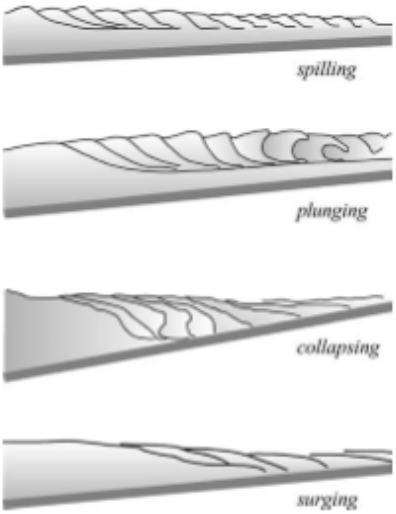

(a) The four main types of breaking waves (after Galvin, 1968). All intermediate states may appear on a real beach [2].

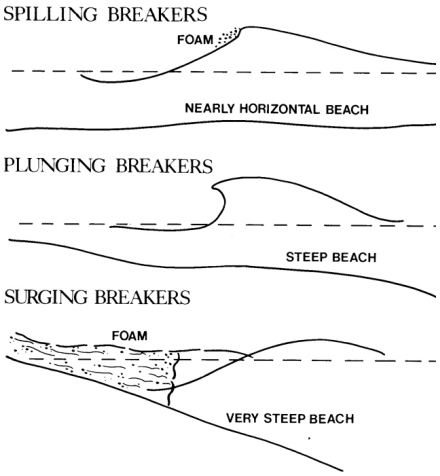

(b) Depth-induced wave-breaking: spilling, plunging and surging [16]

Figure 2.14: Wave breaking

- Spilling breakers happens when a wave propagates towards a beach with a very gentle slope, or when a wave is relatively steep and is propagating on a flat beach. As the wave approaches the shore, it slowly releases energy, and the crest gradually spills down its face until it is all whitewater.
- Plunging breakers occurs when an incoming wave propagates towards a steep seabed. It causes the wave to suddenly lose a lot of its speed, which results in a large increase in wave amplitude and a sudden collapse of wave crest.
- Surging breakers are produced when a wave approach a very steep seabed. These waves usually never becomes steep enough to break at the surf zone, but instead propagates towards the steep beach, dissipates a lot of its energy at a point and the rest surges forward.
- Collapsing breakage is a transition type between plunging and surging.

[17][18][9]

Chapter 3

Modelling of coastal waves

3.1 What is SWAN

SWAN is a third-generation wave model for obtaining realistic estimates of wave propagation in coastal areas from given wind, bottom and current conditions.

SWAN as any other third-generation wave model for ocean waters, models the processes of wind generation, white-capping, quadruplet wave-wave interactions and bottom friction dissipations.

Coastal regions experiences additional processes that needs to be included in order to model these areas. This requires for the adaptation of the spectral action balance equation to include effects like triad wave-wave interactions, depth-induced wave breaking, refraction and shoaling.

Third-generation oceanic wave models like WAM and WAVE-WATCH use an explicit method for numerical propagation. This makes it very computational expensive to use at domain scales lower that 20-30 km and water depths less than 20-30 m. This method cannot be used for coastal models, which demand more grid points for accuracy. This can be solved by using implicit propagation schemes (There is more to it, this is an rough explanation) [19].

Propagation processes that are represented in SWAN;

- Propagation through geographic space,
- Refraction due to spatial variations in bottom and current,
- Diffraction[1] - only approximations,
- Shoaling due to spatial variation in bottom and current,
- Blocking and reflections by opposing currents,
- Transmission through, blockage by or reflection against obstacles.

Generation and dissipation processes that are represented in SWAN;

- Generation by wind,
- Dissipation by whitecapping,
- Dissipation by depth-induced wave breaking,
- Dissipation by bottom friction,
- Wave-wave interactions in both deep and shallow water [20].

[1] Diffraction is modelled in a restrict sense. Spectral models are efficient partially because they neglect diffraction.

Source Term	Reference	SWAN Added	SWAN WAM 3	SWAN WAM 4
Linear wind growth	*Cavaleri and Malanotte-Rizzoli* [1981]	x		
Exponential wind growth	*Komen et al.* [1984]		xx	
	Janssen [1991a]			x
Whitecapping	*Komen et al.* [1984]		xx	
	Janssen [1991a] and *Komen et al.* [1994]			x
Quadruplet wave-wave interactions	*Hasselmann et al.* [1985]		xx	xx
Bottom friction	*Hasselmann et al.* [1973]		xx	xx
	Collins [1972]	x		
	Madsen et al. [1988]	x		
Depth-induced breaking	*Battjes and Janssen* [1978]	xx		
Triad wave-wave interactions	*Eldeberky* [1996]	xx		

Figure 3.1: Options of Third-generation source terms in SWAN [19].

3.1.1 Spectral action balance equation

All information about the sea surface is contained in the energy density $E(\sigma,\theta)$. Energy density describes the evolution of the wave spectrum over radian frequencies σ and propagation directions θ. Due to simplicity in wave propagation in the presence of ambient currents, the spectral action balance equation is used. The action balance equation is defined as $N(x,y,t;\sigma,\theta) = E(x,y,t;\sigma,\theta)/\sigma$ [2].

The full spectral action balance equation is;

$$\frac{\delta N(x,y,t;\sigma,\theta)}{\delta t} + \frac{\delta c_{g,x} N(x,y,t;\sigma,\theta)}{\delta x} + \frac{\delta c_{g,y} N(x,y,t;\sigma,\theta)}{\delta y} + \frac{\delta c_\theta N(x,y,t;\sigma,\theta)}{\delta \theta} + \frac{\delta c_\sigma N(x,y,t;\sigma,\theta)}{\delta \sigma} = \frac{S_{tot}(x,y,t;\sigma,\theta)}{\sigma}$$

The first term on the left-hand side represents the local rate of change of action density in time, the second and third term represent propagation of waves in geographic space (with propagation velocities $c_{g,x}$, $c_{g,y}$ for x- and y- space, respectively). The fourth term represents depth-induced and current-induced refraction (with propagation velocities c_θ in θ- space). The fifth term represents shifting of the relative frequencies due to variations in depth and currents (with propagation velocities c_σ in σ-space)[19].

The right hand side contains $S_{tot}(\sigma,\theta)$, which is the non-conservative source/sink term of energy density, that represents all physical processes which generate, dissipate, or redistribute wave energy at a point.

The right hand side equation $S_{tot}(\sigma,\theta)$ in shallow water is described by six processes.

$$S_{tot} = S_{in} + S_{nl3} + S_{nl4} + S_{ds,w} + S_{ds,b} + S_{ds,br} \tag{3.1}$$

These terms denote, respectively, wave growth by the wind, nonlinear transfer of wave energy through three-wave and four-wave interactions and wave decay due to white-capping, bottom friction and depth-induced wave breaking [20][21]. For more information regarding the formulations of these processes see "SWAN scientific and technical documentation" by SWAN team.

3.1.2 Boundary conditions

In SWAN the boundaries are either water or land. Land in SWAN is fully absorbing of the wave energy, while water requires further planning.

Often no wave conditions are known along boundaries, unless we give it one. SWAN assumes that no wave enters the area, but it can leave freely. This may involve potential errors that needs to be addressed while modelling.

The boundary conditions at the lateral boundary of the computational domain are completely unknown. These boundaries, if not taken into account can potentially influence the credibility of the results. For most situations it is recommended to create a domain that is sufficiently wide, so that it minimizes the erroneous effects of the lateral boundary (Recommended). What also can be done is to apply a incoming wave spectrum at a segment of the lateral boundary, if proper wave information are available. This is although very situations.

3.2 Wave spectrum

Waves in SWAN are described with the two-dimensional (frequency [f] and direction [θ]) wave action density spectrum $E(f,\theta)$. This is also the case for nonlinear processes at the surf zone.This makes it so that the waves cannot be fully described statistically. This is why it appears that the energy density increases at the surf zone.

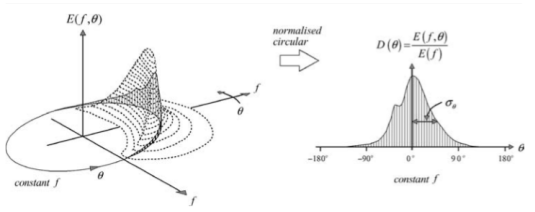

Figure 3.2: The 2D directional spectrum and the directional distribution [2].

The two-dimensional directional spectrum are described with the one-dimensional spectrum with introduced directional distribution $D(\theta)$. Together they define a 2D spectrum; $E(f,\theta) = E(f)D(\theta)$. It is essentially the cross-section through the two-dimensional spectrum at a given frequency, normalized such that its integral over the directions is unity. This integral is shown as follows;

$$\int_0^{2\pi} D(\theta)\,d\theta = \int_0^{2\pi} \frac{E(f,\theta)}{E(f)}\,d\theta = \frac{\int_0^{2\pi} E(f,\theta)\,d\theta}{E(f)} = \frac{E(f)}{E(f)} = 1 \tag{3.2}$$

The directional spreading of the waves can be defined as the (one-sided) directional width of $D(\theta)$, denoted as σ_θ, and thereafter the standard deviation of the directional distribution is defined as;

$$\sigma_\theta^2 = \left(\frac{180}{\pi}\right)^2 \int_0^{2\pi} \left[2\sin\left(\frac{1}{2}\theta\right)\right]^2 D(\theta)\,d\theta \tag{3.3}$$

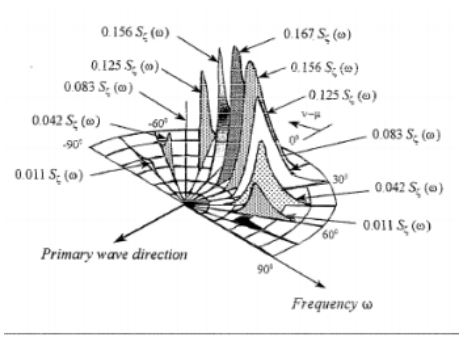

(a) Directional distribution[3]

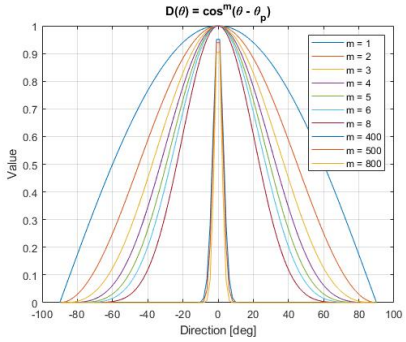

(b) SWAN's directional distribution $D(\theta) = cos^m(\theta - \theta_p)$

Figure 3.3

The directional width (σ_θ) of the directional distribution ($D(\theta)$) is called "DSPR" in SWAN, where it can be defined with the power m.

In SWAN the directional distribution of incident wave energy is given by;

$$D(\theta) = cos^m(\theta - \theta_p) \tag{3.4}$$

Where θ is the wave direction and θ_p is the peak wave direction. The above parameter "m" is related to the one-sided directional spreading of the waves (σ_θ) and the values are shown in table 3.1.

m	σ_θ (Deg)
1	37.5
2	31.5
3	27.6
4	24.9
5	22.9
6	21.2
8	18.8
400	2.9
500	2.56
800	2.0

Table 3.1: Directional spreading, for full table see SWAN User Manual p.106

The spectrum in SWAN is discretized with a constant directional resolution $\Delta\theta$ and a frequency resolution $\Delta f / f$ (logarithmic frequency distribution, see SWAN User Manual p.33). The discrete frequencies are defined between a fixed low-frequency cutoff (flow) and a fixed high-frequency cutoff (fhigh).

If the frequency resolution is too low, the wave spectrum will not represent the desired wave conditions.

We can consider a conditions where the desired significant wave height is 1.0 m and a peak frequency of 1/10 Hz. If the frequency distribution is low, we might end up with the closest calculated frequency, which is either higher or lower. This spans a

lower energy density. SWAN will thereafter start the simulation with a wave height that is lower than the one we wanted. This applies to every spectrum shape.

In SWAN we can input four "spectrum" shapes at boundaries, JONSWAP, Pierson and Moskowitz, Gaussian and a single frequency column (BIN). Where the Gaussian shape describes the surface elevation, which can be used to describe initial waves. As for BIN, we can initiate a regular wave. These shapes will be shown and explained later.

Before showing these spectral distributions we can consider a setup that will be used. The significant wave height H_s = 1.0 m, peak wave period T_p = 10 s, number of meshes in θ-space 180 (This gives a directional resolution of $\Delta\theta = \frac{360^\circ}{180} = 2^\circ$) and the spectral distribution Δf = 50 (This gives the number of frequencies of 51). These parameters will be used throughout the next sections.

BIN (Regular waves)

BIN is a command in SWAN that lets you create regular waves. SWAN locates the energy into one frequency column (bin). This frequency column will be the closest one to the peak wave period, where the width and therefore the accuracy is dependant on the spectral distribution Δf.

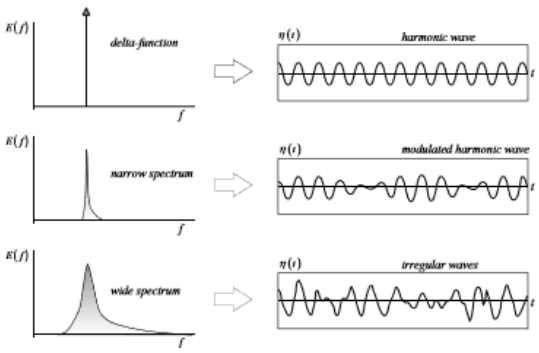

Figure 3.4: The (ir)regular character of the waves for three different widths of the spectrum[2].

To obtain the regular wave with the peak period of 10 s, we want to distribute the frequencies over a very narrow frequency range. For this case we can setup the lowest-frequency range [flow] to 0.09 Hz and the highest-frequency range [fhigh] to 0.11 Hz. This increases our likelihood of getting the frequency and the energy density we want. The result of this can be seen in figure 3.5.

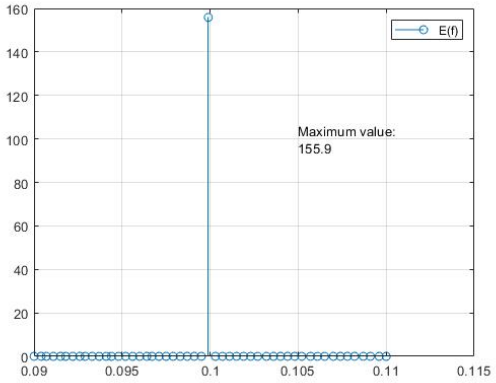

Figure 3.5: 1D frequency BIN in frequency domain [f]

For a simple regular wave in deep water, we can easily make a hand calculations of the significant wave height for a given one-dimensional spectral wave energy density $E(f)$.

This as to check if the simulated significant wave height will be the same as the input significant wave height.

The total energy density at a frequency is defined as;

$$E(f) = \int_0^{2\pi} E(f,\theta)d\theta = \int_0^{2\pi} E(f)D(\theta)d\theta \tag{3.5}$$

Furthermore the variance of the sea surface elevation $\underline{\overline{\eta}}^2$ can be defined as;

$$\underline{\overline{\eta}}^2 = \int_0^{+\infty} E(f)df \tag{3.6}$$

For a regular wave the variance of the sea surface elevation can be easily calculated by hand for a regular wave (see figure 3.6). That is because the variance will be equal to the sea surface elevation. So that $\underline{\overline{\eta}}$ can be simply written as η.

$$\underline{\overline{\eta}}^2 = \int_a^b E(f)df = E(f_m)(f_b - f_a) \Rightarrow \eta^2 = 155.9\frac{m^2}{Hz}\cdot(0.1003Hz - 0.0999Hz) = 0.06236m^2 \tag{3.7}$$

The variance of the sea surface elevation is also given by the zero-th moment of the energy density spectrum $m_0 = \underline{\overline{\eta}}^2$. This defines the significant wave height for deep water as;

$$H_s = 4\sqrt{m_0} = 4\sqrt{\underline{\overline{\eta}}^2} \Rightarrow 4\sqrt{\eta^2} = 4\sqrt{0.06236m^2} = 0.999m \approx 1.0m \tag{3.8}$$

The significant wave height was set up to be 1 meter, which is the value that we got.

Total energy of this one wave;

$$J_{tot} = \frac{1}{2}\rho_w g\underline{\overline{\eta}}^2 \Rightarrow \frac{1}{2}\rho_w g\eta^2 = \frac{1}{2}\cdot 1025\frac{kg}{m^3}\cdot 9.81\frac{m}{s^2}\cdot 0.06236m^2 = 313.52\frac{J}{m^2} \tag{3.9}$$

The point of these calculations is to show the consequences of choosing a wrong spectral distribution Δf and frequency ranges. The comparisons will be done with a narrow Gaussian shape a bit later.

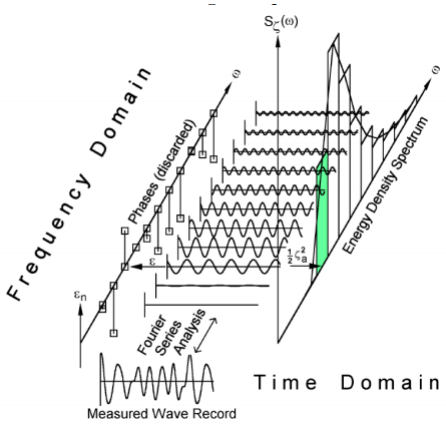

Figure 3.6: Energy density spectrum[3]

A 2D directional energy density spectrum $E(f,\theta)$ describes how the energy is spread out in the domain. The directional spectrum in figure 3.7a has been modelled with a high power "m" of 500, this gives a directional spreading σ_θ 2.56° (see table 3.1). This makes the energy density to be concentrated at one direction (the peak wave direction θ_p), which makes it long crested.

As for the figure 3.7b, the power "m" has been set to 3, which makes it short crested. This plot is very thin, that is because the waves are of only one frequency bin.

If we integrate the 2D directional energy density spectrum $E(f,\theta)$ over the directions θ we get the concentrated energy in a 1D energy density spectrum as shown in figure 3.5. This is the case for both long and short crested waves (shapes will differ).

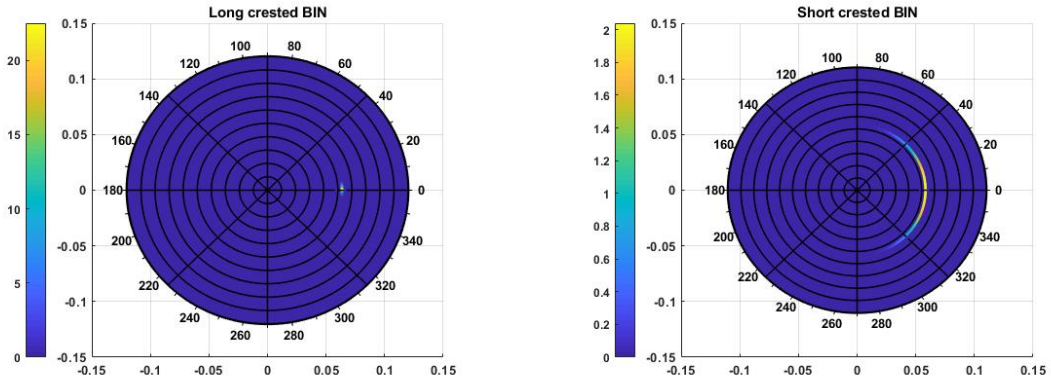

(a) Long crested frequency BIN. *(b) Short crested frequency BIN.*

Figure 3.7: A 2D directional wave spectrum for long and short crested frequency BIN in θ- and f-space.

GAUSS -shape (Sea-surface elevation)

In the linear approximation of ocean waves, the instantaneous sea-surface elevation is a Gaussian distribution. Assuming the mean to be zero, the Gaussian probability density function can be written as [22]:

$$p(\eta) = \frac{1}{(2\pi m_0)^{1/2}} exp\left(-\frac{\eta^2}{2m_0}\right) \tag{3.10}$$

Where η is the sea-surface elevation and m_0 is the zero-th moment of the energy density spectrum.

The width of the Gaussian-shape frequency spectrum is controlled by the standard deviation $\overline{\eta}$ (σ_{fr} in SWAN). The larger the number the more the frequencies will be spread out in its domain (larger amount of random waves). This difference can be seen in figure 3.8 for a 1D spectrum and in figure 3.9 for 2D spectrum.

By decreasing the standard deviation ($\overline{\eta}$) we make the Gaussian shape to be narrower, which when narrow enough can represent a regular wave. This can be seen in figure 3.8a.

For simplicity we consider the same significant wave height and the peak wave period as before.

The frequency range of the spectrum shown in figure 3.8a and figure 3.8b is [flow] = 0.03 Hz and [fhigh] = 0.2 Hz. This is acceptable for the case in figure 3.8b, but not for the case in figure 3.8a. The latter one when compared to the frequency bin as shown in figure 3.5, got the same spectral distribution ($\Delta f = 50$) over a larger range. It so happens that we missed the desired frequency because of this. The frequency used to calculate the energy density for a regular wave is always the closest one. In this case it is $f = 0.1010$ Hz instead of $f = 0.1$ Hz. This does not sound much, but when considered that this spectrum is still not narrow enough, we result in a significant wave height (H_s) of 0.9699 meters.

Gaussian distribution is symmetrical, figure 3.8c show that the lowest frequency cut out is too high to show the entire shape. In this case the the lowest frequency [flow] would need to be somewhere between -0.3 Hz, or the peak wave frequency (f_p) would need to be moved to higher frequency of around 0.3 Hz ($T_p = 7s$).

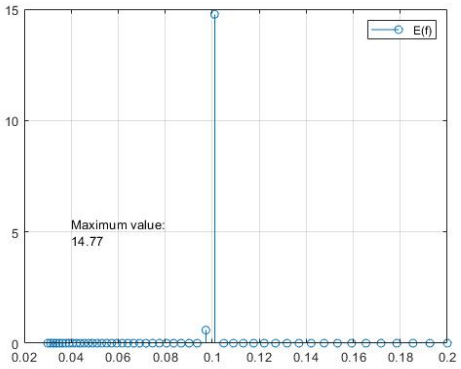

(a) 1D Gauss distribution for standard deviation $\overline{\eta} = 0.001$.

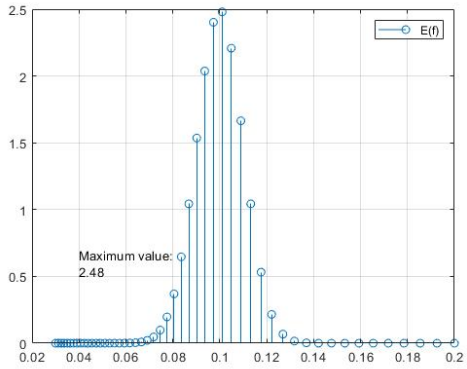

(b) 1D Gauss distribution for standard deviation $\overline{\eta} = 0.01$.

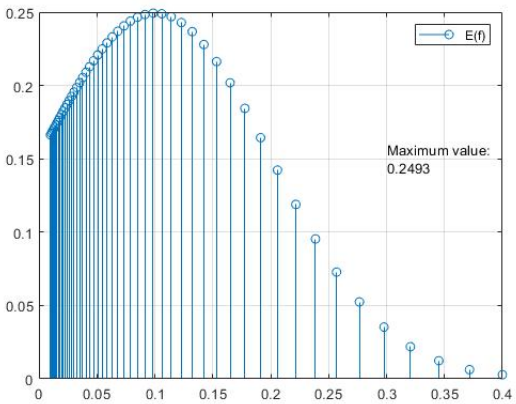

(c) 1D Gauss distribution for standard deviation $\overline{\eta} = 0.1$.

Figure 3.8

The same set of calculations can be done for figure 3.8a as previously with BIN, but since the frequency range is much larger, we cannot expect the same result.

$$\underline{\overline{\eta}}^2 = \int_a^b E(f)df = E(f_m)(f_b - f_a) \Rightarrow \eta^2 = 14.77\frac{m^2}{Hz} \cdot (0.1049Hz - 0.1010Hz) = 0.0576m^2 \tag{3.11}$$

For the significant wave height;

$$H_s = 4\sqrt{m_0} = 4\sqrt{\underline{\overline{\eta}}^2} \Rightarrow 4\sqrt{\eta^2} = 4\sqrt{0.0576m^2} \approx 0.9600m \tag{3.12}$$

Values for the significant wave height obtained from SWAN are 0.9699 m.

Thereafter we can calculate the total energy J_{tot} of one harmonic wave;

$$J_{tot} = \frac{1}{2}\rho_w g\underline{\overline{\eta}}^2 \Rightarrow \frac{1}{2}\rho_w g\eta^2 = \frac{1}{2} \cdot 1025\frac{kg}{m^3} \cdot 9.81\frac{m}{s^2} \cdot 0.0576m^2 = 289.59\frac{J}{m^2} \tag{3.13}$$

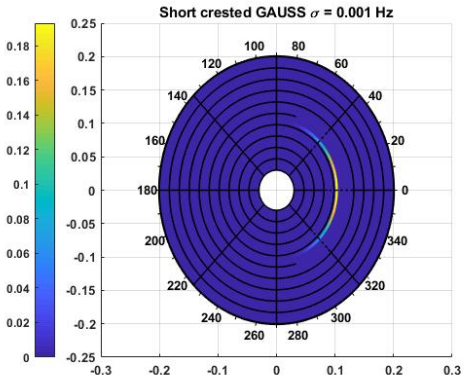

(a) Standard deviation $\underline{\overline{\eta}} = 0.001$.

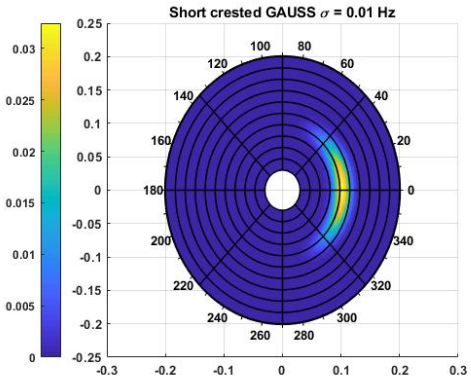

(b) Standard deviation $\underline{\overline{\eta}} = 0.01$.

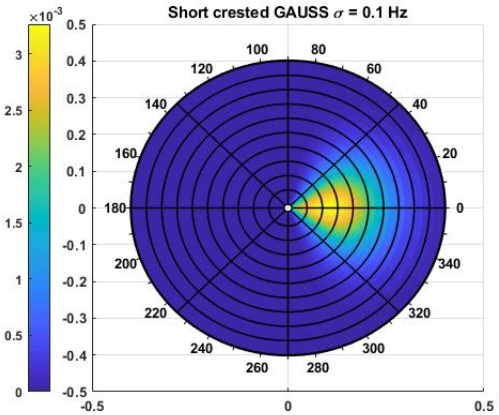

(c) Standard deviation $\underline{\overline{\eta}} = 0.1$.

Figure 3.9: 2D directional short crested GAUSS-shaped distribution.

In figures above we can clearly see how the wave energy is redistributed in f- and θ- space. Where figure 3.9c got its energy noticeable more redistributed over different frequencies than the other figures.

Pierson and Moskowitz

Pierson and Moskowitz is the second most used spectral shape behind JONSWAP, but it is also the simplest for defining the irregular ocean waves.

The assumption here is that if wind blew steadily for a long time over a large area, the wave would come into equilibrium with the wind. This is called a fully developed spectrum or sea, which occurs only in spacial cases [23].

In SWAN we can simulate sea behaviour by defining the waves at the boundary as a Pierson and Moskowitz spectrum.

The fully developed spectrum (Pierson and Moskowitz) is described as [22];

$$E_{PM}(f) = \frac{\alpha_{PM} g^2}{(2\pi)^4 f^5} exp\left(-\frac{5}{4}\left(\frac{f}{f_{PM}}\right)^{-4}\right) \tag{3.14}$$

Where α_{PM} is the energy scale value for PM and f_{PM} is the peak frequency value for PM (for more information see "Waves in oceanic and coastal waters" p. 155 by Leo H. Holthuijsen).

To show this spectrum shape we limited the frequency range to the lowest frequency [flow] 0.03 Hz and the highest frequency [fhigh] 0.2 Hz. When we look at the figure 3.10b we see that this range could have been moved a little bit towards the lower frequencies.

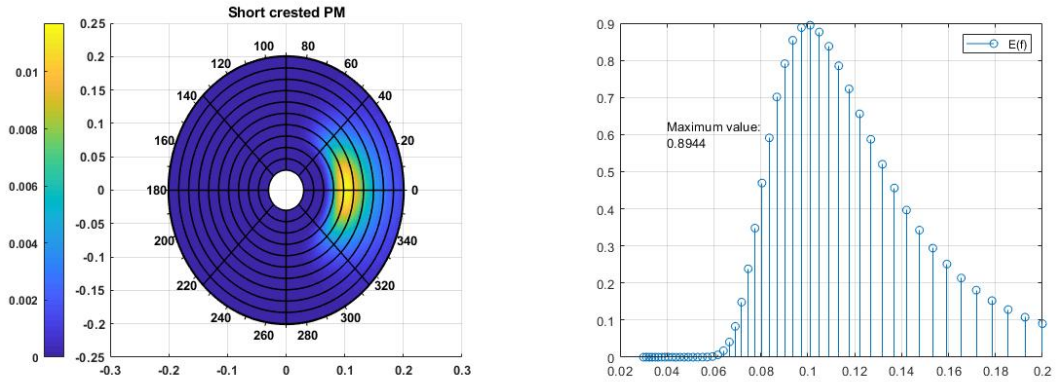

(a) 2D short crested directional PM spectrum. *(b) 1D short crested PM spectrum*

Figure 3.10: Pierson and Moskowitz spectrum done in SWAN.

The shape of a JONSWAP spectrum is based on Pierson and Moskowitz with added peak enhancement parameter (γ), which is a parameter that increases the peakedness of this spectrum. If this parameter is set to one ($\gamma = 1$), the JONSWAP shape will be the same as a Pierson and Moskowitz shape, this is shown in figure 3.12.

JONSWAP

JONSWAP (JOint North Sea WAve Project) is the most important wave spectrum for defining the irregular oceanic waves.

The spectra observed during the JONSWAP appeared to have a sharper peak than the Pierson and Moskowitz spectrum. To account for this in a parametrisation of the observations, the scientists of JONSWAP chose to sharpen the Pierson and Moskowitz spectrum (not its energy scale or frequency scale) and to enhance its peak with a peak-enhancement function $G(f)$:

$$G(f) = \gamma^{exp\left[-\frac{1}{2}\left(\frac{f/f_{PM}-1}{\sigma_j}\right)^2\right]} \tag{3.15}$$

Where γ is the peak-enhancement factor and σ_j is the pea-width parameter ($\sigma_j = \sigma_a$ for $f \leq f_p$ and $\sigma_j = \sigma_b$ for $f > f_p$)

This sharpens the spectrum peak, but has no effect on other parts of the spectrum. This idealised spectrum is called the JONSWAP spectrum. Its complete expression is [22];

$$E_{JONSWAP}(f) = \underbrace{\underbrace{\frac{\alpha_{PM}g^2}{(2\pi)^4 f^5} exp\left(-\frac{5}{4}\left(\frac{f}{f_{PM}}\right)^{-4}\right)}_{\text{Pierson and Moskowitz shape}} \gamma^{exp\left[-\frac{1}{2}\left(\frac{f/f_{PM}-1}{\sigma_j}\right)^2\right]}}_{\text{JONSWAP}} \tag{3.16}$$

Where α_{PM} is the energy scale value for PM and f_{PM} is the peak frequency value for PM (for more information about JONSWAP see "Waves in oceanic and coastal waters" p. 160 by Leo H. Holthuijsen).

In figures below we can see the effect that the peak-enhancement factor γ has on the shape of the JONSWAP spectrum. This yields both for the 1D and 2D spectrum.

Almost all models done in this rapport, are done with the JONSWAP spectrum with the peak-enhancement factor γ = 3.3 has been used. These figures have been used to determine the correct frequency range for Sulafjord wave models, where there are different peak frequencies.

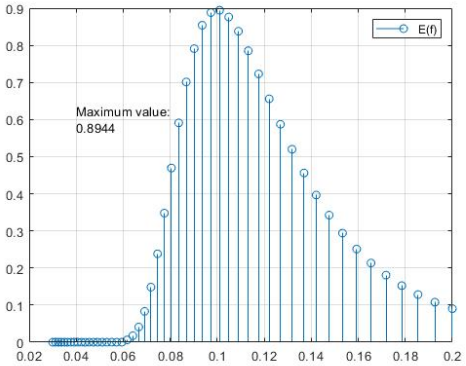

(a) peak-enhancement factor $\gamma = 1$

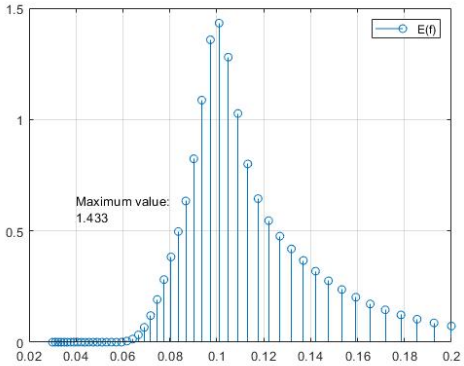

(b) peak-enhancement factor $\gamma = 2$

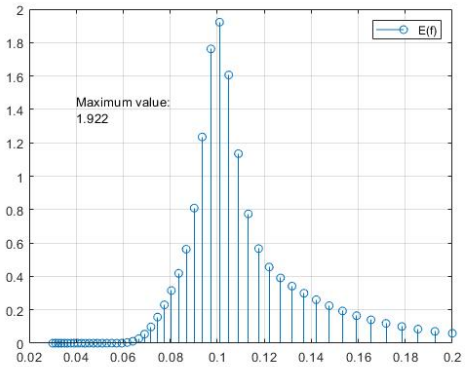

(c) peak-enhancement factor $\gamma = 3.3$

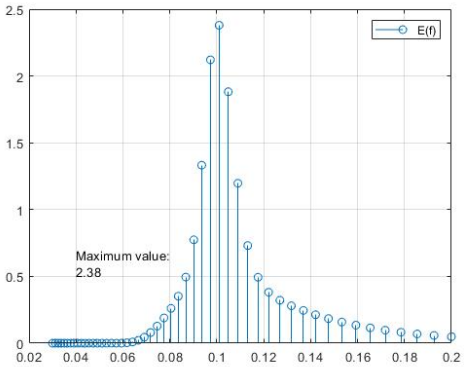

(d) peak-enhancement factor $\gamma = 5$

Figure 3.11: 1D short crested JONSWAP spectrum for the peak-enhancement factors $\gamma = 1$, $\gamma = 2$, $\gamma = 3.3$ and $\gamma = 5$

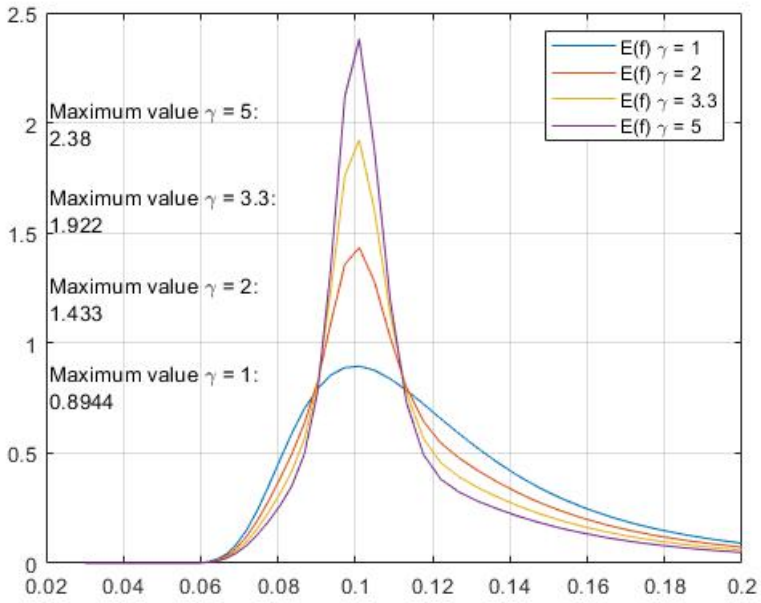

Figure 3.12: Multiple 1D plots of JONSWAP spectrum for the peak-enhancement factors $\gamma = 1$, $\gamma = 2$, $\gamma = 3.3$ and $\gamma = 5$

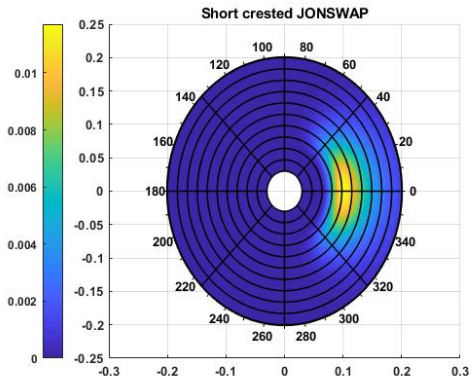

(a) peak-enhancement factor $\gamma = 1$

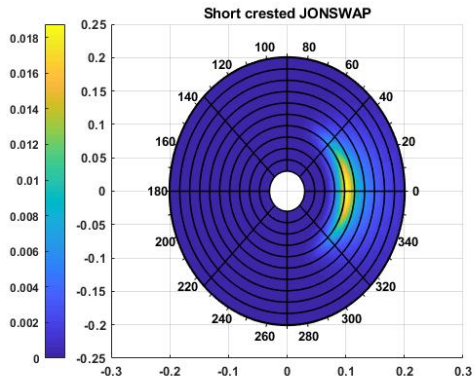

(b) peak-enhancement factor $\gamma = 2$

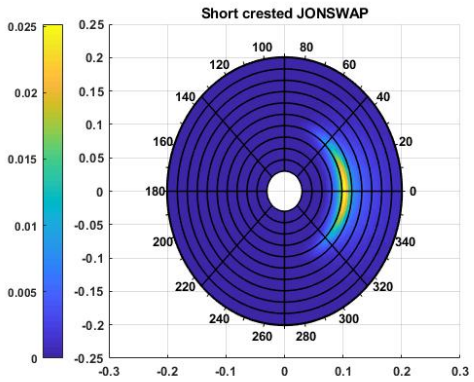

(c) peak-enhancement factor $\gamma = 3.3$

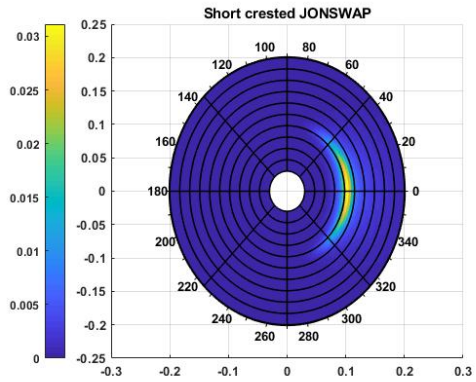

(d) peak-enhancement factor $\gamma = 5$

Figure 3.13: 2D directional short crested JONSWAP spectrum for the peak-enhancement factors $\gamma = 1$, $\gamma = 2$, $\gamma = 3.3$ and $\gamma = 5$

3.3 Wave models

3.3.1 Shoaling

As the wave propagates into shallower water, the phase speed approaches the group velocity and the wave becomes less and less dispersive.

Both the phase speed and the group velocity approach zero at the waterline. This has serious consequences for the applicability of the linear wave theory under such conditions, because it causes the wave amplitude to go to infinity (see below).

$$a_2 = \sqrt{\frac{c_{g,1}}{c_{g,2}}} a_1 \tag{3.17}$$

Where a is the wave amplitude and c_g is the group velocity.

The above energy balance shows that, as the group velocity approaches zero at the waterline, the wave amplitude theoretically goes to infinity. Obviously, the theory breaks down long before that. In addition, other processes such as refraction and wave breaking may well cause a totally different evolution of the waves over an arbitrary seabed topography.

Phase speed and group velocity;

$$c_p = \sqrt{\frac{g}{k}\tanh(kd)} \qquad c_g = \frac{1}{2}\left[1 + \frac{2kd}{\sinh(2kd)}\right]c_p \tag{3.18}$$

Where k is the wave number, d is the water depth and g is the gravitational acceleration.

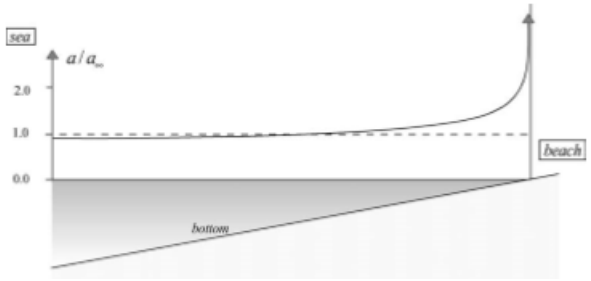

Figure 3.14: Wave amplitude evolution due to shoaling [2].

Shoaling wave model

We can present a simple model of shoaling in SWAN. For this we can consider a wave propagating perpendicularly towards the beach for two slopes, a small and a large slope. That way we can can show effects that occur on larger slopes, effects like wave setdown.

If we look at figure 3.18a, which shows the significant wave height for a large slope. We can notice a decline in the significant wave height at approx. 300 meters. This happens persistently when a wave propagates from relatively deep to shallow water, over a large slope, where the effect spikes (can also be observed later in figure 3.38a). This effect will be explained later.

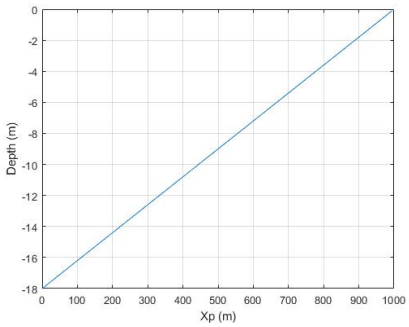

Figure 3.15: Depth = 18.0 m

It has been mentioned above that the phase speed and the group velocity will both eventually approach zero at the waterline. This caused for the wave amplitude to shoot up to infinity. In reality the wave will break before that happens.

In figure 3.18a and 3.17a we can notice that the wave amplitude does indeed go to infinity. To counteract this, we can introduce depth-induced breaking into this numerical model. This will make sure that the energy will dissipate accordingly when the wave propagates.

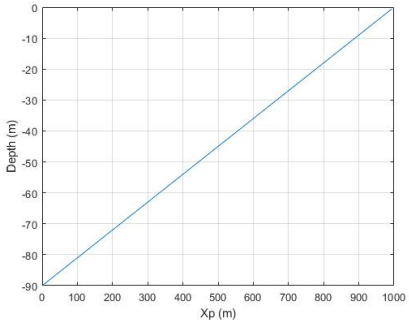

Figure 3.16: Depth = 90 m

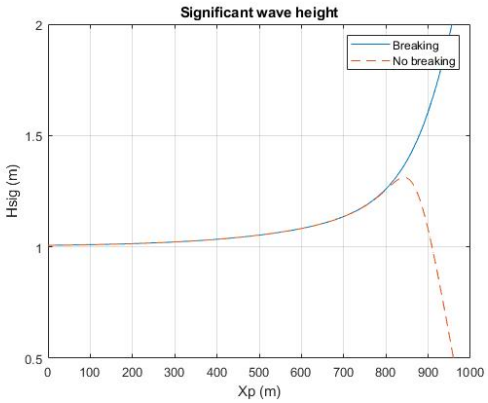

(a) Significant wave height at depth 18.0 meters.

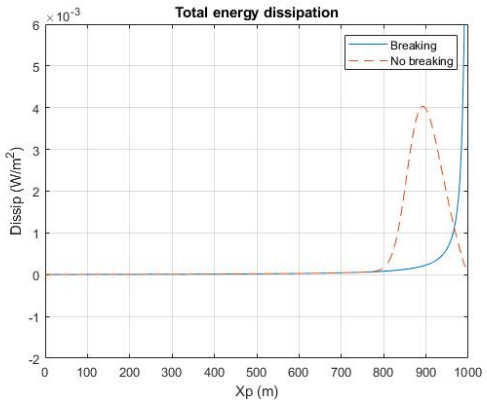

(b) Total energy dissipation at depth 18.0 meters (S_{tot})

Figure 3.17

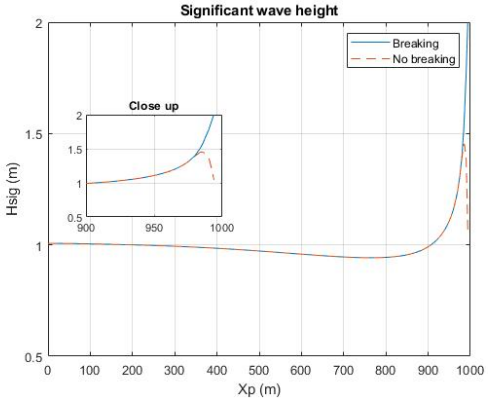

(a) Significant wave height at depth 90.0 meters.

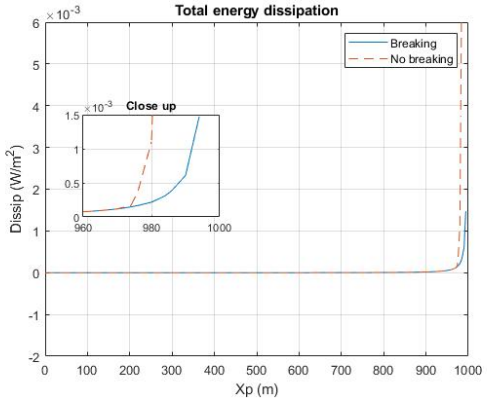

(b) Total energy dissipation at depth 90.0 meters (S_{tot})

Figure 3.18

Wave setup and setdown

In fluid dynamics, wave setup is the increase in mean water level due to the presence of breaking waves. Similarly, wave setdown is a wave-induced decrease of the mean water level before the waves break (during the shoaling process). For short, the whole phenomenon is often denoted as wave setup, including both increase and decrease of mean elevation. This setup is primarily present in and near the coastal surf zone [24].

There is a command in SWAN called "setup", which accounts for the wave-induced setup.

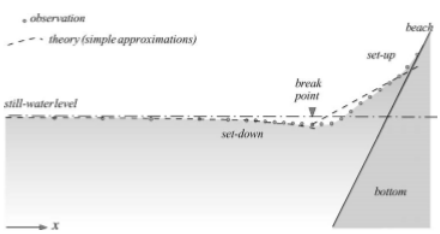

Figure 3.19: Step-up and step-down induced by waves approaching a very steep beach[2].

3.3.2 Refraction

When waves propagate towards land at an angel the wave crest will be turned towards the land and get aligned parallel with the depth contours, as mentioned is section 2.3.2. This is due to the change is Phase speed $[c_p]$ along the wave crest.

The part of the wave in shallower water will move slower than parts of the wave in deeper water, which will have a bending effect of the wave crest turning it towards the shallower depth. When the waves enter shallow water the phase speed $[c_p]$ becomes a function of water depth instead of wavelength as in deep water.

The equation of the phase speed at a arbitrary depth is;

$$c_p = \sqrt{\frac{g}{k} \cdot \tanh kd} \tag{3.19}$$

This equation can be further simplified to an equation for deep water ($\tanh kd \Rightarrow 1$) and shallow water ($\tanh kd \Rightarrow 0$).

$$c_{pD} = \sqrt{\frac{g}{k}} \qquad\qquad c_{pS} = \sqrt{g \cdot d} \tag{3.20}$$

Where c_{pD} is the phase speed for the deep water, c_{pS} is the phase speed for the shallow water, k is the wave number, d is the water depth and g is the gravitational acceleration.

For simpler cases where the depth contours are parallel the change of wave direction can be calculated by a simplified use of Snel's law.

$$\frac{\sin\theta}{c_p} = \text{Constant} \tag{3.21}$$

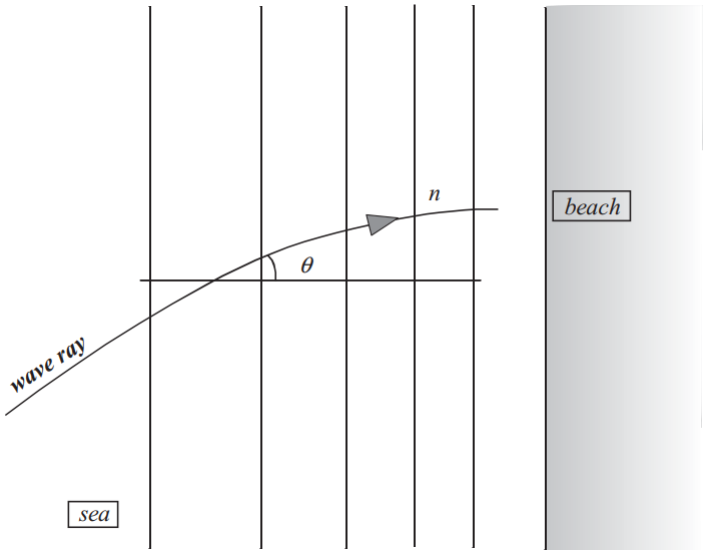

Figure 3.20: The angle θ in Snel's Law is taken between the wave ray and the normal to the straight and parallel depth contours[2].

Refraction wave model

To show the effect of refraction in SWAN a simple wave model was created. We modeled a simple wave propagating towards a beach, with parallel depth contours, at an angel of 30 degrees with respect to the width . The wave initial wave height was set to 1m and other inputs like wind and currents was ignored for this simulation.

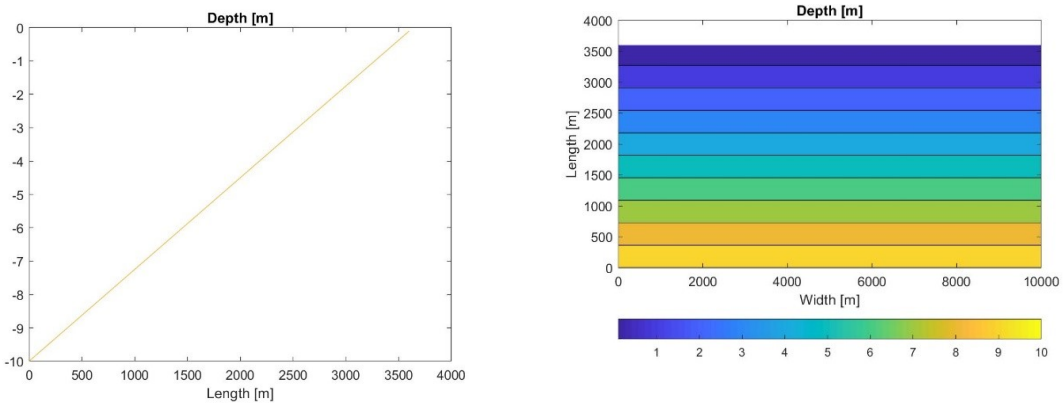

(a) One dimensional depth *(b) Two dimensional depth*

Figure 3.21

The case we are running is a cutout from a considered long straight beach, with parallel depth contours going out in the water. Therefor we also included a segmented wave boundary on half of the east side in addition to the wave boundary on the whole of south side to get more realistic results.

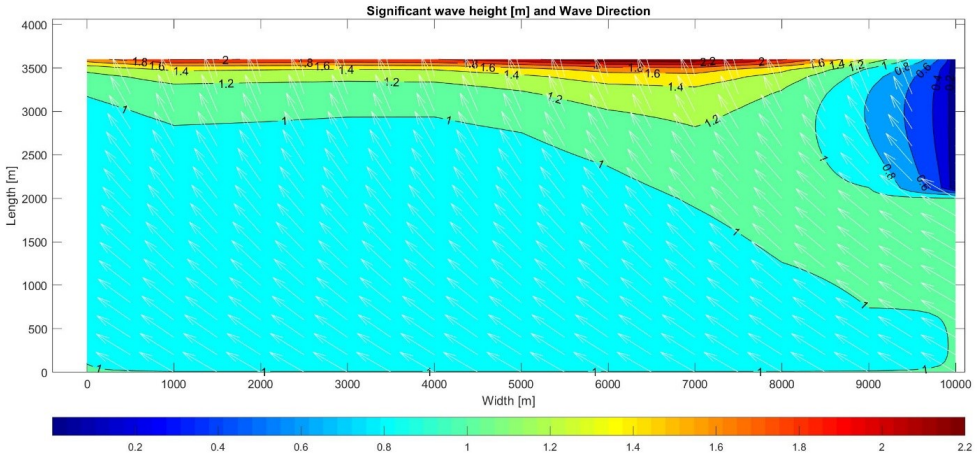

Figure 3.22: Resulting significant wave height with arrow showing the wave direction at $\theta_m = 30°$

As explained by the theory, we can clearly see the waves initially propagating at an angel of 30 degrees change direction towards the beach as they propagate along the

width of the beach.

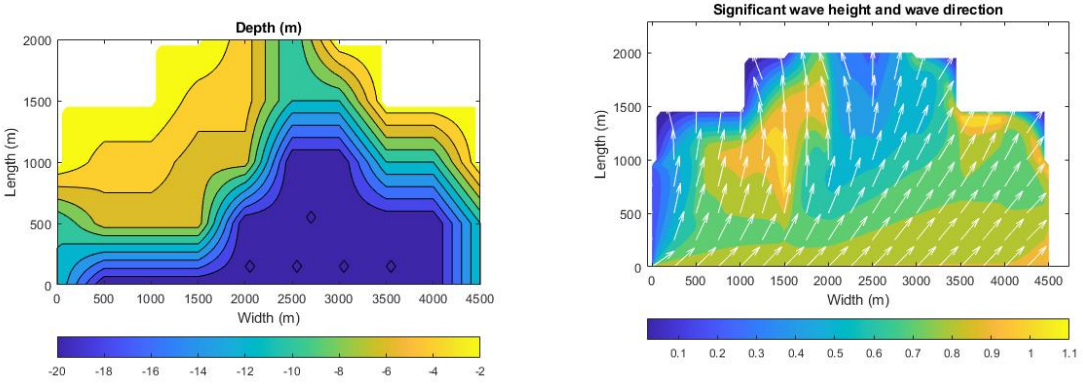

(a) A more complex depth

(b) Resulting significant wave height with arrow showing the wave direction at $\theta_m = 30°$

Figure 3.23

3.3.3 Diffraction

Diffraction in SWAN is very limited. Spectral action balance equation models usually neglects diffraction in order to be more computational friendly. The same goes for SWAN.

To accommodate diffraction in SWAN simulations, a phase-decoupled refraction-diffraction approximation is suggested. This allows for SWAN to still make simple diffraction approximations.

Nevertheless diffraction in SWAN should not be used when;

- An obstacle or coastline covers a significant part of the down-wave view.
- The distance to that obstacle or coastline is small (less than a few wave length).
- The reflection off that obstacle or coastline is coherent.
- The reflection coefficient is significant.

This implies that the SWAN diffraction approximation can be used in most situations near absorbing or reflecting coastlines of ocean, seas, bays, lagoons and fjords with an occasional obstacle such as islands, breakwaters, or headlands but NOT in harbour or in front of reflecting breakwaters or near wall-defined cliff walls. The SWAN results seem reasonable if the above conditions are met [20].

Diffraction wave model

To model diffraction in SWAN, we need to create a depth that involves absorbing breakwaters.

A command in SWAN called "obstacle" cannot be used since it models reflecting obstacles. This will usually yield no result after computation. What can be done instead is to model a land mass in the bottom file.

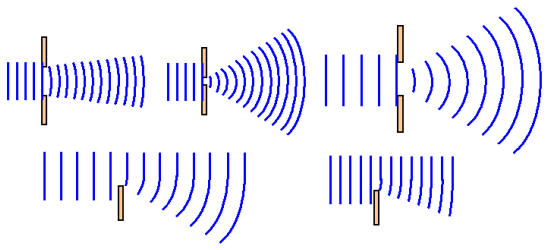

Figure 3.24: Simple cases that show diffraction

The boundaries in SWAN are either land or water. Land in SWAN does not generate waves and it fully absorbs wave energy (which is what we need for diffraction to work).

	Aperture $[m]$	$\Delta x[m]$	$\Delta y[m]$	$\lambda_p[m]$
Figure 3.25a	50	50	25	6.25
Figure 3.25b	150	50	25	6.25

Table 3.2

We assume a monochromatic[2] wave propagating from the west side of the domain. Its significant wave height (H_s) is 0.2 meters and peak wave period (T_p) is 2.0 sec.

Plots of diffraction done in SWAN can be seen on the next page.

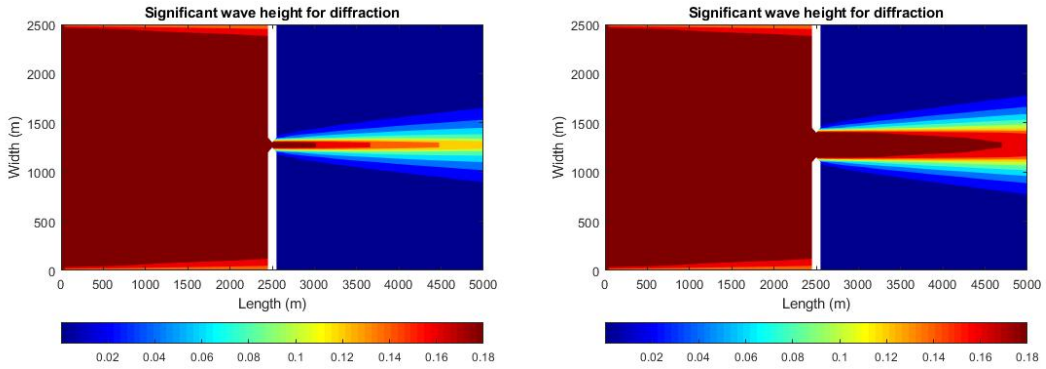

(a) *(b)*

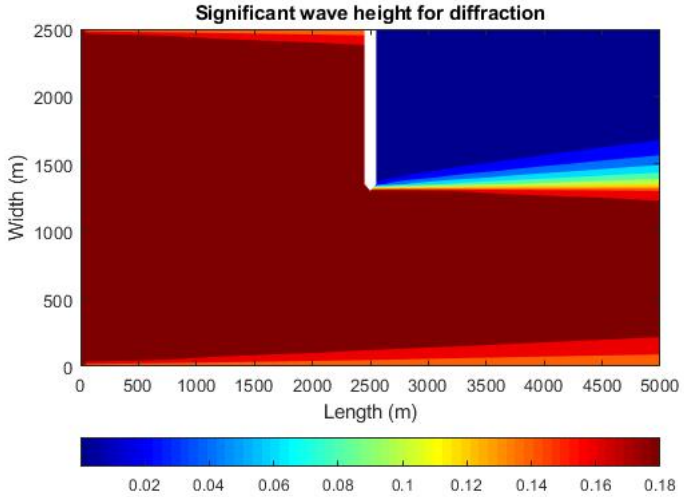

(c)

Figure 3.25

[2] It's a wave with a single wavelength and frequency. Harmonic and long crested.

3.3.4 Depth-Induced breaking

Wave breaking is arguably the most important process that waves are subjected to. Unfortunately it is also one of the most difficult process to describe mathematically.

At shallow waters, the waves energy dissipate decisively due to the influence of the bottom depth. Depth can cause the wave to plunge when a certain wave steepness is reached, it can cause the wave to spill its energy to the sides (spilling) or also cause it to surge when the beach slope is large. The model of wave breaking in SWAN corresponds to the theory, where the slopes of the seabed will be gradually increased. in SWAN there is no clear way to identify what kind of breaking occurs. For this this section will include the iribarren number, which will help use understand what breaking should theoretically happen.

In this section we will use the iribarren number to determine the range of these different breakages (as mentioned in section 2.3.4). Thereafter model them accordingly to get spilling, plunging and surging breakage, and run a simulation with SWAN. The collapsing breaking will be ignored, since it happens between a plunging and surging breaking, with no clear definition of its own. This data might be proven useful further when looking at the results of Sulafjorden.

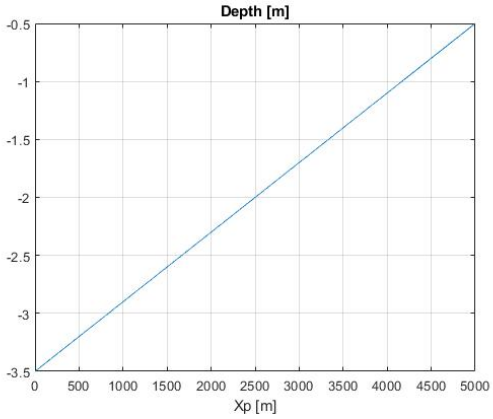

Figure 3.26: A depth used to simulate spilling breaking, with a slope of 3:5000.

Spilling breaking

Spilling breaking occurs when a wave propagates in shallow water along a flat, or a very small sloped seabed. A spilling breakage is defined when the iribarren number (the surf similarity parameter) is below 0.5 ($\xi_\infty < 0.5$).

The wave will gradually spill its energy over the distance traveled towards the shore, it will result in a steady decline in wave amplitude and wave length due to it slowing down, until it reaches land or it loses all of its energy while propagating.

We want to create a model to simulate that satisfies these conditions. For this purpose we decided to input a significant wave height as one meter (H_s = 1.0 meter), the peak wave period (T_p) as 10.0 seconds, directional width σ_θ = 27.6° and a JONSWAP-shaped frequency spectrum with a peak enhancement parameter γ = 3.3.

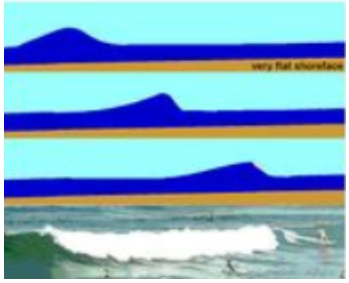

Figure 3.27: Spilling breaking

As the wave propagates, the energy is supposed to spill gradually to the base or to the sides. This will cause a continuous decline in the significant wave height, this can be seen in figure 3.28a.

This dissipation is mainly caused due to surf effect (figure 3.28b.), but also due to the bottom friction and the triad wave-wave interactions.

The calculation of iribarren number;

$$\xi_\infty = \frac{\tan\alpha}{\sqrt{H_\infty/\lambda_\infty}} = \frac{3/5000}{\sqrt{1.0m/156.0m}} = 7.5\cdot 10^{-3} \tag{3.22}$$

The iribarren number shown in 3.22 is much lower than the limit number where the spilling should occur ($7.5 * 10^{-3} << 0.5$). The parameters can be changed to a slope of 0.04 ($\alpha = 2.0°$), which gives a depth of approx. 200 meters. These values can be used next time when simulating spilling.

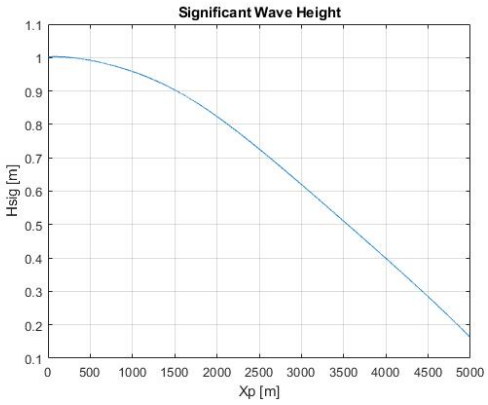

(a) Significant wave height. for spilling breaking (H_s)

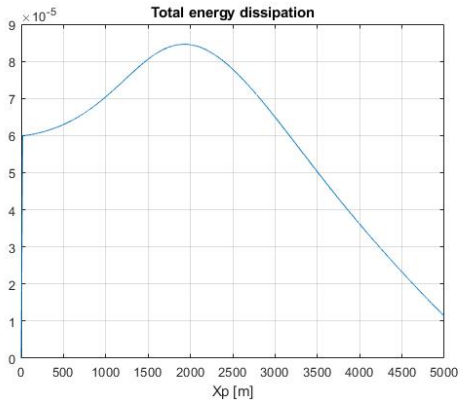

(b) Total energy dissipation (S_{tot})

Figure 3.28

A spilling breaking cannot reach a steepness $\left(\frac{H_s}{\lambda_a}\right)$ ratio that will cause it to break by plunging. To validate this model we need to determine the wave steepness, and compare it to the breaking criterion $H_b/\lambda_a = 0.142. * \tanh(kd)$. Where H_b is the maximum wave height, λ_a is the average wave length, k is the wave number and d is the water depth. The steepness values from SWAN are calculated by taking a ration between the significant wave height over the average wave length at each point.

The plots of these values can be seen in figure 3.29.

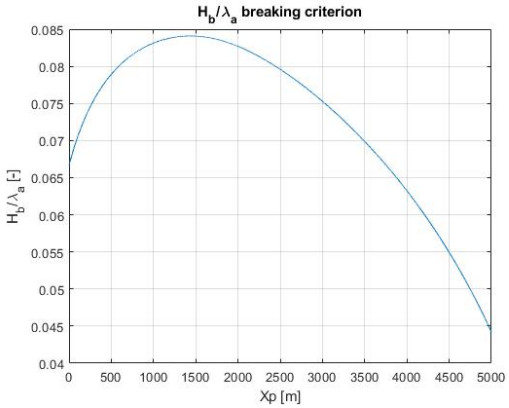

(a) Breaking criterion. Steepness at which the wave should break.

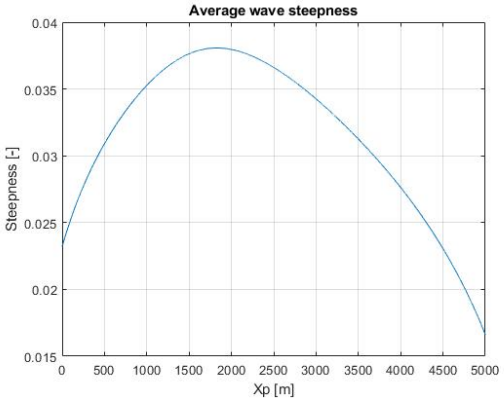

(b) Average wave steepness. Calculated from SWAN.

Figure 3.29: Steepness limit and steepness value

The occurring effects are expected to happen, which satisfies the general theory behind spilling breaking. To our understanding SWAN gave satisfactional results based on the theoretical input. This comes from a conclusion that the wave steepness does not exceed the breaking criterion, the significant wave height and the energy dissipation gradually decreases, which is what we expected.

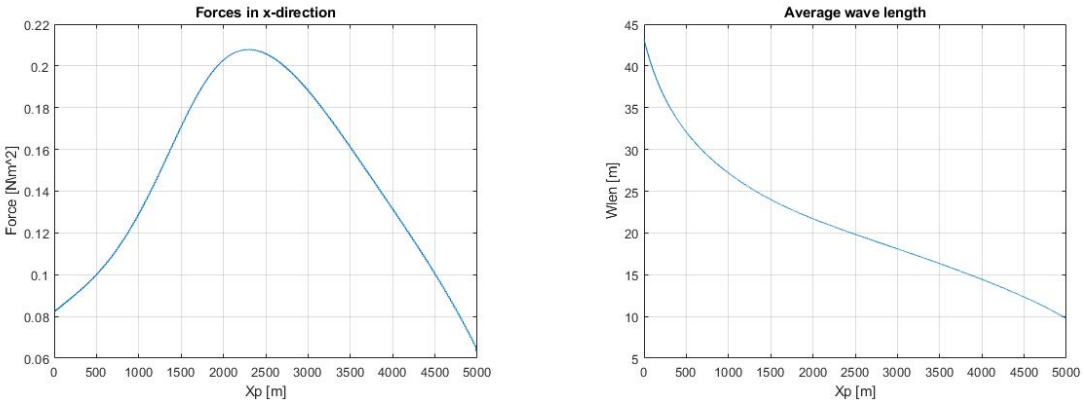

(a) Forces *(b) Average wave length.*

Figure 3.30: Forces in x-direction and average wave length

Plunging breaking

A wave plunges when the front face become vertical, where it eventually falls into the base of the wave. This happens when the wave approaches a moderately steep seabed. Where, eventually at a point the wave becomes too steep and breaks.

A plunging breaking is defined when the iribarren number is between 0.5 and 3.3 ($0.5 < \xi_\infty < 3.3$).

To verify the effects of plunging breaking in SWAN we can consider the same wave parameters as mentioned previously.

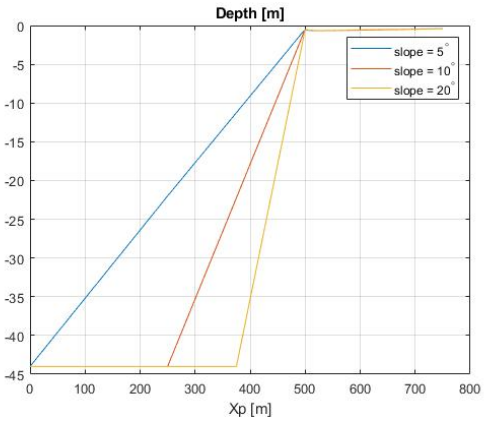

Figure 3.31: A depth used to simulate and compare plunging breaking of different slopes. Slopes used are 11:125, 22:125 and 44:125.

To better show this effect we can consider a wave propagating towards a bottom angle of 5°, 10° and 20°.

We can also compare them by making the slopes end at the same point, and give them the same maximum depth.

Seabed angle (α)	Slope	Iribarren number (ξ_∞)
5°	11:125	1.1
10°	22:125	2.2
20°	44:125	4.4

Table 3.3: Iribarren number for these three slopes.

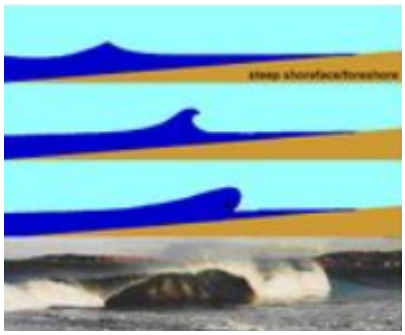

Figure 3.32: Plunging breaking

Table 3.3 gives the values of iribarren number at each slope.

We can notice that the iribarren number for the slope of $\alpha = 20°$ is way above the limit. This indicates that the breaking should be either a surging or a collapsing. The thing that is certain is that it will have many similarities to the surging breaking shown next.

Before proceeding to show the results, we can make some assumption as to how the waves will behave.

When we look at the depths shown in figure 3.31 we can conclude that the significant wave height will start increasing at the lowest slope first, this will cause a gradual surf dissipation at first. As for the higher slopes the energy dissipation will be more sudden and the wave amplitude will steepen faster. These results can be observed in figure 3.34.

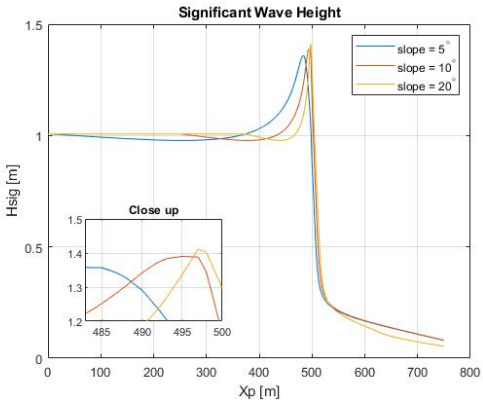

(a) Significant wave height, for plunging breaking.

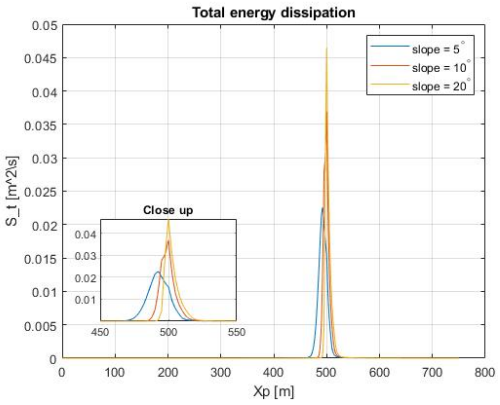

(b) Close up of the total energy dissipation.

Figure 3.33

A plot of wave steepness generated from SWAN can be seen on figure 3.34b. We can notice that at the point of discontinuity (500 meters), the steepness is way above the breaking limit. If we look closer at these figures 3.34, we can also notice that few meters before the discontinuity, the steepness of these cases are equal to the limit shown in figure 3.34a. This matches the significant wave height shown in figure 3.33a quite well.

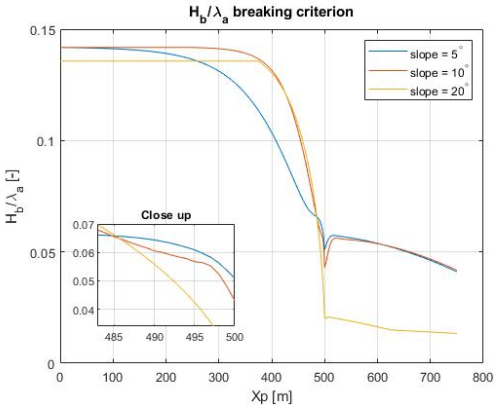

(a) Steepness at which the wave should break. Breaking limit.

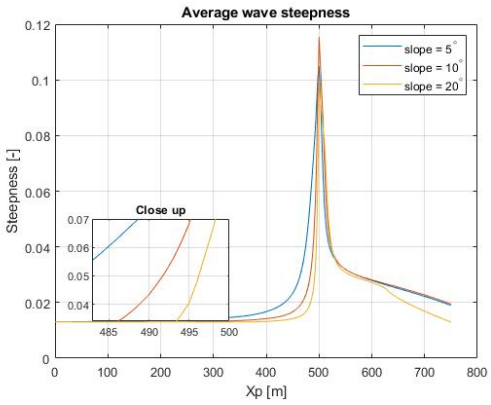

(b) Average wave steepness, computed from SWAN.

Figure 3.34: Steepness limit and steepness value

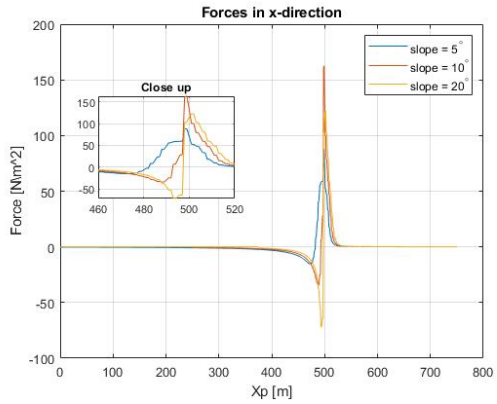

(a) Wave-induced force per unit surface area

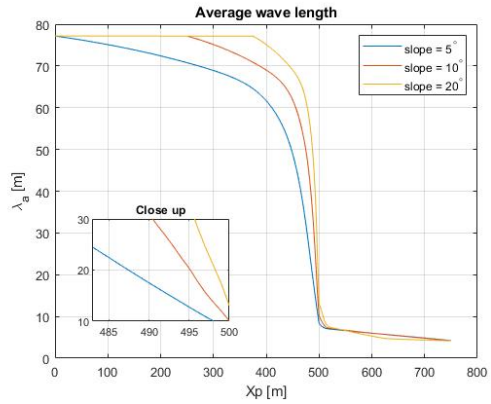

(b) Average wave length

Figure 3.35: Wave-induced force and average wave length

When a wave breaks it turns its wave energy into a turbulent energy. For larger slopes this energy will spike around one location. This may cause severe structural damage. In SWAN we can plot the wave induced forces. Forces for plunging breaking can be seen in figure 3.35.

As mentioned before, we cannot determine what kind of breaking will occur. What we can conclude is that the waves break at around the maximum wave height as they are supposed to.

What also happened is that the largest slope does not look that much different from the other two, but it does hold a lot of similarities to a surging breakage. The wave steepness for this case do exceed the breaking criterion. This do seem like a collapsing breaking. The wave height and the setdown effect did spike more for this slope.

Surging breaking

A surging breaking occurs when a wave approaches a relatively steep seabed. These waves do not break, instead they surge up and down the slope with most of its energy being reflected. Surging wave breaking is defined at iribarren number larger than 3.3 ($\xi_\infty > 3.3$).

To recreate this process in SWAN, we assume a large slope of 200:250, this gives a angle of approx. 40°. The significant wave height and peak period still remains as 1.0 meters and 10 seconds.

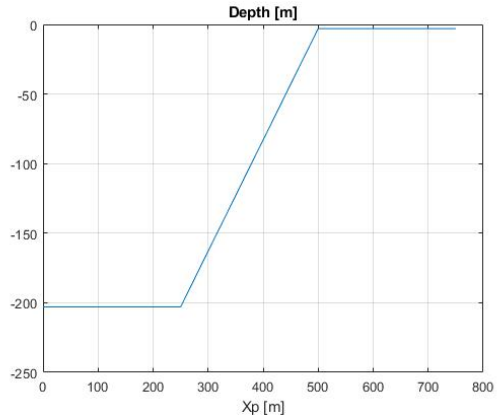

Figure 3.36: A depth used to simulate surging breaking at slope 200:250.

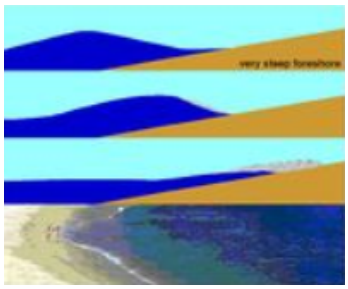

Figure 3.37: Surging breaking

The calculation of iribarren number;

$$\xi_\infty = \frac{\tan\alpha}{\sqrt{H_\infty/\lambda_\infty}} = \frac{200/250}{\sqrt{1.0m/156.0m}} = 10 \tag{3.23}$$

In equation 3.23 we can notice that the iribarren number for this slope is way above the definition value (10 >> 3.3). The slope can be significantly reduced, this will cause for the results to be similar to the previous case in plunging (seabed angle α = 20°). To be within the limits, we could have change the parameters to a bottom slope of 0.2642, seabed angle α = 14.8°, which gives a depth = 66m and a domain length of 250 m. Regardless, the value of 10 can be still used as an example.

As the wave propagates towards the shore, the wave will quickly steepen and cause a large portion of its energy to dissipate fast. This is because of the seabed slope being large, which causes a fast transition between depth contours. The rest of the energy will dissipate later while it propagates further into land. This can be seen in figure 3.38b.

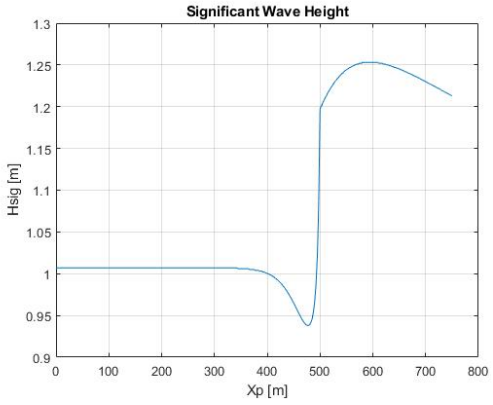

(a) Significant wave height for a surging breakage.

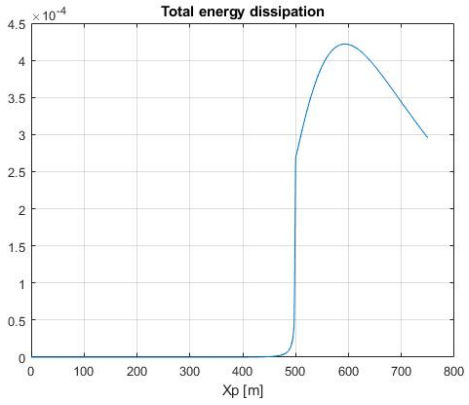

(b) Total energy dissipation

Figure 3.38

It has been mentioned before that a surging breakage is not supposed to break. To check if that is true in this case, we need to plot a figure that shows the steepness of the wave and the wave breaking criterion, exactly like before. The results can be seen in figure 3.39.

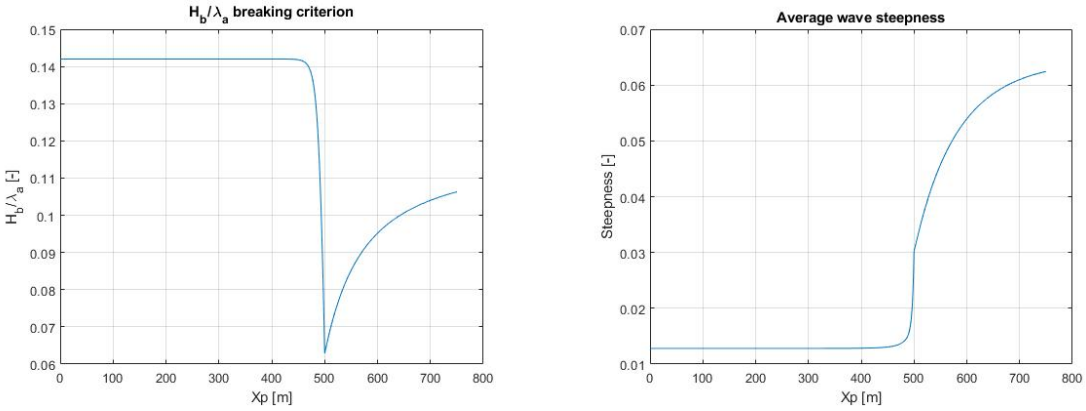

(a) Breaking criterion *(b) Average steepness of the wave*

Figure 3.39: Breaking criterion and the average steepness with close up windows

There are few things that can be concluded from running this model. The first is that the wave does not seem to break like the waves shown in plunging section.

A surging breaking is supposed to be reflecting and when we look at the figure 3.40b we can see that there is a much larger force reflection than in the previous cases. This seems to satisfy the theory.

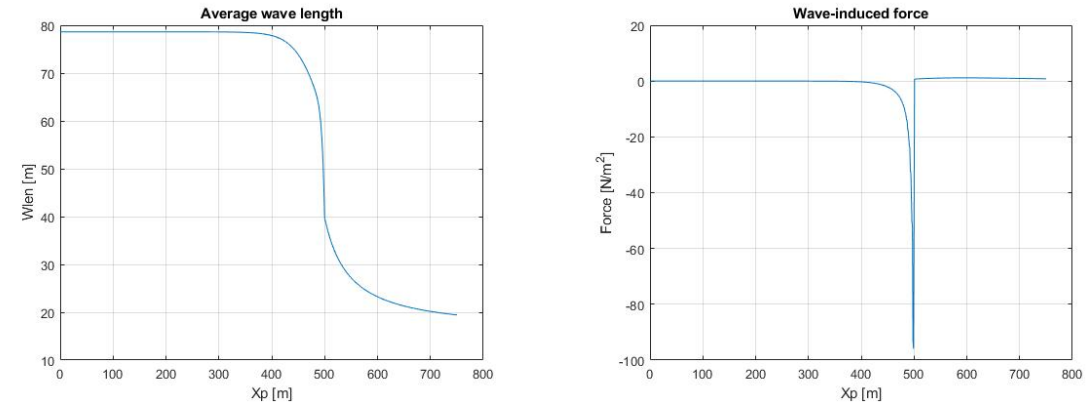

(a) Average wave length *(b) Forces in x-direction*

Figure 3.40

Chapter 4

Sulafjord

4.1 Introduction

Statens vegvesen's ferry-free Norway is a major engineering project, which aims to remove all ferry transport on E39 from Kristiansand to Trondheim. Sulafjorden is one of the challenging areas where the construction will be conducted.

This chapter is entirely dedicated to the modelling and simulating of Sulafjorden. This chapter will cover the plan for modelling of Sulafjorden, the execution of it and analyzation.

This chapter is divided into 5 sections, introduction, location, modelling, results and conclusion. Where the section about location, will be dedicated to explaining the local location of Sulafjorden, the buoy placements, the approximate distance from the buoy D to the other buoys and the domain-and depth meshing (discretization).

The next section is about the modelling, where there will be explained the four real cases based on the buoy data. In addition, this section will also cover some mistakes and clarify few thing.

The last sections will explain the numeric results, show few plots with a detailed explanation of one of them and at last a conclusion.

4.2 Location

(a) A partial map of Sunnmøre, with buoy placements.

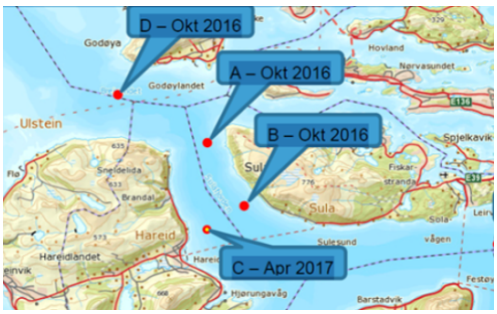

(b) Sulafjord with buoy

Figure 4.1

For the ease of navigation and explanation of few situations, a map without the buoy locations is included in figure 4.2.

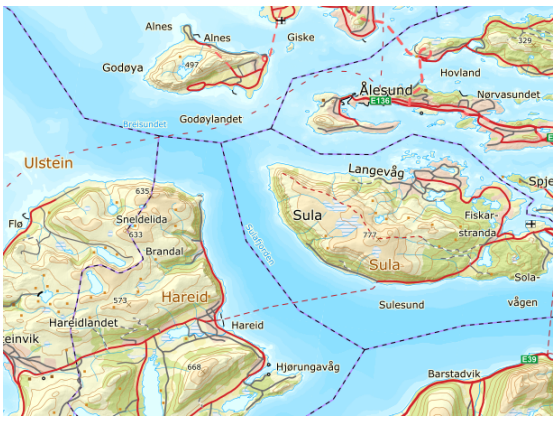

Figure 4.2: A map of Sulafjord

Buoy information			
Buoy	Latitude	longitude	depth [m]
A	62.428°	006.049°	375
B	62.404°	006.083°	325
C	62.391°	006.052°	450
D	62.442°	005.929°	345

Table 4.1

Time elapsed from buoy D				
Buoy	Distance [km]	Peak period T_p	Wave length λ_p	Time [min]
D-A	6.0	12	224.8	5.3
D-B	10.0	12	224.8	8.9
D-C	10.6	12	224.8	9.43

Table 4.2: A rough estimation of the time elapsed from the buoy D (Calculated over deep water)

Domain					
Length [km]	Width [km]	Δx [m]	Δy [m]	$\Delta\theta$ [Deg]	Δf [Hz]
20	17	180	180	360	50
Bottom					
Length [km]	Width [km]	Δx [m]	Δy [m]	Elements nx	Elements ny
20	17	50	50	400	340

Table 4.3: Domain and bottom discretization

4.3 Modelling

Before proceeding further into modelling, some things needs to be addressed. The waves at the inlet are pretty much unknown. This makes it necessary to make some guesses as to how much do the waves transform when propagating from the inlet to the first buoy. There is no clear answer other than trying and failing, until the values seem reasonable.

The inlet is located at the north-west side of the computational domain, west of Godøya. This is where the wave boundary will be placed.

Since that there are two sides, one at the west and the other at the north. There needs to be defined two separate boundaries. The western one is the easy one. This side can be entirely covered with the expected wave, due to there being land along the rest of the side. The consequence of it is that the land to the south of the boundary will experience a concentration of energy dissipation at an point close it. The influence seems to be minimal anyways, therefore the entire side will be covered.

The input wave at the northern boundary, cannot be applied on the entire side of the computational domain. By doing so, the model would receive larger than usual waves propagating from the east side of Godøya. This is highly undesirable. For this reason, the waves will be applied only at a segment of this side. This segment will stretch from the north-western corner of the computational domain in to Godøya.

This seem to be reasonable, but it will get the same consequences as the western boundary.

For the simplifications, the rest of the northern boundary (east of Godøya) will not experience any incoming waves. This will cause some errors in the results for the buoy A, B and C.

For the purpose of sparing some room in tables, the dates chosen for the simulations are labeled in minutes from the start of the month.

- 470 min = 01 January 2019 07:50
- 730 min = 01 January 2019 12:10
- 3760 min = 02 January 2019 14:40
- 19140 min = 12 January 2019 07:00

All of the modelled cases of Sulafjord are simulated with no wind and currents present. That reason for this was time constraints.

This, with the addition of absent wave boundary east of Godøya will have a influence on the overall results. This report do not cover by how much will it influence the results, this is also due to the lack of time.

With the removal of the wind, physical source effects like white-capping and quadruplet wave-wave interactions can be also removed. This will spare some time when running the simulations. Nevertheless, other physical source effects like depth-induced wave breaking, bottom friction, triad wave-wave interactions, refraction and diffraction are included in the computations.

For the sake of simplicity, the results are compared at the same time. The reasoning is that the values usually do not vary that much between measured time increments.

The last things that needs to be mentioned, is that the results are in relation to the cartesian coordinates. Where the mean wave direction is showing the wave propagating towards the respected direction and lastly that the real values of the buoy B for the last case [19140] are erroneous. There was no time to pick different values after noticing this error.

4.4 Results

4.4.1 Buoy comparisons - numerical results

01 January 2019 07:50

Boundary input					
Run [min]	$H_s[m]$	$T_p[s]$	$\theta_m[deg]$	$power"m"$	$\sigma_\theta[deg]$
[470]	6.3	11.1	320	≈2	33.5

Buoy D					
Time $[min]$	$H_s[m]$	$T_p[s]$	$T_m[s]$	$\theta_m[deg]$	$\sigma_\theta[deg]$
470	5.0	11.04	8.59	319.22	24.61
Buoy D - SWAN					
Run [min]	$H_s[m]$	$T_p[s]$	$T_m[s]$	$\theta_m[deg]$	$\sigma_\theta[deg]$
[470]	5.02	10.94	9.16	332	23.70

Buoy A					
Time $[min]$	$H_s[m]$	$T_p[s]$	$T_m[s]$	$\theta_m[deg]$	$\sigma_\theta[deg]$
470	3.24	9.86	8.11	339.6	13.4
Buoy A - SWAN					
Run [min]	$H_s[m]$	$T_p[s]$	$T_m[s]$	$\theta_m[deg]$	$\sigma_\theta[deg]$
[470]	2.43	10.94	8.88	322	8.46

Buoy B					
Time $[min]$	$H_s[m]$	$T_p[s]$	$T_m[s]$	$\theta_m[deg]$	$\sigma_\theta[deg]$
470	1.25	9.38	5.18	338.2	18.98
Buoy B - SWAN					
Run [min]	$H_s[m]$	$T_p[s]$	$T_m[s]$	$\theta_m[deg]$	$\sigma_\theta[deg]$
[470]	1.44	10.94	8.68	315	5.76

Buoy C					
Time $[min]$	$H_s[m]$	$T_p[s]$	$T_m[s]$	$\theta_m[deg]$	$\sigma_\theta[deg]$
470	1.465	9.67	4.30	291	70.31
Buoy C - SWAN					
Run [min]	$H_s[m]$	$T_p[s]$	$T_m[s]$	$\theta_m[deg]$	$\sigma_\theta[deg]$
[470]	0.48	10.94	8.92	292	6.08

01 January 2019 12:10

Boundary input					
Run [min]	$H_s[m]$	$T_p[s]$	$\theta_m[deg]$	$power"m"$	$\sigma_\theta[deg]$
[730]	8.8	14.85	320	8	18.8

Buoy D					
Time $[min]$	$H_s[m]$	$T_p[s]$	$T_m[s]$	$\theta_m[deg]$	$\sigma_\theta[deg]$
730	8.09	14.844	11.523	318.516	17.58
Buoy D - SWAN					
Run [min]	$H_s[m]$	$T_p[s]$	$T_m[s]$	$\theta_m[deg]$	$\sigma_\theta[deg]$
[730]	7.95	13.77	11.65	325.16	15.55

Buoy A					
Time $[min]$	$H_s[m]$	$T_p[s]$	$T_m[s]$	$\theta_m[deg]$	$\sigma_\theta[deg]$
730	4.06	15.04	10.45	336.8	10.55
Buoy A - SWAN					
Run [min]	$H_s[m]$	$T_p[s]$	$T_m[s]$	$\theta_m[deg]$	$\sigma_\theta[deg]$
[730]	2.98	13.77	10.96	318.9	5

Buoy B					
Time $[min]$	$H_s[m]$	$T_p[s]$	$T_m[s]$	$\theta_m[deg]$	$\sigma_\theta[deg]$
730	2.358	15.77	8.64	331.875	32.345
Buoy B - SWAN					
Run [min]	$H_s[m]$	$T_p[s]$	$T_m[s]$	$\theta_m[deg]$	$\sigma_\theta[deg]$
[730]	2.454	13.77	10.82	315.9	4.8

Buoy C					
Time $[min]$	$H_s[m]$	$T_p[s]$	$T_m[s]$	$\theta_m[deg]$	$\sigma_\theta[deg]$
730	1.069	15.53	4.25	296.02	56.25
Buoy C - SWAN					
Run [min]	$H_s[m]$	$T_p[s]$	$T_m[s]$	$\theta_m[deg]$	$\sigma_\theta[deg]$
[730]	0.8	13.77	11.85	289.8	5.15

02 January 2019 14:40

Boundary input					
Run [min]	$H_s[m]$	$T_p[s]$	$\theta_m[deg]$	$power"m"$	$\sigma_\theta[deg]$
[3760]	2.47	7.77	334	5	22.9

Buoy D					
Time $[min]$	$H_s[m]$	$T_p[s]$	$T_m[s]$	$\theta_m[deg]$	$\sigma_\theta[deg]$
3760	2.0654	7.764	5.957	333.98	21.094
Buoy D - SWAN					
Run [min]	$H_s[m]$	$T_p[s]$	$T_m[s]$	$\theta_m[deg]$	$\sigma_\theta[deg]$
[3760]	2.19	7.925	6.21	325.9	15.93

Buoy A					
Time $[min]$	$H_s[m]$	$T_p[s]$	$T_m[s]$	$\theta_m[deg]$	$\sigma_\theta[deg]$
3760	1.35	7.715	6.152	341.02	15.47
Buoy A - SWAN					
Run [min]	$H_s[m]$	$T_p[s]$	$T_m[s]$	$\theta_m[deg]$	$\sigma_\theta[deg]$
[3760]	0.994	7.57	6.06	319.12	5.38

Buoy B					
Time $[min]$	$H_s[m]$	$T_p[s]$	$T_m[s]$	$\theta_m[deg]$	$\sigma_\theta[deg]$
3760	0.747	7.129	6.104	327.76	7.03
Buoy B - SWAN					
Run [min]	$H_s[m]$	$T_p[s]$	$T_m[s]$	$\theta_m[deg]$	$\sigma_\theta[deg]$
[3760]	0.825	7.57	6.02	316.31	5.11

Buoy C					
Time $[min]$	$H_s[m]$	$T_p[s]$	$T_m[s]$	$\theta_m[deg]$	$\sigma_\theta[deg]$
3760	0.22	8.45	5.42	294.61	28.125
Buoy C - SWAN					
Run [min]	$H_s[m]$	$T_p[s]$	$T_m[s]$	$\theta_m[deg]$	$\sigma_\theta[deg]$
[3760]	0.2	7.924	6.06	292.49	5.27

12 January 2019 07:00

Boundary input					
Run [min]	$H_s[m]$	$T_p[s]$	$\theta_m[deg]$	$power"m"$	$\sigma_\theta[deg]$
[19140]	6.11	13.5	330	6	21.2

Buoy D					
Time $[min]$	$H_s[m]$	$T_p[s]$	$T_m[s]$	$\theta_m[deg]$	$\sigma_\theta[deg]$
19140	5.61	13.48	9.62	320	20.39
Buoy D - SWAN					
Run [min]	$H_s[m]$	$T_p[s]$	$T_m[s]$	$\theta_m[deg]$	$\sigma_\theta[deg]$
[19140]	5.73	13.15	11.04	333	17.70

Buoy A					
Time $[min]$	$H_s[m]$	$T_p[s]$	$T_m[s]$	$\theta_m[deg]$	$\sigma_\theta[deg]$
19140	3.25	13.48	7.76	335	28.3
Buoy A - SWAN					
Run [min]	$H_s[m]$	$T_p[s]$	$T_m[s]$	$\theta_m[deg]$	$\sigma_\theta[deg]$
[19140]	2.91	13.15	10.42	325	7.65

Buoy B					
Time $[min]$	$H_s[m]$	$T_p[s]$	$T_m[s]$	$\theta_m[deg]$	$\sigma_\theta[deg]$
19140	0.015	24.95	18.60	304	46.41
Buoy B - SWAN					
Run [min]	$H_s[m]$	$T_p[s]$	$T_m[s]$	$\theta_m[deg]$	$\sigma_\theta[deg]$
[19140]	1.58	13.15	10.13	317	5.62

Buoy C					
Time $[min]$	$H_s[m]$	$T_p[s]$	$T_m[s]$	$\theta_m[deg]$	$\sigma_\theta[deg]$
19140	0.98	13.82	3.71	289	52.03
Buoy C - SWAN					
Run [min]	$H_s[m]$	$T_p[s]$	$T_m[s]$	$\theta_m[deg]$	$\sigma_\theta[deg]$
[19140]	0.54	13.15	10.82	291	6.12

The tables above contains the boundary input, real buoy data and the SWAN simulations results corresponding to the four buoys. When we look closely at the values, we can notice that the results for the significant wave height are somewhat satisfactional for most cases, other than the buoy A. The reason for it might be due to the lack of the wave boundary east of Godøya or simply due to no inclusion of the wind and currents, which is more likely.

The peak wave period do have some large difference for case [730], while it seems to be fine for all the others. The reason for it might be that the set up frequency range [flow] and [fhigh] (mentioned in section 3.2) is misplaced. The other two influences might be the absent wave boundary east of Godøya or the absent wind and current. Nevertheless, these effects do not seem to hold that large of a influence. That is because other cases seem to be mostly alright.

What seems to be off in almost all cases, is the mean wave direction and the directional spreading. This may be caused by several elements. The errors in the mean wave direction might have been caused by placing a wrong input direction at the inlet, it might be caused by the lack of wind and currents, even lack of the other boundary.

The directional spreading vary immensely at all other buoys other than the first one (buoy D). This seems to have the same implications as the mean wave direction.

These are only educated guesses, but a good start for further study.

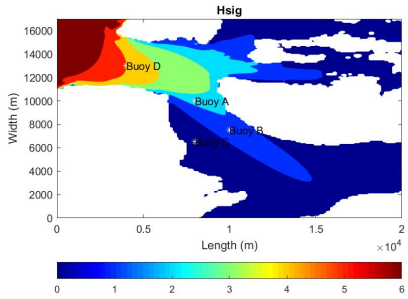

(a) Input H_s = 6.3m and T_p = 11.1s [470]

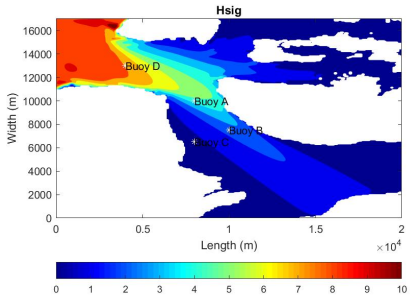

(b) Input H_s = 8.8m and T_p = 14.85s [730]

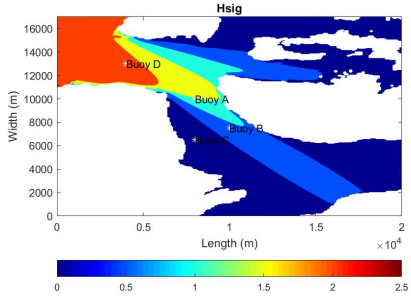

(c) Input H_s = 2.47m and T_p = 7.77s [3760]

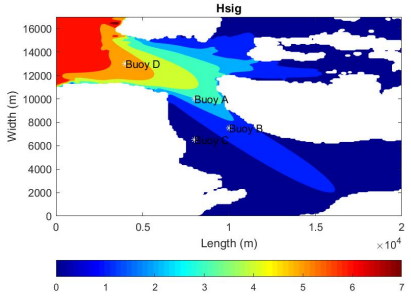

(d) Input H_s = 6.11m and T_p = 13.5s [19140]

Figure 4.3: Plots of the significant wave height for four conditions

4.4.2 Detailed explanation for the second case

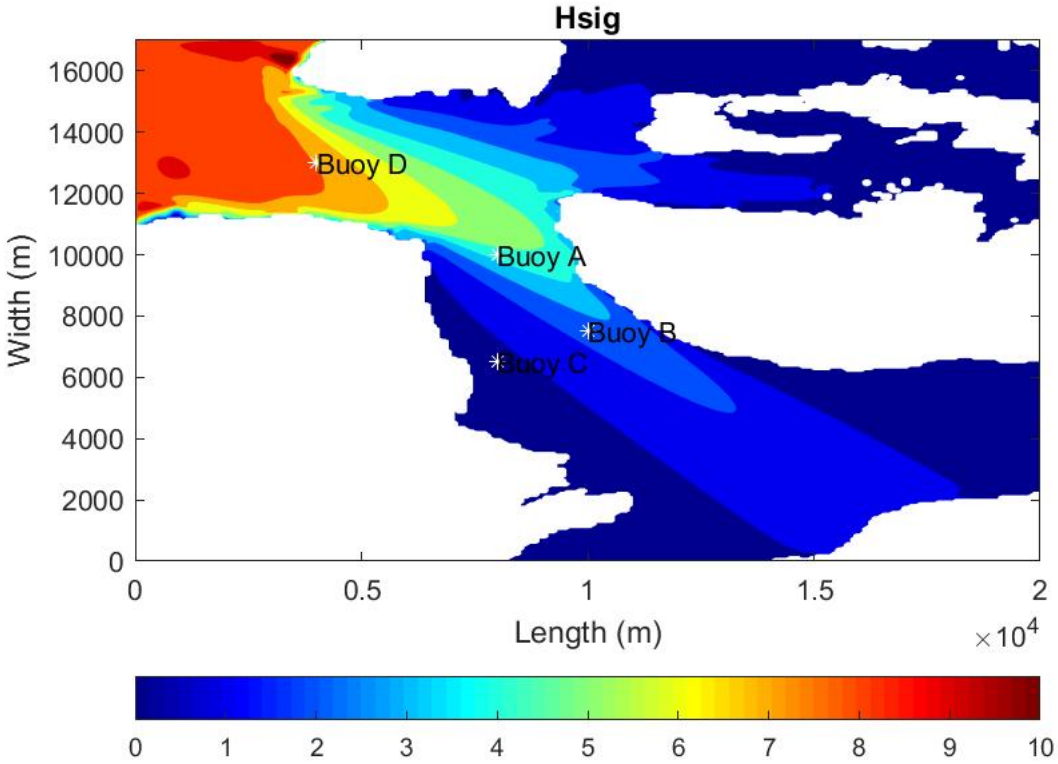

Figure 4.4: Input $H_s = 8.8m$ and $T_p = 14.8s$ [730]

This plot shows how the significant wave height changes throughout the domain of Sulafjorden. The wave height of the waves is significantly reduced from buoy D to Buoy A as the waves pass through Godøya and Hareidlandet and turn southwards toward buoy A.

The wave height continues to decrease rapidly further down Sulafjorden, and even large waves of 6 meters and more are reduced to almost 1 -2 meters inside Sulafjorden. From the plots and the data collected from the buoys we can see that the larger waves propagate inwards along Sula down Sulafjorden, and on the other side of Sulafjorden we get a “Quite zone” around Buoy C, with relatively smaller waves.

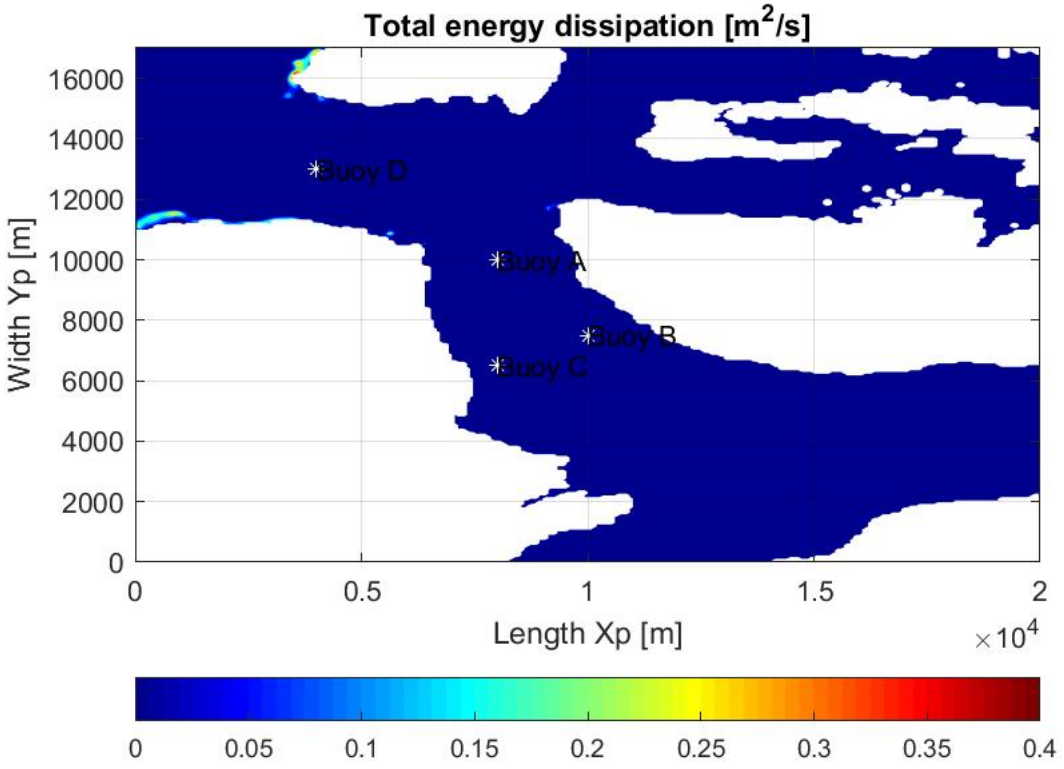

Figure 4.5: Input $H_s = 8.8m$ and $T_p = 14.8s$ [730]

The total energy dissipation plot makes it is possible to locate where wave energy is being dissipated.

SWAN calculates the "Total wave energy dissipation" by adding the effects of wave energy dissipation due to bottom friction, surf breaking, white-capping, and other few less significant effects.

White-capping cannot occur in this simulation because this model did not include any wind and currents. Therefore it could have been turned off for the simulation to spare some memory.

The remaining major dissipative effects are therefore bottom friction and depth-induced wave breaking.

From the significant wave height figure, it is possible to see that large waves of 6 meters and more come in from the sea at the north east corner of the map and are reduced by 1-1,5 meters as the waves meet Godøya and Hareidlandet. That information fits well with the figure 4.5, showing energy being dissipated along the south-west tip of Godøya and at the north part of Hareidlandet.

Figure 4.5 also shows a lot of energy being dissipated at the west side of Godøya. The other noticeable place where the energy dissipate is at the north-west corner of Hareidlandet, and the rest at the north west tip of Sula.

To establish as to why the dissipation occurs particularly at these locations, we can use the wave direction (figure 4.9) and the depth (figure 4.8). Also, with the help of the breaking criterion and the wave steepness (see figure 4.6 and 4.7) we can conclude the main dissipative effect at these locations.

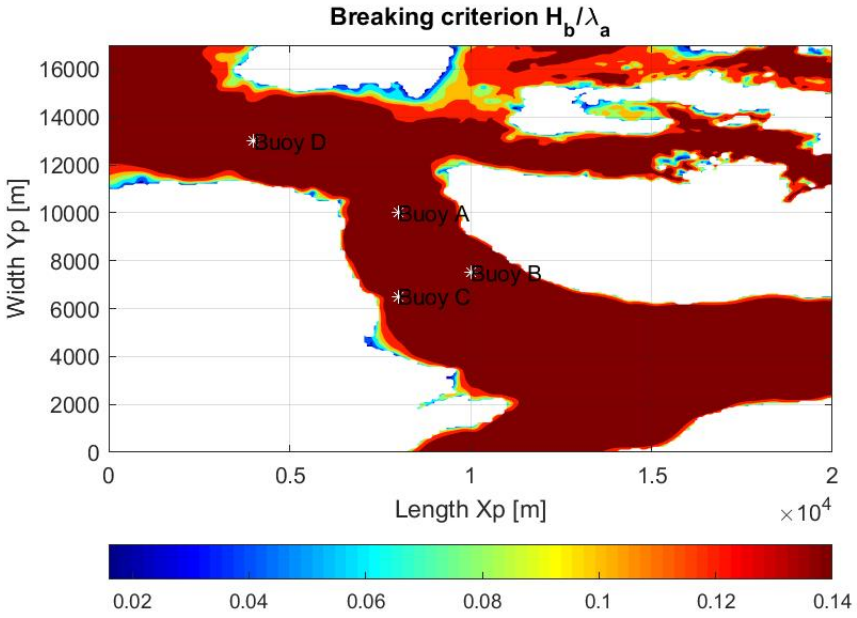

Figure 4.6: Input $H_s = 8.8m$ and $T_p = 14.8s$ [730]

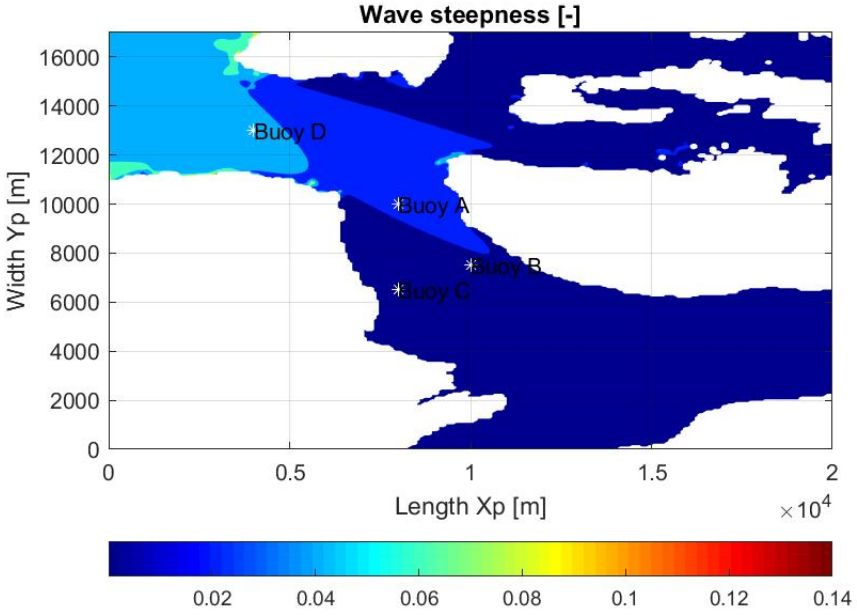

Figure 4.7: Input $H_s = 8.8m$ and $T_p = 14.8s$ [730]

By looking closer at the north west corner of Hareidlandet and the west side of Godøya it can be noticed that the wave steepness is larger or equal to the wave-breaking criterion. This matches well with the information given in the total energy dissipation figure.

While these two are the most exiting, there is still one noticeable dissipative area.

The third spot where the wave steepness is equal or larger than the wave-breaking criterion, is the north-west tip of Sula.

Once again this matches well with the total energy dissipation figure, even though it is much less noticeable.

The major dissipative effect at these three locations is therefore concluded to be caused by the depth-induced breaking. There might be some other places that this occurs, but it is harder to spot.

Lastly, by compering the wave steepness (figure4.7), the wave-breaking criterion (figure 4.6) and the depth (figure 4.8), we might assume what kind of breaking occur at these locations. For certainty, it is usually better to survey these locations.

Unfortunately, SWAN cannot identify for us what kind of breaking happen. For more detailed information see section 3.3.4.

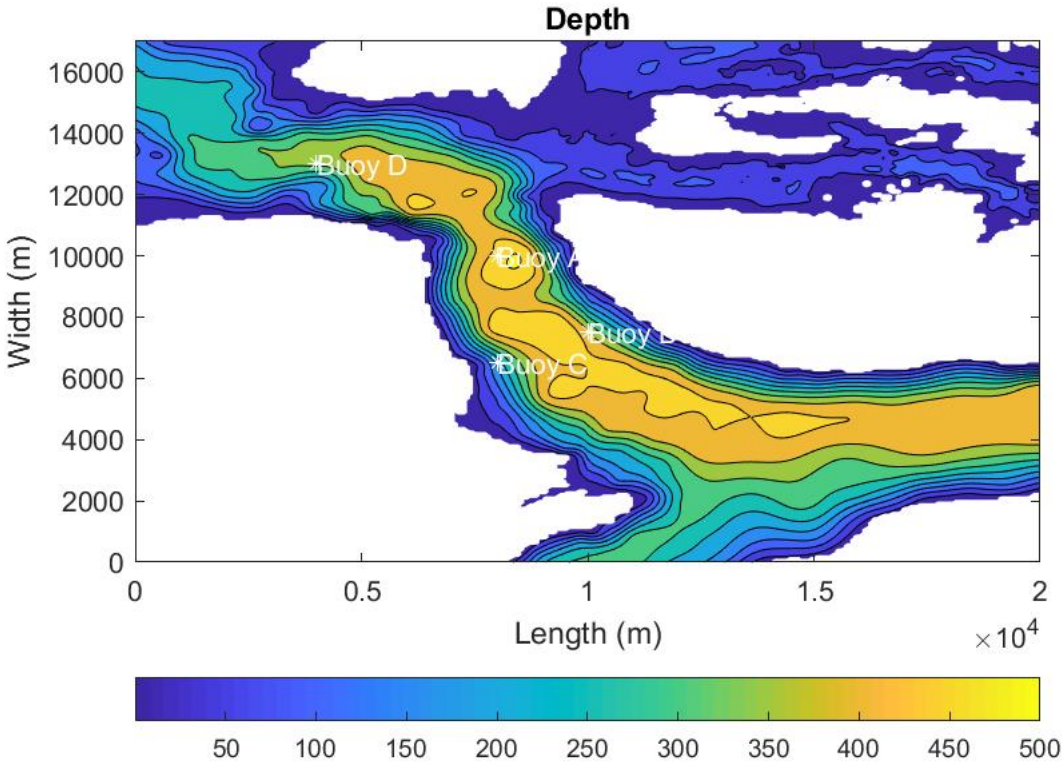

Figure 4.8: Input $H_s = 8.8m$ and $T_p = 14.8s$ [730]

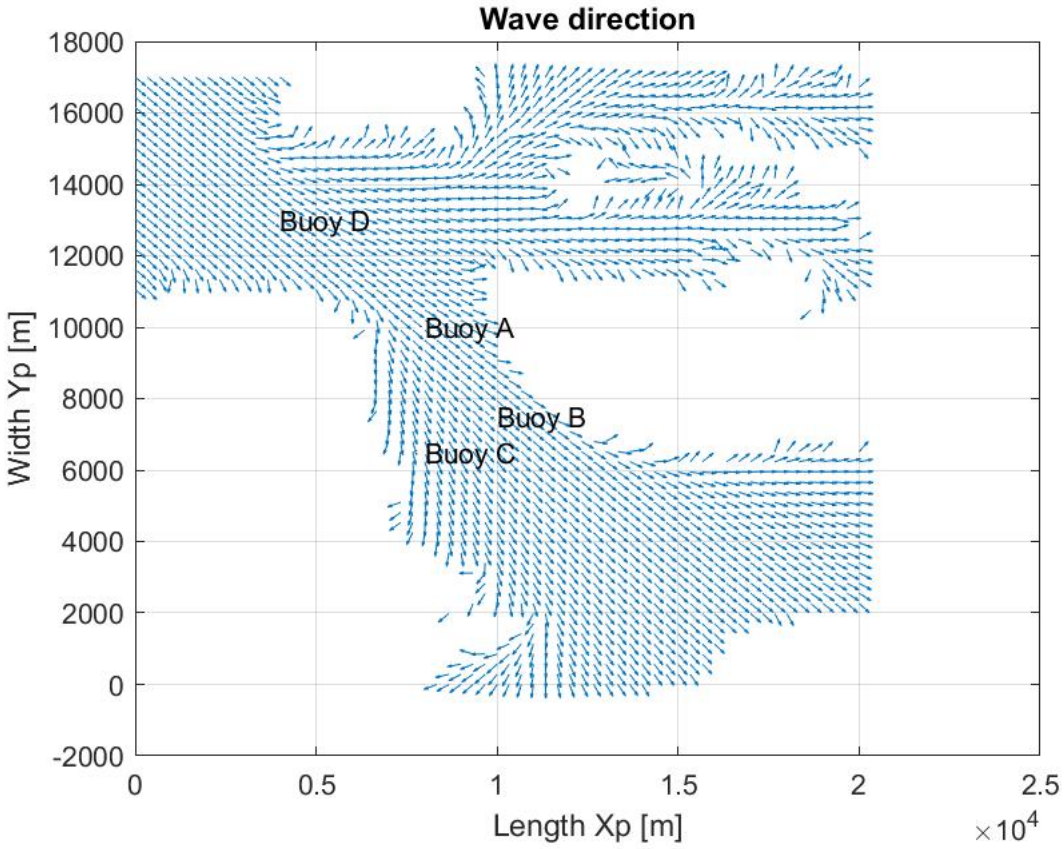

Figure 4.9: Input $H_s = 8.8m$ and $T_p = 14.8s$ [730]

The wave direction plot shows that the waves coming in from the sea are redirected in several directions.

As the waves propagate inwards the fjord between Godøya, Hareidlandet and Sula the wave direction plot show that the waves are redirected towards the islands along the sides. This is explained by the effect of refraction, see section 2.3.2.

One can also expect the effect of focused refraction, which might have caused a higher wave height around the two headlands at the south-west tip of Godøya and the north-west tip of Sula. See section 2.3.2 for more detailed information.

As the waves pass buoy D the water depth suddenly increases from 350 meters to 450 meters. The peak wave length and the mean wave length at these depths looks to be unchanged. This means that the change in depth do not hold a noticeable influence on the wave propagation.

4.5 Simulation conclusion

As stated earlier in the previous chapter a boundary wave propagating from the north around the east side of Godøya was not considered. We did not have much information about this area, and as most waves propagate from the west towards the east it was believed to have little effect on the overall computations. That being said, it is still an error to take into consideration.

What was also absent from the model, was the wind and currents input. The reasoning for this was the time constraints. This is believed to hold the most significance on the results.

If this boundary were to be included, along with the wind and current conditions, this would most likely change the overall direction of the waves propagating in Sulafjorden for the better. Possibly improving the significant wave height in buoy A, which was the only one we had struggle to match with our results. It would also decisively improve the results on the directional spreading.

It is believed that the large amount of dissipation at these specific locations is partially because of the bathymetry and the effect of refraction, but mainly because of the initial wave direction. It is also worth noticing that at the west side of Godøya and nort-west corner of Hareidlandet, the high dissipation shown on the plot could also be influenced by the fact that the wave boundary spans from the left up-most corner of the domain to the land for both boundaries.

Due the the lack of the wind, the effects like white-capping and quadruplet wave-wave interactions are also removed. This made it that the remaining two major dissipative effects where the bottom friction and the depth-induced wave breaking, where the latter one is the dominating.

We are quite happy with the results. The values of the significant wave height in almost all cases were satisfactional.

Due to the absent wind, the returned values of the directional spreading were wildly below the buoy data. That is not the case for the buoy D.

The variation in the mean wave direction is believed to be also caused by the lack of wind, but mostly due to the wrong input.

Chapter 5

Conclusion

The first part of this report, briefly explains the basic theories of waves in coastal areas, where it covers the theory of shoaling, refraction, diffraction and depth-induced wave breaking. The purpose of this was to give a brief explanation of the phenomenal occurring at coastal areas, before proceeding further.

The second part of this paper takes the theory from the first part and presents them in SWAN. This is where shoaling, diffraction, depth-induced wave breaking and wave spectrum that are presented in SWAN.

In the section dedicated to the shoaling, there has been shown the effects of wave-induced setup and setdown, and concluded that this effect is more noticeable on larger seabed slopes. Unfortunately, there was no time to further explore its influence and how to handle it in SWAN.

In the section dedicated to refraction it was covered how the wave direction changes in shallow water due to the change of phase speed along the wave crest. After running some simulations in SWAN we could clearly see the change of wave direction as an effect of refraction according to what could be expected.

In the section dedicated to diffraction, it has been concluded that SWAN can only calculate estimates of diffraction, and only in areas where there are no sever reflection or not in closed areas like harbours.

The section dedicated to the depth-induced wave breaking, covers the three main types of breaking (spilling, plunging and surging) and holds a brief mention of collapsing wave breaking. The reasoning for this was that SWAN cannot identify what kind of breaking that is occurring, and since collapsing breaking is somewhat in between a plunging and surging breaking, it became irrelevant.

The conclusion is that the waves for a plunging breaking do seem to break around when its steepness exceed the breaking criterion, which matches with the evolution of the significant wave height for the respected case. The waves in a spilling breaking do not break, but instead lose its energy while propagating, which satisfies the theory. The surging breaking seems to reflect most of its energy while not breaking like in plunging. Nevertheless, mistakes were made when modelling the slopes for most of these cases. They do not take anything away from the results.

When Sulafjord was considered, we wanted to include both wind and currents, but due to time constraints they needed to be scrapped. This was unfortunate since it showed that the results other than the significant wave height were significantly worse

without the inclusion of winds and currents.

With the removal of wind, few physical effects have been removed aswell due to them being influenced mostly be wind. This led to the two main remaining dissipative effects being bottom friction and surf breaking.

The numerical results from SWAN at the locations of the buoys are influenced by few objects, where the most significant is believed to be the lack of wind and currents.

The total energy dissipation was concentrated mainly at two points, with a faint one at tip of Sula. The main cause of it is due to the initial wave direction and refraction. As for the main dissipative effect, it is the surf breaking.

In addition there were few chosen time frames where the buoy data were erroneous. This was found out after conducting many simulations.

SWAN seems to return good values, even though many simplifications had been made. Which, with little information SWAN delivers a lot of good values very fast. For certainty, more cases needs to be developed, which included all of the remaining effects, but mainly winds and currents.

Refleksjonsnotat (10009)

Hensikten med oppgaven (som nevnt flere ganger) var å finne hvor bra er SWAN i arbeidet sitt. For dette trengte vi først å fremst å lære seg å bruke programmet. Dette viste seg til å være problematisk, siden det var en stor mangel av enkel litteratur å lese seg gjennom. Alt på dette tidspunktet (og mange fortsatt er det) var mye vanskeligere enn det jeg hadde forventet. Om jeg kunne komme tilbake til oppgaven, så ville jeg ha revidert hele først måneden. Den var ganske arbeidsomt, men ofte viste seg å være irrelevant for oppgaven.

Som i mange gode prosjekter blir man lei av å jobbe med det samme, frustrert over at ingenting vil virke og alt er for vanskelig. I god tidspunkt hadde Karl Henning Halse og Henry Piehl gitt oss gode råd, og derfra alt har blitt klarere. Utfordringen var fortsatt der, kanskje mer enn før, men nå hadde vi noe fundamenter.

Jeg har lært ganske mye om oseanografi, om SWAN, om MATLAB, ledelse og samarbeid. Forhåpentligvis, har oppgaven ikke for mangle feil i teorien og om av det vi konkluderte gir meining til en profesjonell leseren. Oppgaven var ikke det jeg hadde forventet, men på denne tidspunktet viste jeg ikke helt selv. Jeg tenkte å ha en oppgave som vil gi meg en god utfordring og denne oppgaven hadde klart det. Nå som jeg er ferdig med hovedoppgaven, så vil jeg bare ferdiglegge SWAN ved å skrive et veilednings dokument og deretter jobbe med nye prosjekter.

Dette har vert et eventyr som jeg har ikke lyst å gjenoppleve, denne oppgaven har tatt over hele livet mitt og jeg vil ikke at dette skal skje på samme nivå igjen.

Med dette forferdelige refleksjonsnotatet vil jeg avslutte tre-års utdanning på denne universitetet, og at jeg hadde klart å komme meg gjennom den overraskende med gode karakterer. Takk for meg.

Refleksjonsnotat (10020)

Hensikten med denne bacheloren var å teste hvor godt og hvor hensiktsmessig SWAN var til å simulere bølger nær kysten. Målet var å kjøre simuleringer for Sulafjorden hvor Statensvegvesen sammen med Runde miljøsenter har over en lengere periode gjort målinger på bølger ved hjelp av målebøyer.

Det var i starten av prosjektet utrolig mye å sette seg inn i. Flere nye programmer å lære seg og sette seg inn, og det var til tider veldig vanskelig å finne god informasjon og hjelp til disse. Takket være 2 meget hjelpsomme og dyktige veiledere på feltet, Karl Henning Halse og Henry Piehl kom vi i gang og fikk dannet et viktig fundament for å kunne begynne på selve oppgaven.

Det gikk altså veldig mye tid og arbeid i starten til å lære seg programvaren, hvor mye gikk ut på å prøve og feile.

Det har vært noe tunge perioder, men vi fikk til slutt benyttet programvarer på en god måte og fikk resultater vi er relativt fornøyd med basert på den tiden vi hadde. Et videre steg i arbeidet hadde vært å inkludere utelatte effekter som vind og strøm i simulasjonene.

Gjennom dette prosjektet har jeg fått repetert og lært mye bølgeteori. Jeg har også lært mye om bruken av dataprogrammer som SWAN og MATLAB, og fått en god innsikt i hvordan å programmer, lage kjørbare skript for slike programmer.

Appendix A

Sulafjord

A.1 Numerical results

A.1.1 Boundary input

Run boundary input						
	Run [min]	$H_s[m]$	$T_p[s]$	$\theta_m[deg]$	$power"m"$	$\sigma_\theta[deg]$
1	[470]	6.3	11.1	320	≈2	33.5
2	[730]	8.8	14.85	320	8	18.8
3	[3760]	2.47	7.77	334	5	22.9
4	[19140]	6.11	13.5	330	6	21.2

Table A.1

A.1.2 01 January 2019 between 07:50 - 08:20

Run boundary input					
Run [min]	$H_s[m]$	$T_p[s]$	$\theta_m[deg]$	$power"m"$	$\sigma_\theta[deg]$
[470]	6.3	11.1	320	≈2	33.5

Buoy D					
Time $[min]$	$H_s[m]$	$T_p[s]$	$T_m[s]$	$\theta_m[deg]$	$\sigma_\theta[deg]$
470	5.0	11.04	8.59	319.22	24.61
480	5.11	10.65	8.59	319.92	28.125
490	5.20	11.52	8.89	319.92	25.31
500	5.845	11.13	9.33	320.62	18.99
Buoy D - SWAN					
Run [min]	$H_s[m]$	$T_p[s]$	$T_m[s]$	$\theta_m[deg]$	$\sigma_\theta[deg]$
[470]	5.02	10.94	9.16	332	23.70

Buoy A					
Time $[min]$	$H_s[m]$	$T_p[s]$	$T_m[s]$	$\theta_m[deg]$	$\sigma_\theta[deg]$
470	3.24	9.86	8.11	339.6	13.36
480	3.25	10.89	8.11	337.5	17.58
490	3.5	10.89	8.2	338.9	16.88
500	3.57	11.52	8.2	340.3	16.88
Buoy A - SWAN					
Run [min]	$H_s[m]$	$T_p[s]$	$T_m[s]$	$\theta_m[deg]$	$\sigma_\theta[deg]$
[470]	0.48	10.94	8.92	292	6.08

Buoy B					
Time $[min]$	$H_s[m]$	$T_p[s]$	$T_m[s]$	$\theta_m[deg]$	$\sigma_\theta[deg]$
470	1.25	9.38	5.18	338.2	18.98
480	1.23	9.23	4.88	339.6	25.31
490	1.17	11.23	4.35	335.4	30.24
500	1.19	10.89	4.54	336.1	38.67
Buoy B - SWAN					
Run [min]	$H_s[m]$	$T_p[s]$	$T_m[s]$	$\theta_m[deg]$	$\sigma_\theta[deg]$
[470]	1.44	10.94	8.68	315	5.36

Buoy C					
Time $[min]$	$H_s[m]$	$T_p[s]$	$T_m[s]$	$\theta_m[deg]$	$\sigma_\theta[deg]$
470	1.465	9.67	4.30	291	70.31
480	1.41	3.81	4.15	298	19.69
490	1.27	3.66	3.96	297	21.1
500	1.16	3.66	3.61	296	14.06
Buoy C - SWAN					
Run [min]	$H_s[m]$	$T_p[s]$	$T_m[s]$	$\theta_m[deg]$	$\sigma_\theta[deg]$
[470]	0.48	10.94	8.92	292	6.08

A.1.3 01 January 2019 between 12:10 - 12:40

Run boundary input					
Run [min]	$H_s[m]$	$T_p[s]$	$\theta_m[deg]$	$power"m"$	$\sigma_\theta[deg]$
[730]	8.8	14.85	320	8	18.8

Buoy D					
Time $[min]$	$H_s[m]$	$T_p[s]$	$T_m[s]$	$\theta_m[deg]$	$\sigma_\theta[deg]$
730	8.09	14.844	11.523	318.516	17.58
740	7.588	15.04	11.38	315	22.5
750	6.841	14.844	11.08	312.19	25.31
760	6.826	15.283	10.84	315.7	26.72
Buoy D - SWAN					
Run [min]	$H_s[m]$	$T_p[s]$	$T_m[s]$	$\theta_m[deg]$	$\sigma_\theta[deg]$
[730]	7.95	13.77	11.65	32.16	15.55

Buoy A					
Time $[min]$	$H_s[m]$	$T_p[s]$	$T_m[s]$	$\theta_m[deg]$	$\sigma_\theta[deg]$
730	4.06	15.04	10.45	336.8	10.55
740	4.131	15.04	10.45	336.8	17.58
750	3.93	15.28	9.91	334.69	18.98
760	3.648	15.283	9.473	336.39	24.61
Buoy A - SWAN					
Run [min]	$H_s[m]$	$T_p[s]$	$T_m[s]$	$\theta_m[deg]$	$\sigma_\theta[deg]$
[730]	2.98	13.77	10.96	318.9	5

Buoy B					
Time $[min]$	$H_s[m]$	$T_p[s]$	$T_m[s]$	$\theta_m[deg]$	$\sigma_\theta[deg]$
730	2.358	15.77	8.64	331.875	32.345
740	2.241	15.283	8.936	329.77	17.58
750	2.3	15.283	9.08	331.172	25.313
760	2.183	15.53	8.11	328.36	33.05
Buoy B - SWAN					
Run [min]	$H_s[m]$	$T_p[s]$	$T_m[s]$	$\theta_m[deg]$	$\sigma_\theta[deg]$
[730]	2.454	13.77	10.82	315.9	4.8

Buoy C					
Time $[min]$	$H_s[m]$	$T_p[s]$	$T_m[s]$	$\theta_m[deg]$	$\sigma_\theta[deg]$
730	1.069	15.53	4.25	296.02	56.25
740	1.025	15.77	4.395	300.234	58.36
750	1.055	15.53	4.05	296.02	73.125
760	1.1133	3.418	3.711	290.39	18.28
Buoy C - SWAN					
Run [min]	$H_s[m]$	$T_p[s]$	$T_m[s]$	$\theta_m[deg]$	$\sigma_\theta[deg]$
[730]	0.8	13.77	11.85	289.8	5.15

A.1.4 02 January 2019 between 14:40 - 15:10

Run boundary input					
Run [min]	$H_s[m]$	$T_p[s]$	$\theta_m[deg]$	$power"m"$	$\sigma_\theta[deg]$
[3760]	2.47	7.77	334	5	22.9

Buoy D					
Time $[min]$	$H_s[m]$	$T_p[s]$	$T_m[s]$	$\theta_m[deg]$	$\sigma_\theta[deg]$
3760	2.0654	7.764	5.957	333.98	21.094
3770	2.124	7.715	6.104	329.77	21.8
3780	2.139	7.52	6.06	333.28	23.2
3790	2.153	7.715	6.152	335.39	22.5
Buoy D - SWAN					
Run [min]	$H_s[m]$	$T_p[s]$	$T_m[s]$	$\theta_m[deg]$	$\sigma_\theta[deg]$
[3760]	2.19	7.925	6.21	325.9	15.93

Buoy A					
Time $[min]$	$H_s[m]$	$T_p[s]$	$T_m[s]$	$\theta_m[deg]$	$\sigma_\theta[deg]$
3760	1.35	7.715	6.152	341.02	15.47
3770	1.377	6.836	6.152	341.72	19.69
3780	1.333	8.35	6.152	340.31	16.17
3790	1.333	8.74	6.15	338.9	15.47
Buoy A - SWAN					
Run [min]	$H_s[m]$	$T_p[s]$	$T_m[s]$	$\theta_m[deg]$	$\sigma_\theta[deg]$
[3760]	0.994	7.57	6.06	319.12	5.38

Buoy B					
Time $[min]$	$H_s[m]$	$T_p[s]$	$T_m[s]$	$\theta_m[deg]$	$\sigma_\theta[deg]$
3760	0.747	7.129	6.104	327.76	7.03
3770	0.7617	8.35	6.25	328.36	8.438
3780	0.7617	8.594	6.152	329.77	8.438
3790	0.7471	8.2031	6.0	328.36	8.438
Buoy B - SWAN					
Run [min]	$H_s[m]$	$T_p[s]$	$T_m[s]$	$\theta_m[deg]$	$\sigma_\theta[deg]$
[3760]	0.825	7.57	6.02	316.31	6.11

Buoy C					
Time $[min]$	$H_s[m]$	$T_p[s]$	$T_m[s]$	$\theta_m[deg]$	$\sigma_\theta[deg]$
3760	0.22	8.45	5.42	294.61	28.125
3770	0.2344	8.40	5.32	290.39	27.422
3780	0.2637	8.594	4.980	293.2	26.02
3790	0.264	7.813	4.94	298.83	21.09
Buoy C - SWAN					
Run [min]	$H_s[m]$	$T_p[s]$	$T_m[s]$	$\theta_m[deg]$	$\sigma_\theta[deg]$
[3760]	0.2	5.27	6.06	292.49	5.27

A.1.5 12 January 2019 between 07:00 - 07:30

Run boundary input					
Run [min]	$H_s[m]$	$T_p[s]$	$\theta_m[deg]$	$power"m"$	$\sigma_\theta[deg]$
[19140]	6.11	13.5	330	6	21.2

Buoy D					
Time $[min]$	$H_s[m]$	$T_p[s]$	$T_m[s]$	$\theta_m[deg]$	$\sigma_\theta[deg]$
19140	5.61	13.48	9.62	320	20.39
19150	5.95	12.94	9.77	317	26.72
19160	5.71	11.38	9.33	321	19.28
19170	5.52	14.01	9.42	323	26.72
Buoy D - SWAN					
Run [min]	$H_s[m]$	$T_p[s]$	$T_m[s]$	$\theta_m[deg]$	$\sigma_\theta[deg]$
[19140]	5.73	13.15	11.04	333	17.70

Buoy A					
Time $[min]$	$H_s[m]$	$T_p[s]$	$T_m[s]$	$\theta_m[deg]$	$\sigma_\theta[deg]$
19140	3.25	13.48	7.76	335	28.3
19150	3.22	12.06	8.06	333	22.50
19160	3.22	14.01	8.06	333	13.23
19170	3.05	13.48	7.86	333	34.45
Buoy A - SWAN					
Run [min]	$H_s[m]$	$T_p[s]$	$T_m[s]$	$\theta_m[deg]$	$\sigma_\theta[deg]$
[19140]	2.91	13.15	10.42	325	7.65

Buoy B					
Time $[min]$	$H_s[m]$	$T_p[s]$	$T_m[s]$	$\theta_m[deg]$	$\sigma_\theta[deg]$
19140	0.0147	24.9512	18.6035	304	46.41
19150	0.0147	24.9512	18.6035	304	46.41
19160	0.0147	24.9512	18.6035	304	46.41
219170	0.0147	24.9512	18.6035	304	46.41
Buoy B - SWAN					
Run [min]	$H_s[m]$	$T_p[s]$	$T_m[s]$	$\theta_m[deg]$	$\sigma_\theta[deg]$
[19140]	1.58	13.15	10.13	317	5.62

The buoy B was unfortunately erroneous at the chosen time.

Buoy C					
Time $[min]$	$H_s[m]$	$T_p[s]$	$T_m[s]$	$\theta_m[deg]$	$\sigma_\theta[deg]$
19140	0.98	13.82	3.71	289	52.03
19150	0.98	13.82	3.71	289	52.03
19160	1.03	11.23	3.81	289	50.63
19170	0.95	11.77	3.66	295	46.41
Buoy C - SWAN					
Run [min]	$H_s[m]$	$T_p[s]$	$T_m[s]$	$\theta_m[deg]$	$\sigma_\theta[deg]$
[19140]	0.54	13.15	10.82	291	6.12

A.2 Sulafjord plots

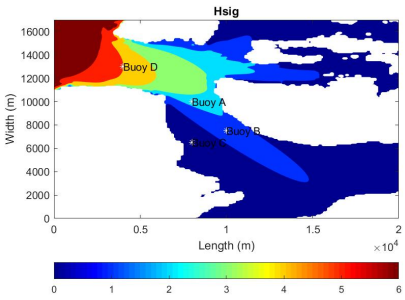

(a) Input H_s = 6.3m and T_p = 11.1s [470]

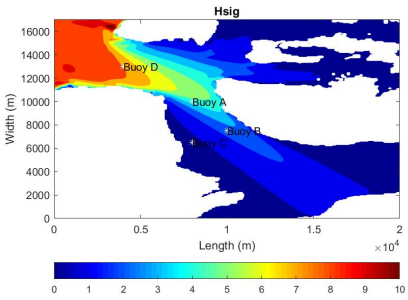

(b) Input H_s = 8.8m and T_p = 14.85s [730]

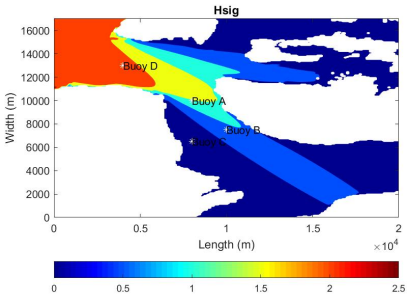

(c) Input H_s = 2.47m and T_p = 7.77s [3760]

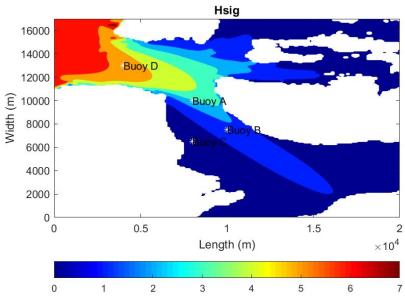

(d) Input H_s = 6.11m and T_p = 13.5s [19140]

Figure A.1: Plots of the significant wave height for four conditions

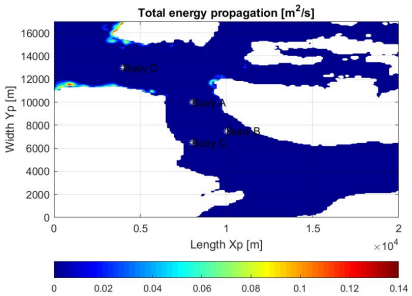

(a) Input H_s = 6.3m and T_p = 11.1s [470 min]

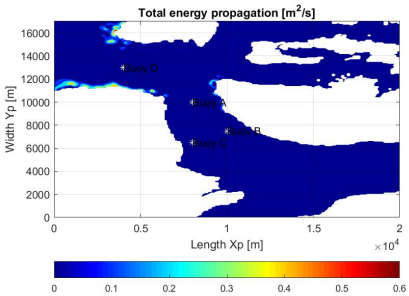

(b) Input H_s = 8.8m and T_p = 14.85s [730 min]

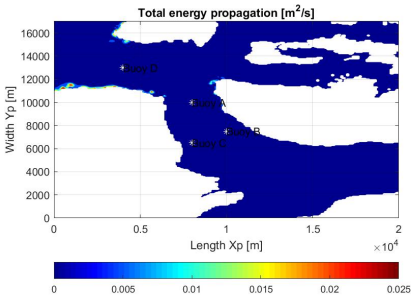

(c) Input H_s = 2.47m and T_p = 7.77s [3760 min]

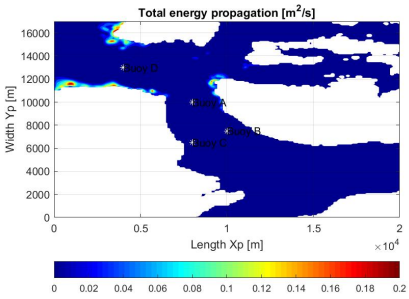

(d) Input H_s = 6.11m and T_p = 13.5s [19140 min]

Figure A.2: Plots of the total energy propagation for four conditions

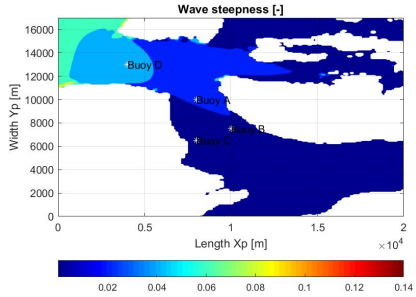

(a) Input H_s = 6.3m and T_p = 11.1s [470 min]

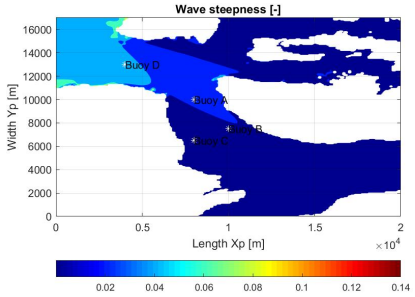

(b) Input H_s = 8.8m and T_p = 14.85s [730 min]

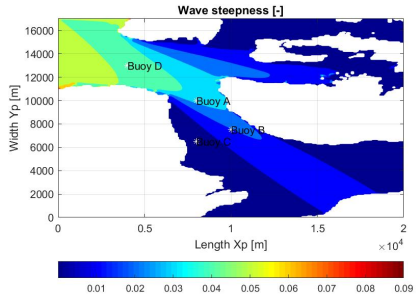

(c) Input H_s = 2.47m and T_p = 7.77s [3760 min]

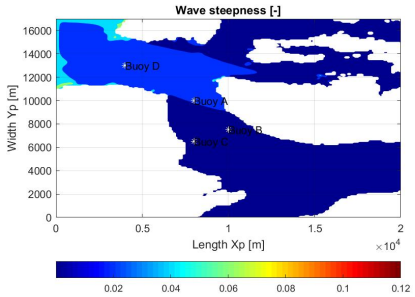

(d) Input H_s = 6.11m and T_p = 13.5s [19140 min]

Figure A.3: Plots of the wave steepness for four conditions

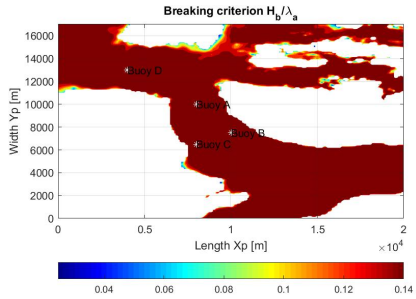

(a) Input H_s = 6.3m and T_p = 11.1s [470 min]

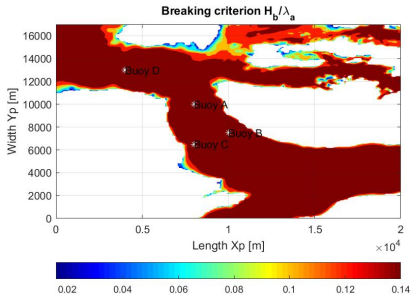

(b) Input H_s = 8.8m and T_p = 14.85s [730 min]

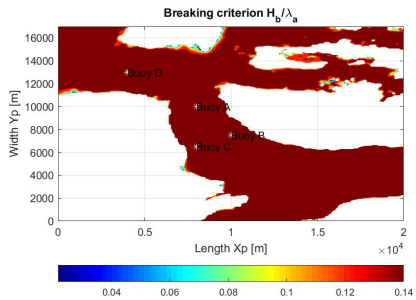

(c) Input H_s = 2.47m and T_p = 7.77s [3760 min]

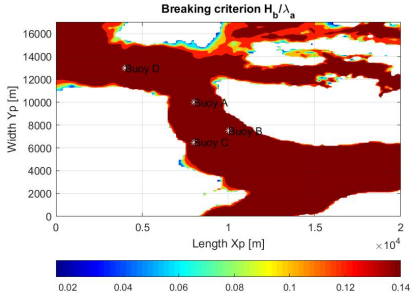

(d) Input H_s = 6.11m and T_p = 13.5s [19140 min]

Figure A.4: Plots of the wave breaking criterion for four conditions

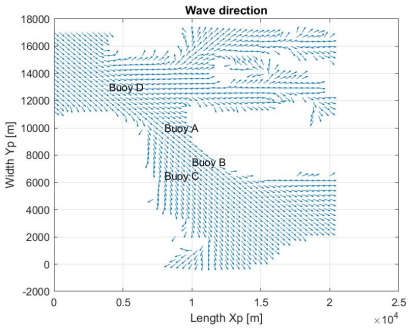

(a) Input H_s = 6.3m and T_p = 11.1s [470 min]

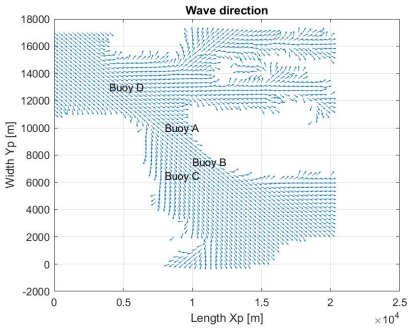

(b) Input H_s = 8.8m and T_p = 14.85s [730 min]

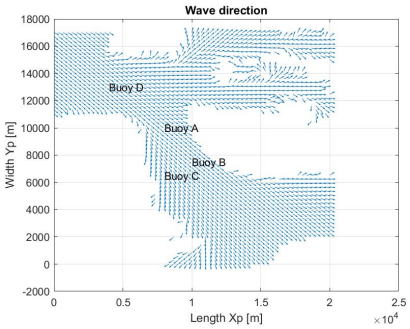

(c) Input H_s = 2.47m and T_p = 7.77s [3760 min]

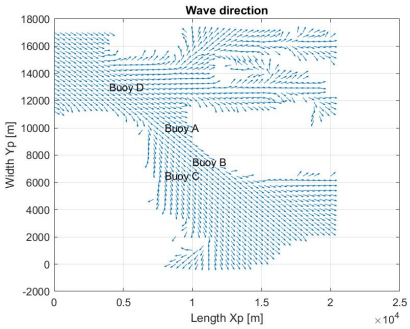

(d) Input H_s = 6.11m and T_p = 13.5s [19140 min]

Figure A.5: Plots of the wave direction for four conditions

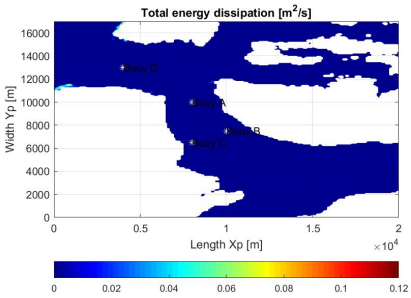

(a) Input H_s = 6.3m and T_p = 11.1s [470 min]

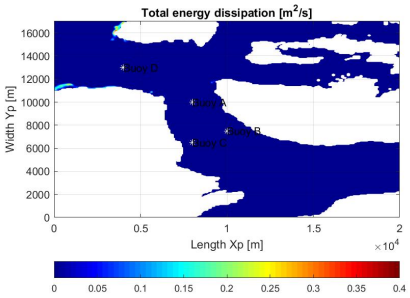

(b) Input H_s = 8.8m and T_p = 14.85s [730 min]

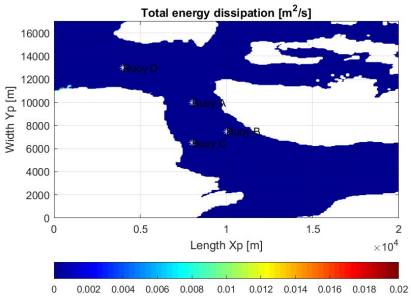

(c) Input H_s = 2.47m and T_p = 7.77s [3760 min]

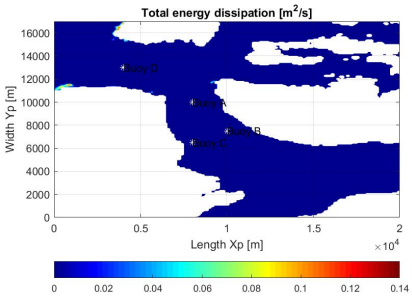

(d) Input H_s = 6.11m and T_p = 13.5s [19140 min]

Figure A.6: Plots of the total energy dissipation for four conditions

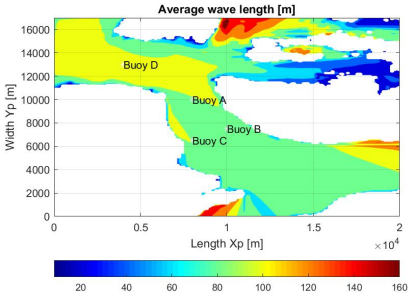

(a) Input H_s = 6.3m and T_p = 11.1s [470 min]

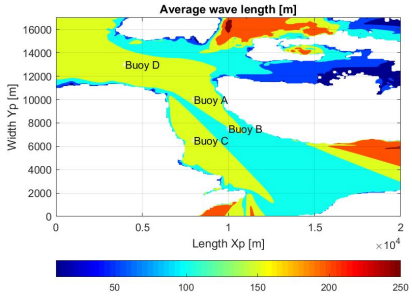

(b) Input H_s = 8.8m and T_p = 14.85s [730 min]

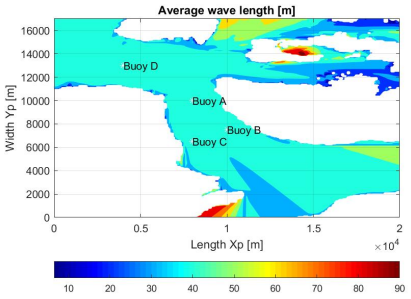

(c) Input H_s = 2.47m and T_p = 7.77s [3760 min]

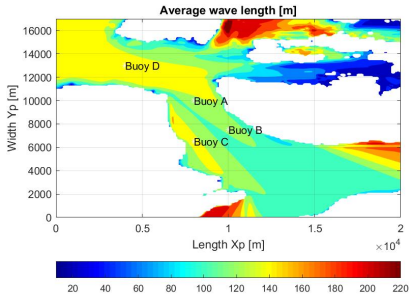

(d) Input H_s = 6.11m and T_p = 13.5s [19140 min]

Figure A.7: Plots of the average wave length for four conditions

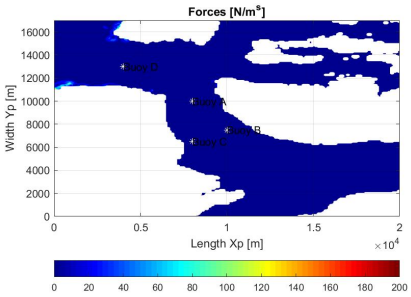

(a) Input H_s = 6.3m and T_p = 11.1s [470 min]

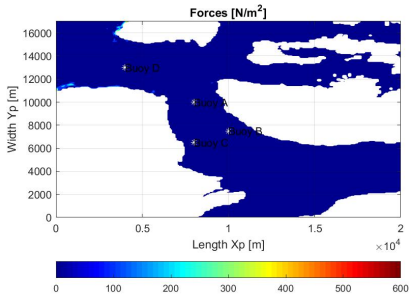

(b) Input H_s = 8.8m and T_p = 14.85s [730 min]

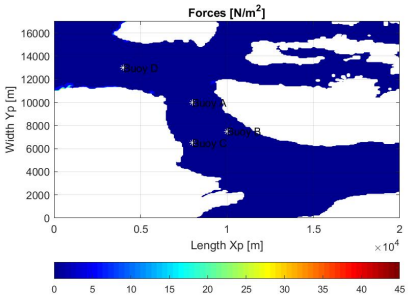

(c) Input H_s = 2.47m and T_p = 7.77s [3760 min]

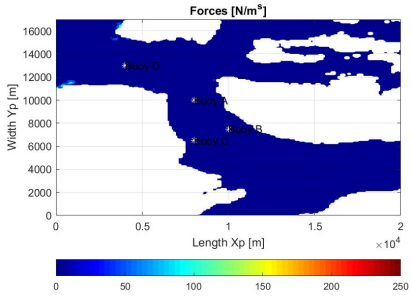

(d) Input H_s = 6.11m and T_p = 13.5s [19140 min]

Figure A.8: Plots of the wave forces for four conditions

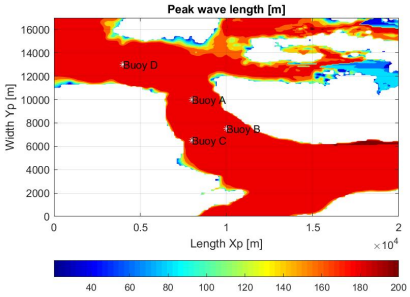

(a) Input H_s = 6.3m and T_p = 11.1s [470 min]

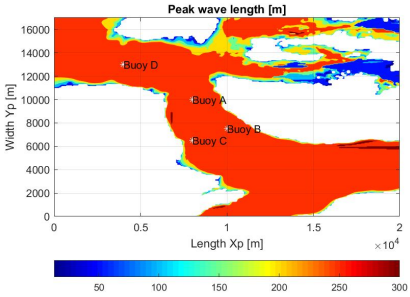

(b) Input H_s = 8.8m and T_p = 14.85s [730 min]

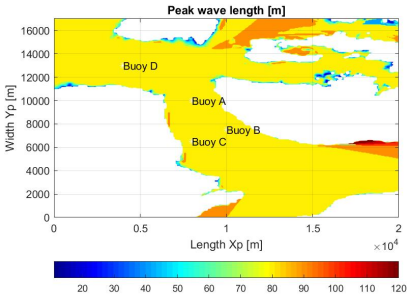

(c) Input H_s = 2.47m and T_p = 7.77s [3760 min]

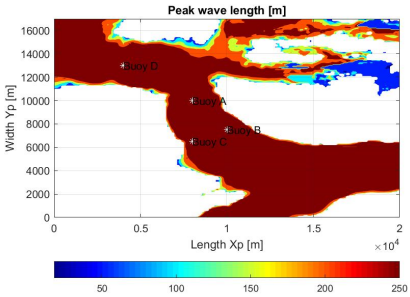

(d) Input H_s = 6.11m and T_p = 13.5s [19140 min]

Figure A.9: Plots of the peak wave length for four conditions

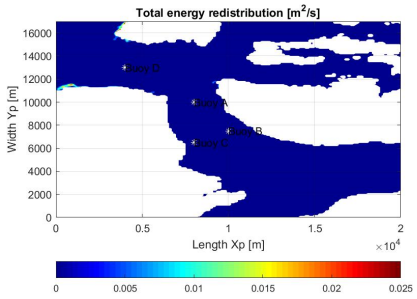

(a) Input H_s = 6.3m and T_p = 11.1s [470 min]

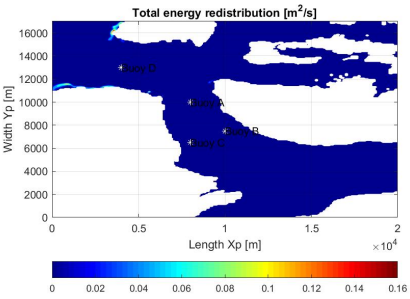

(b) H_s = 8.8m and T_p = 14.85s [730 min]

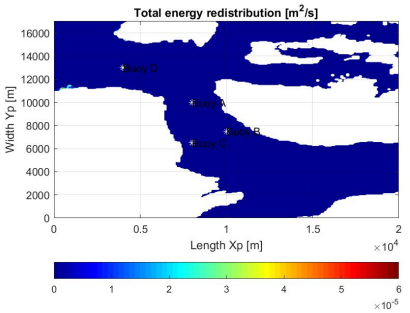

(c) Input H_s = 2.47m and T_p = 7.77s [3760 min]

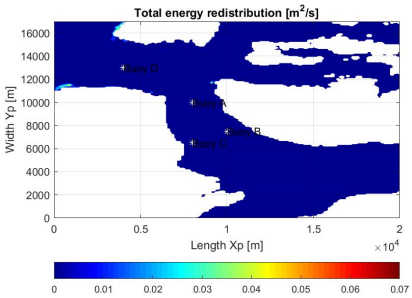

(d) Input H_s = 6.11m and T_p = 13.5s [19140 min]

Figure A.10: Plots of the total energy redistribution for four conditions

A.2.1 Sulafjord 01.01.19 - 07:50 (large)

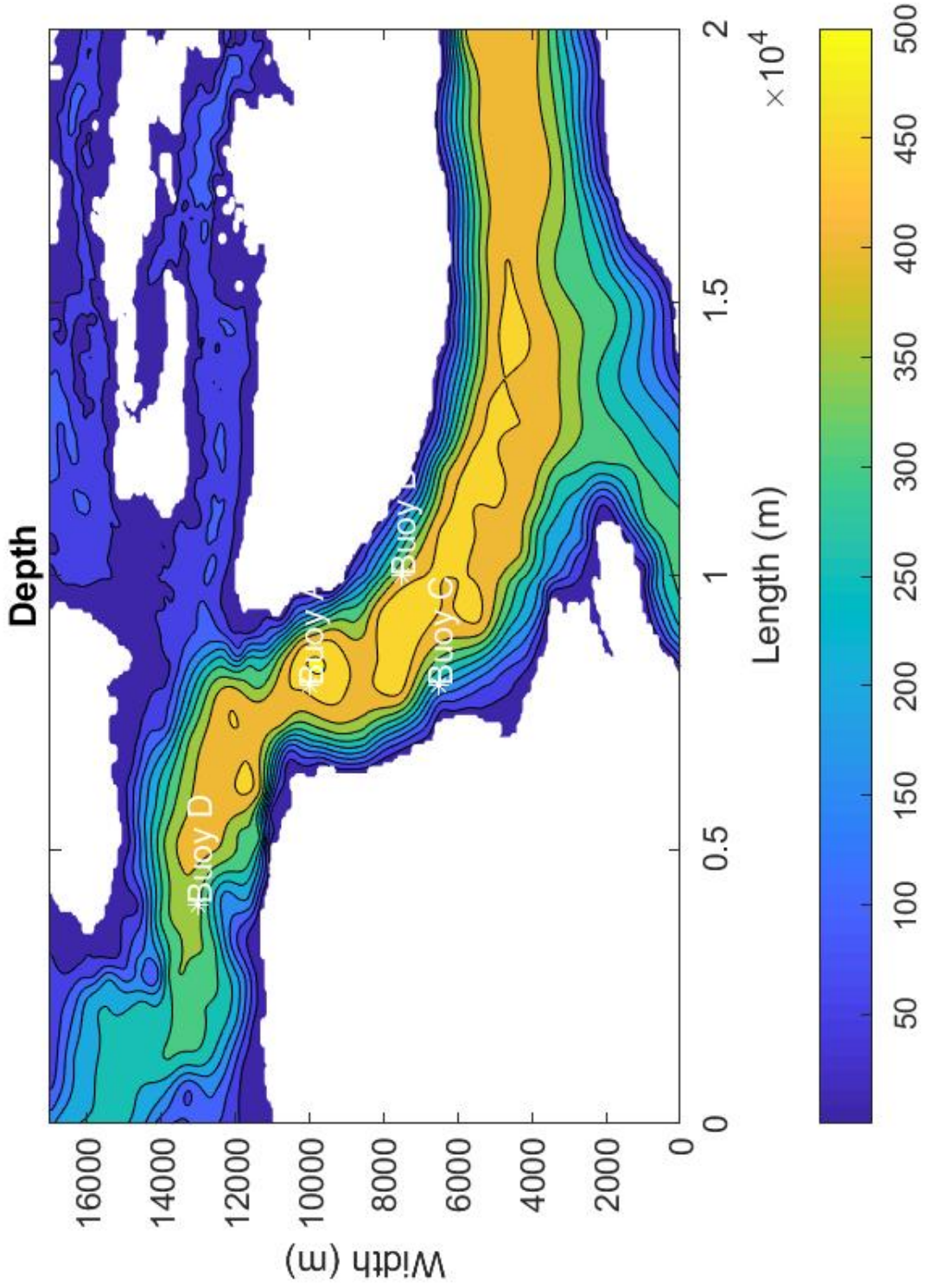

Figure A.11: Depth

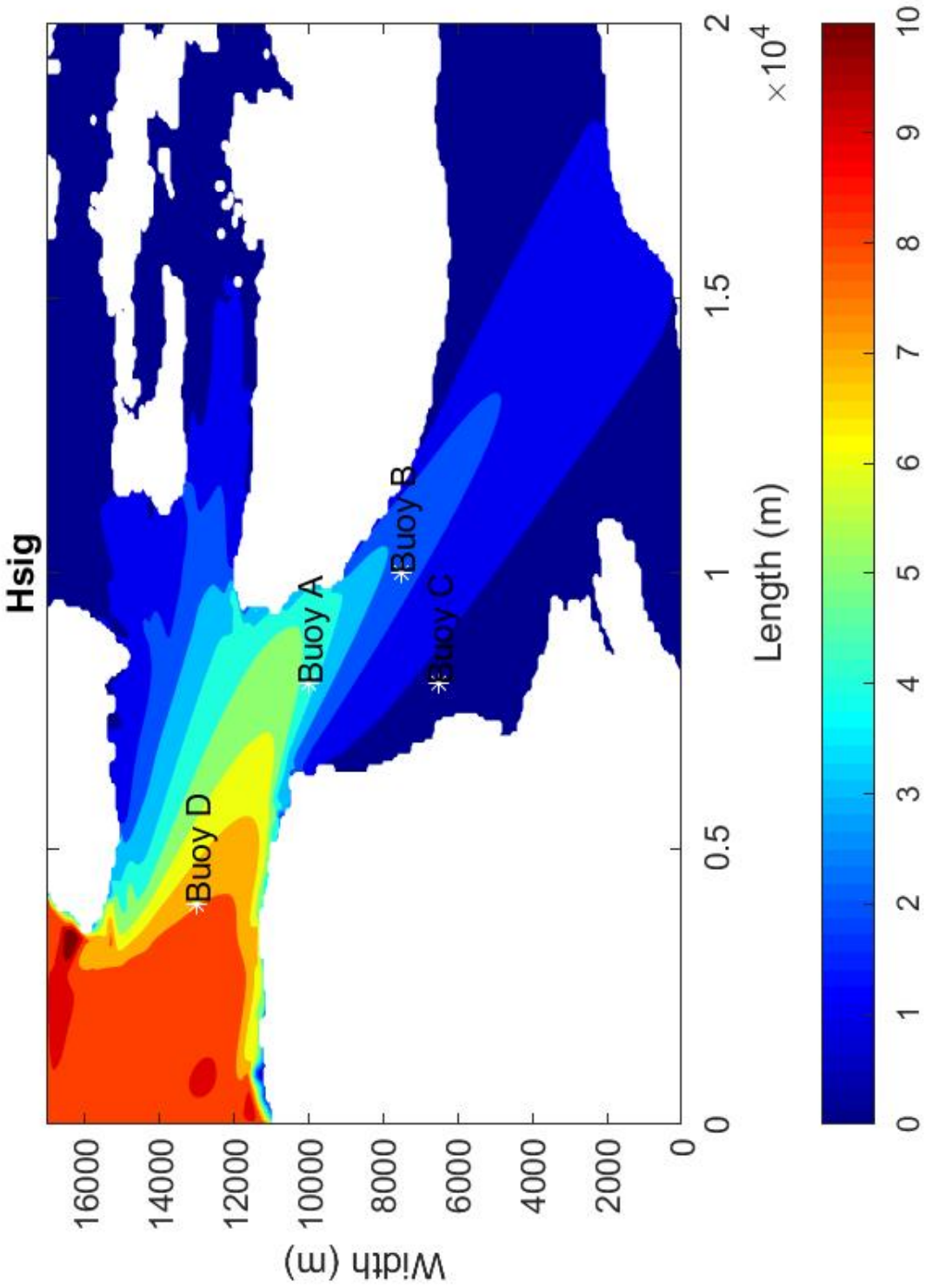

Figure A.12: The significant wave height for 01.01.19 - 07:50

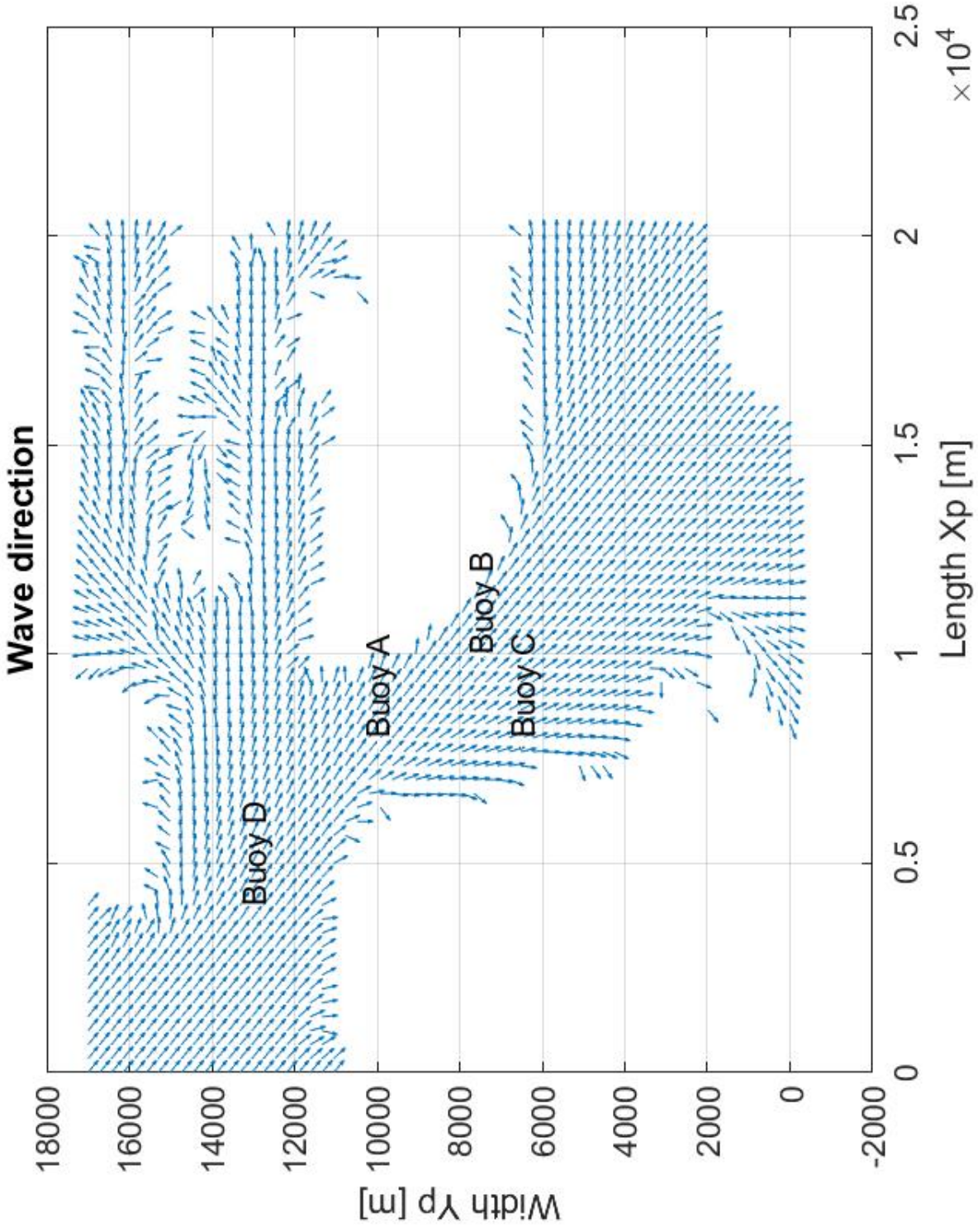

Figure A.13: Mean wave direction for 01.01.19 - 12:10

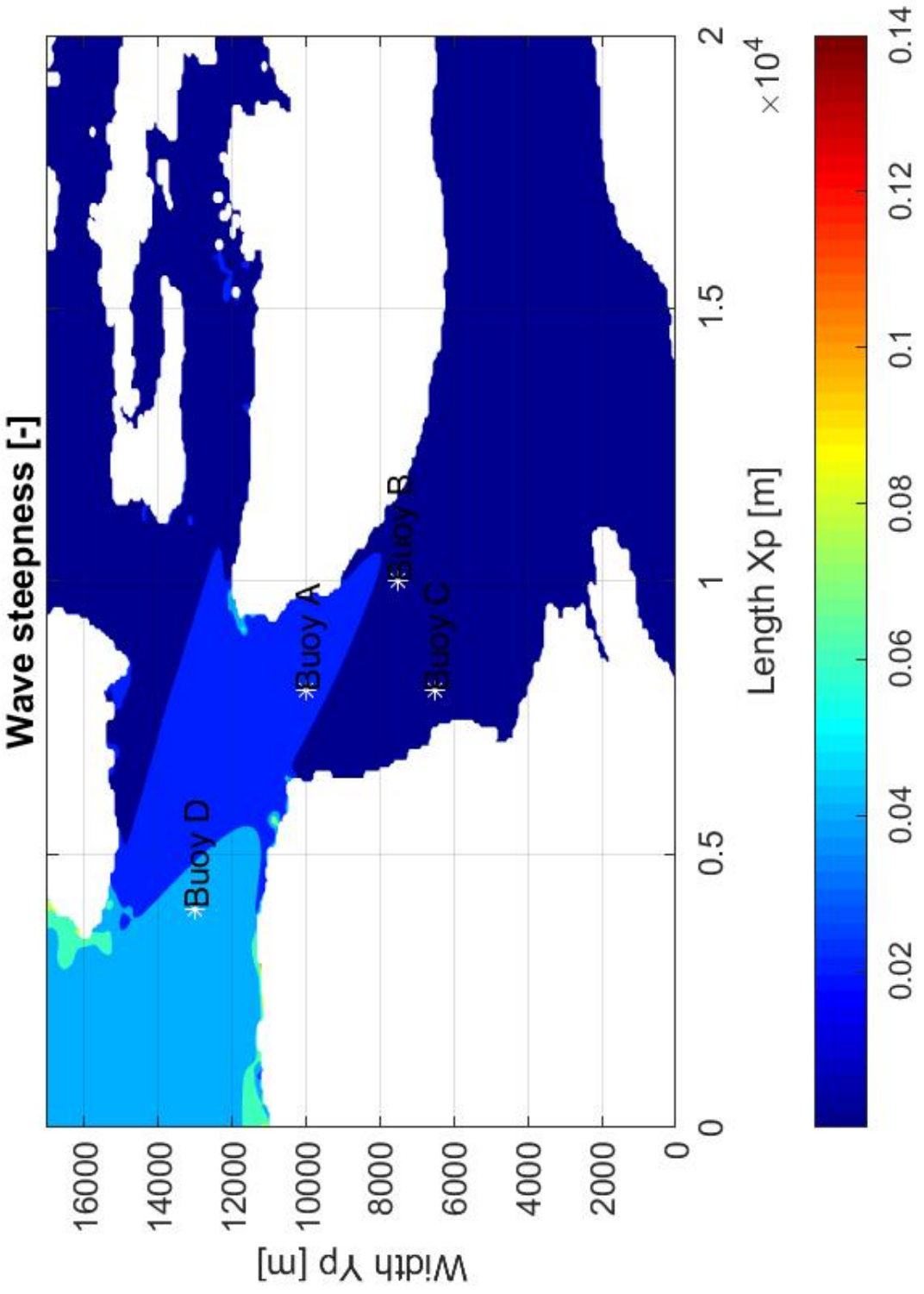

Figure A.14: Mean wave steepness for 01.01.19 - 12:10

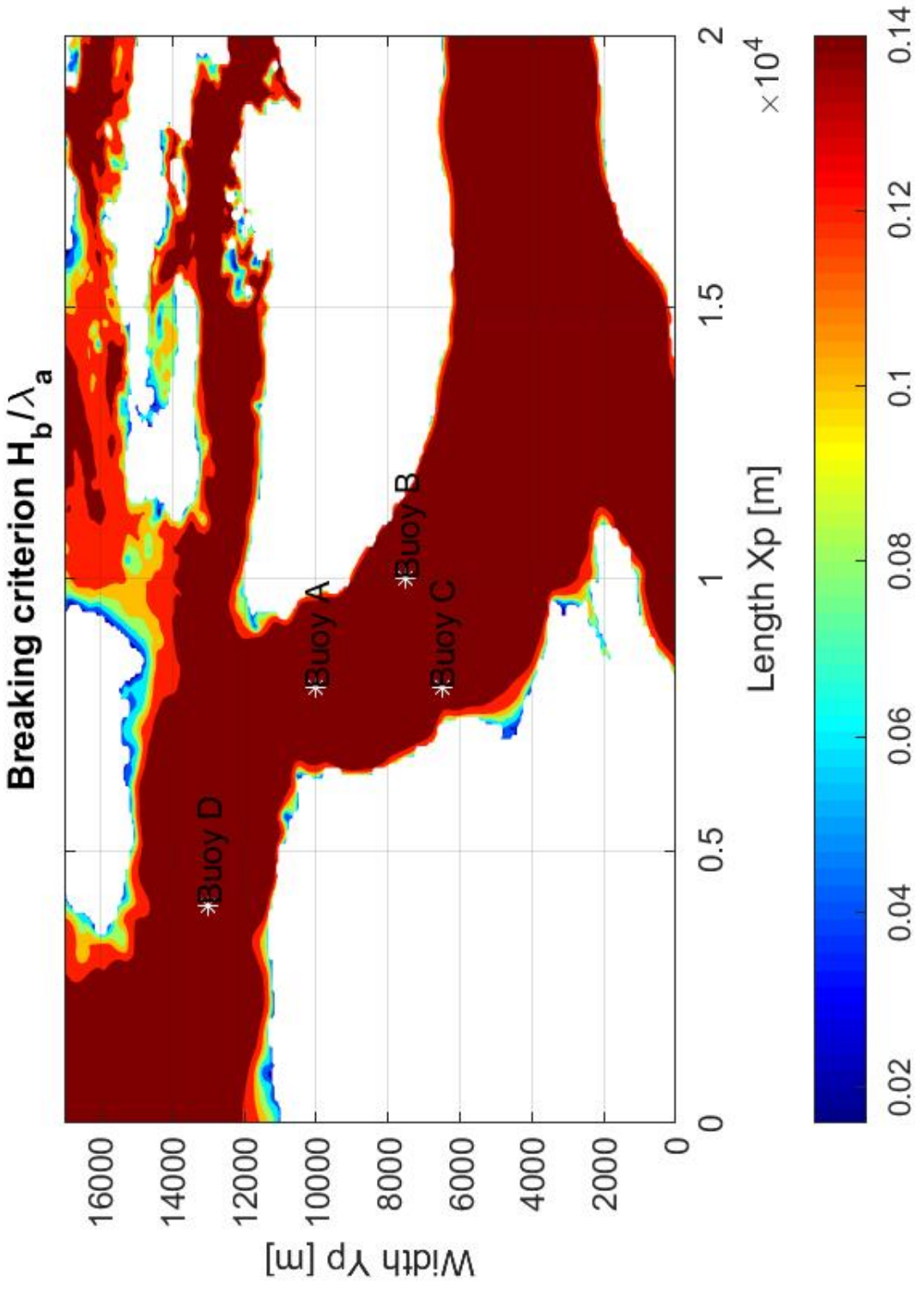

Figure A.15: Breaking criterion for 01.01.19 - 12:10

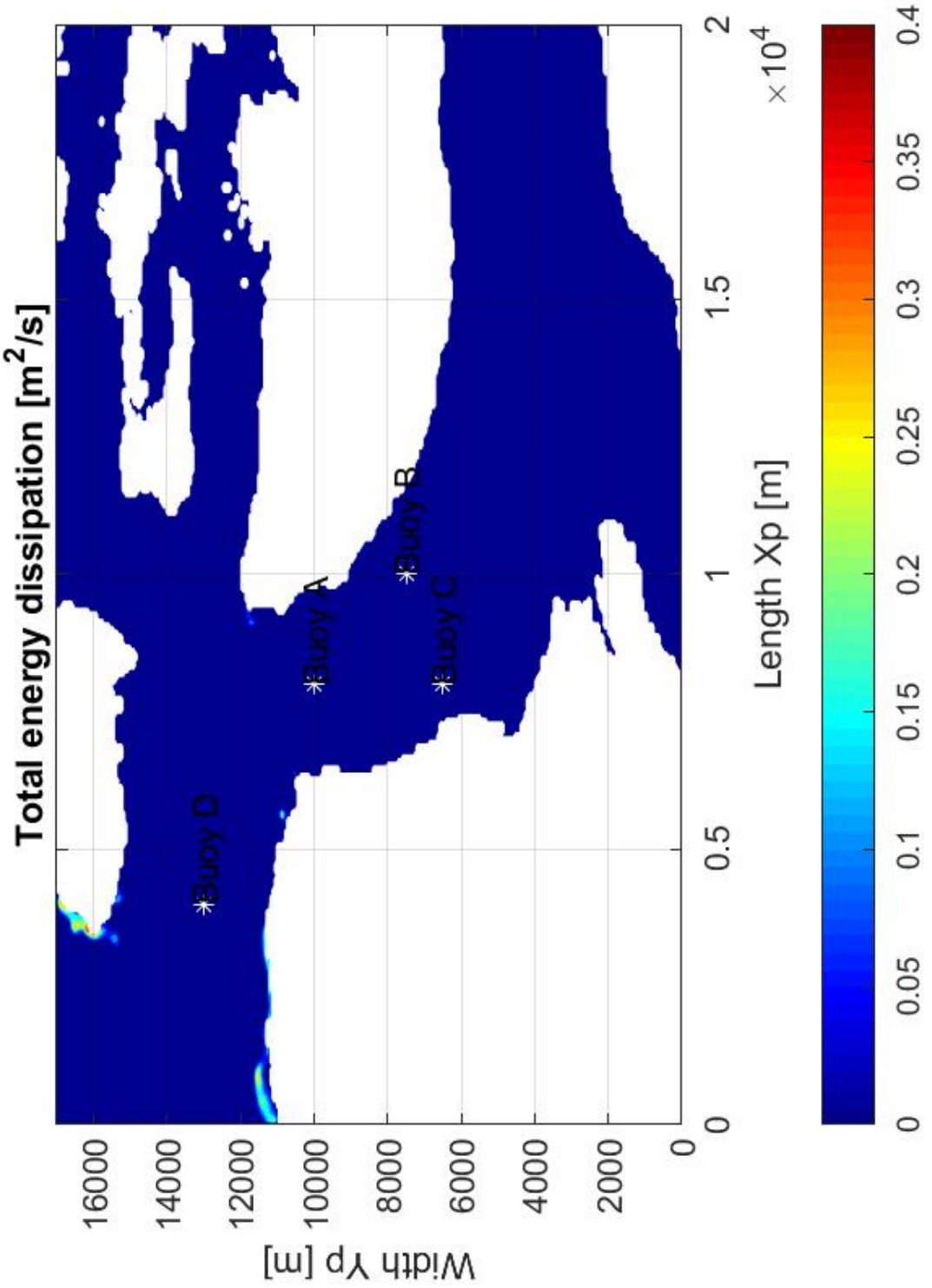

Figure A.16: Total energy dissipation for 01.01.19 - 12:10

Appendix B

Wave data

B.1 Full month

B.1.1 Buoy A

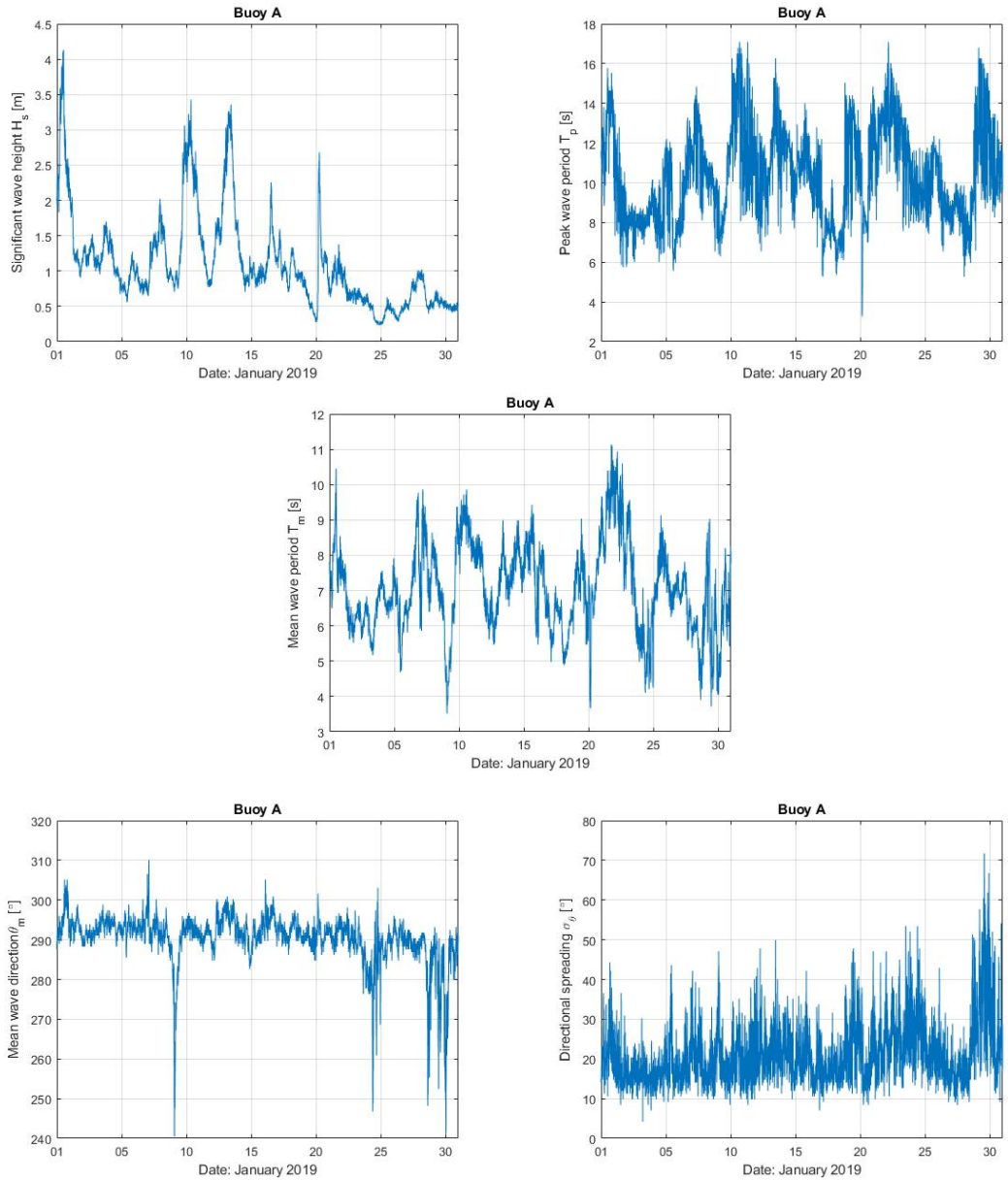

Figure B.1: Buoy A- wave data

B.1.2 Buoy B

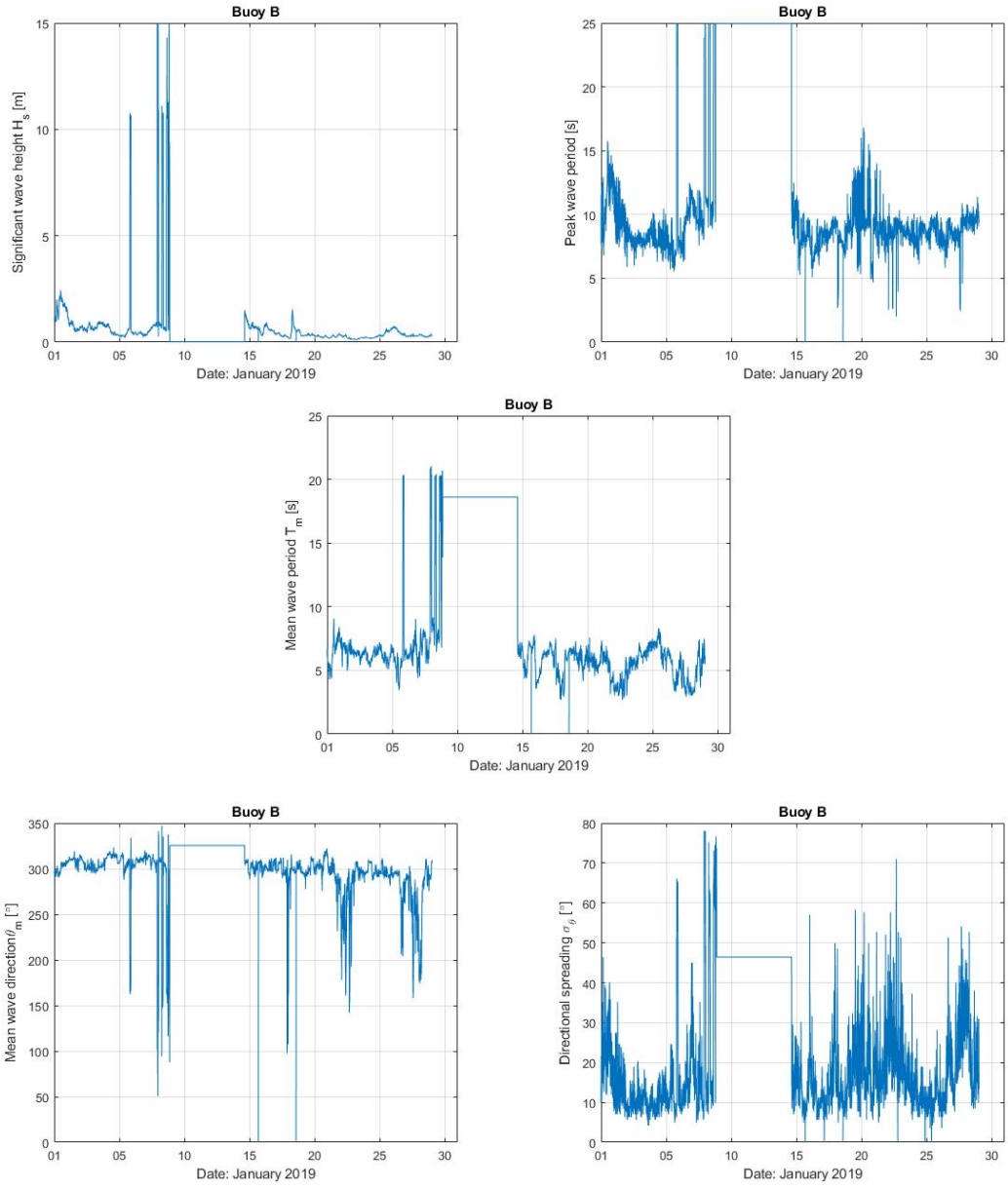

Figure B.2: Buoy B- wave data

B.1.3 Buoy C

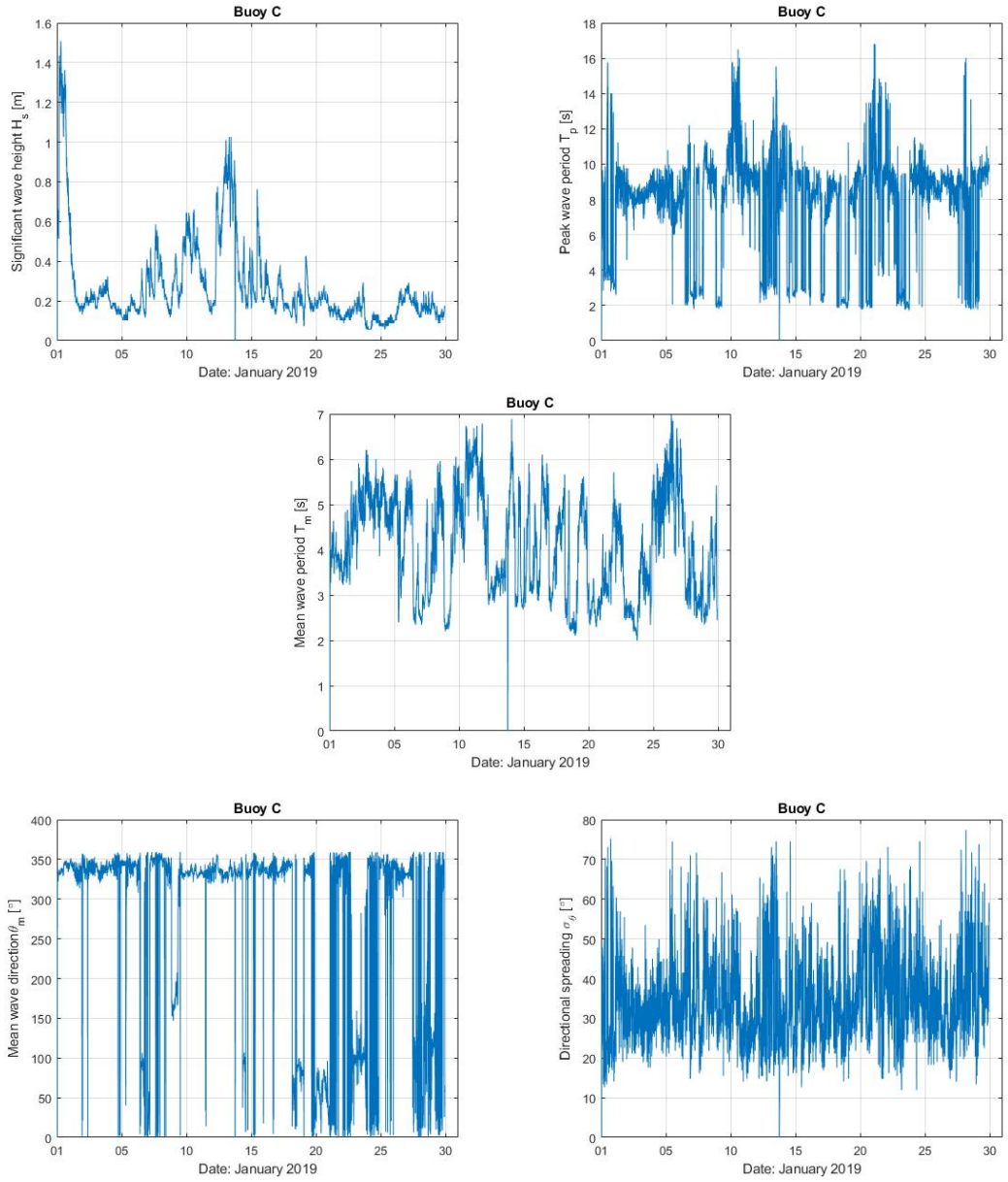

Figure B.3: Buoy C- wave data

B.1.4 Buoy D

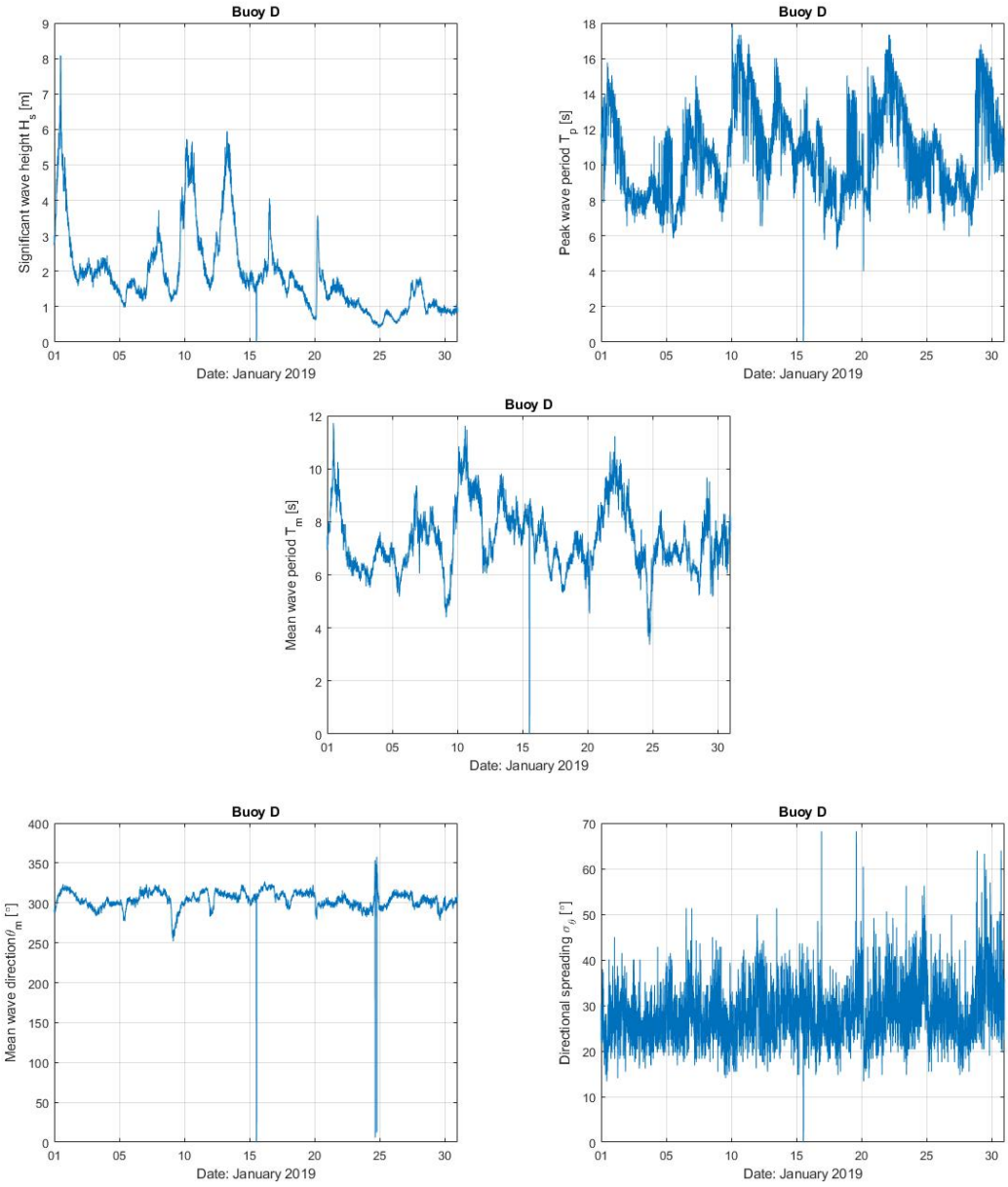

Figure B.4: Buoy D- wave data

B.2 Time increment

B.2.1 Significant wave height

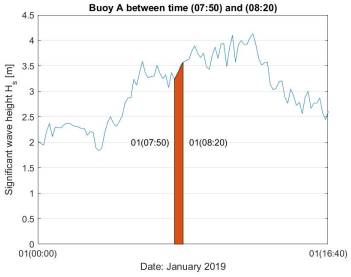

(a) H_s for 01 January between 07:50 - 08:20

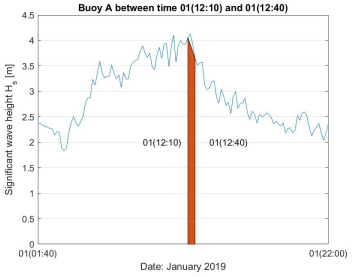

(b) H_s for 01 January between 12:10 - 12:40

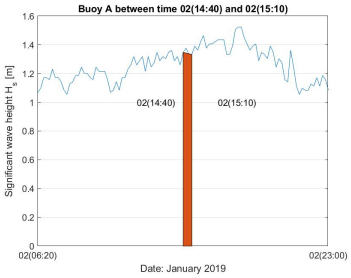

(c) H_s for 02 January between 14:40 - 15:10

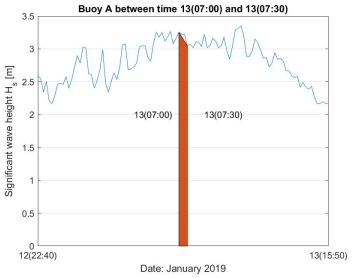

(d) H_s for 12 January between 07:00 - 07:30

Figure B.5: Buoy A

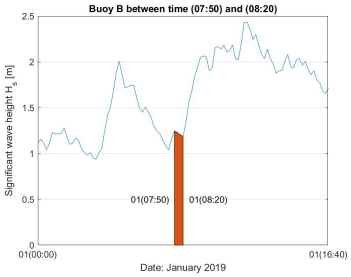

(a) H_s for 01 January between 07:50 - 08:20

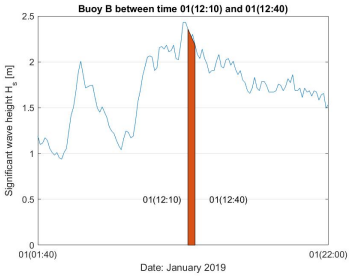

(b) H_s for 01 January between 12:10 - 12:40

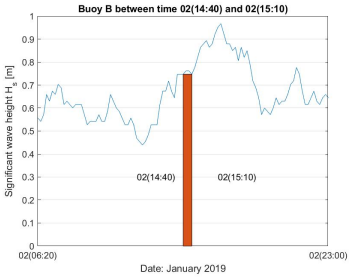

(c) H_s for 02 January between 14:40 - 15:10

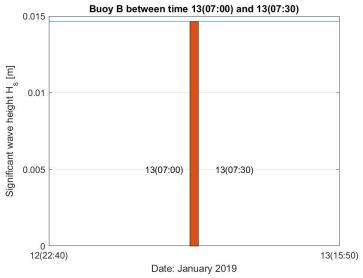

(d) H_s for 12 January between 07:00 - 07:30

Figure B.6: Buoy B

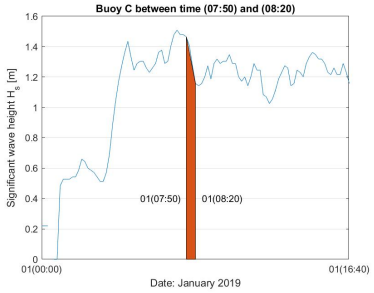

(a) H_s for 01 January between 07:50 - 08:20

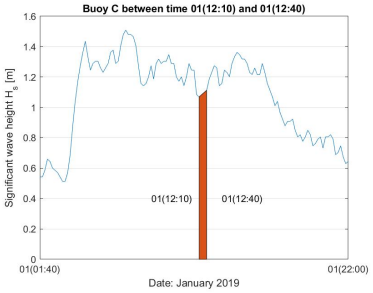

(b) H_s for 01 January between 12:10 - 12:40

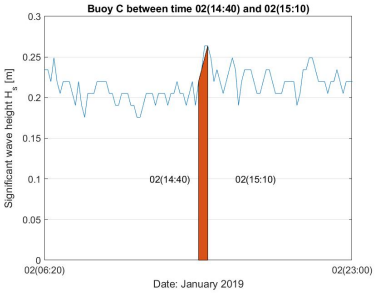

(c) H_s for 02 January between 14:40 - 15:10

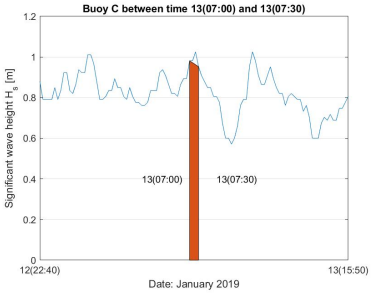

(d) H_s for 12 January between 07:00 - 07:30

Figure B.7: Buoy C

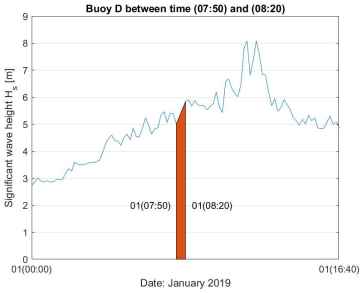

(a) H_s for 01 January between 07:50 - 08:20

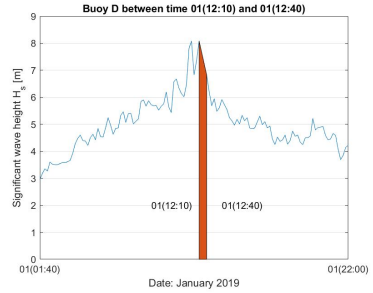

(b) H_s for 01 January between 12:10 - 12:40

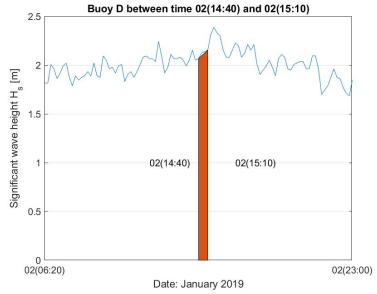

(c) H_s for 02 January between 14:40 - 15:10

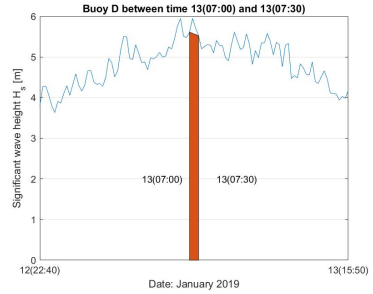

(d) H_s for 12 January between 07:00 - 07:30

Figure B.8: Buoy D

B.2.2 Peak wave period

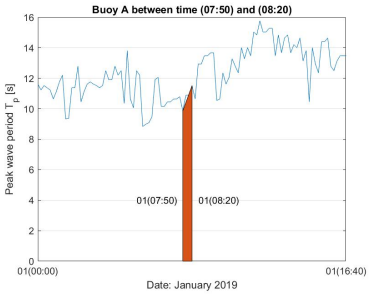

(a) T_p for 01 January between 07:50 - 08:20

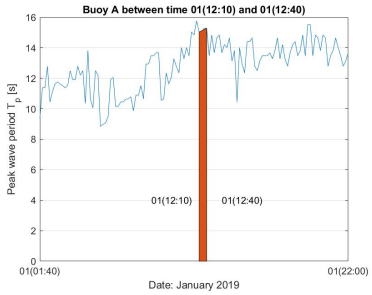

(b) T_p for 01 January between 12:10 - 12:40

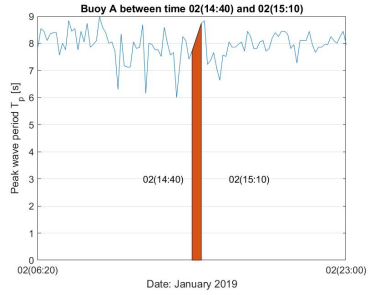

(c) T_p for 02 January between 14:40 - 15:10

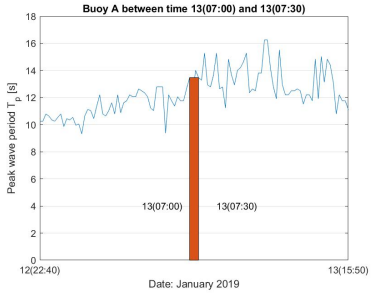

(d) T_p for 12 January between 07:00 - 07:30

Figure B.9: Buoy A

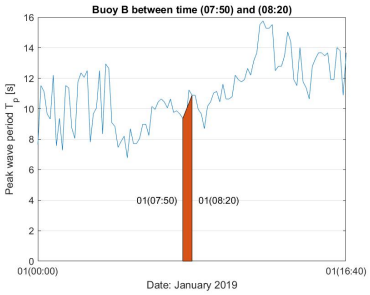

(a) T_p for 01 January between 07:50 - 08:20

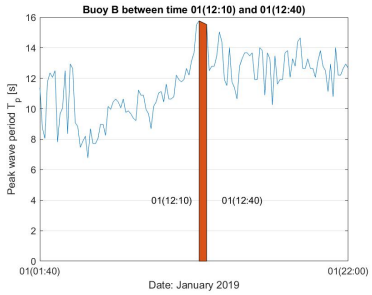

(b) T_p for 01 January between 12:10 - 12:40

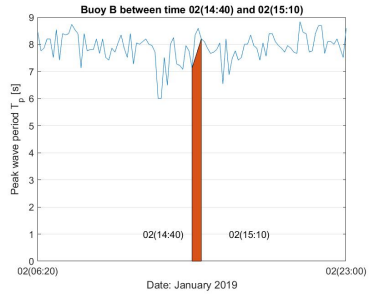

(c) T_p for 02 January between 14:40 - 15:10

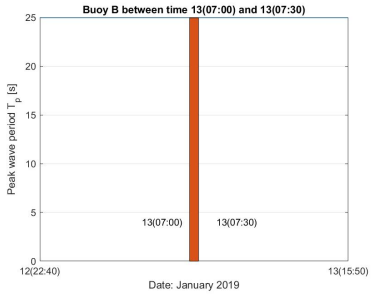

(d) T_p for 12 January between 07:00 - 07:30

Figure B.10: Buoy B

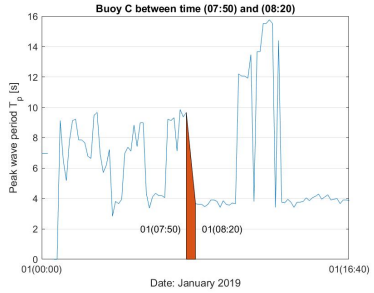

(a) T_p for 01 January between 07:50 - 08:20

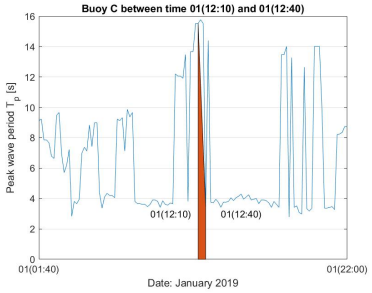

(b) T_p for 01 January between 12:10 - 12:40

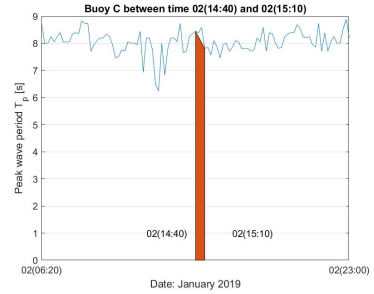

(c) T_p for 02 January between 14:40 - 15:10

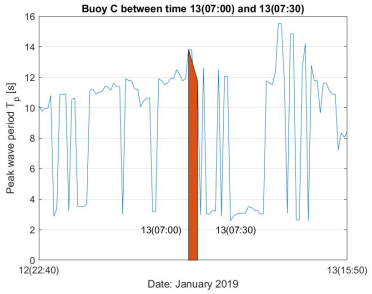

(d) T_p for 12 January between 07:00 - 07:30

Figure B.11: Buoy C

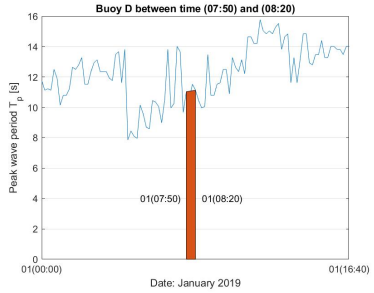

(a) T_p for 01 January between 07:50 - 08:20

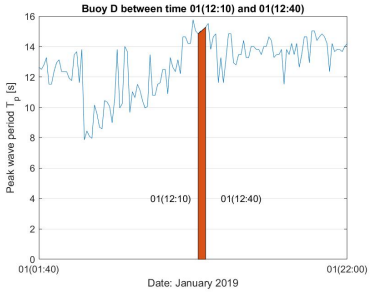

(b) T_p for 01 January between 12:10 - 12:40

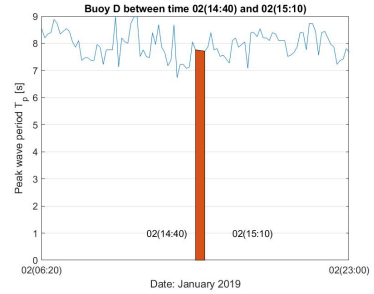

(c) T_p for 02 January between 14:40 - 15:10

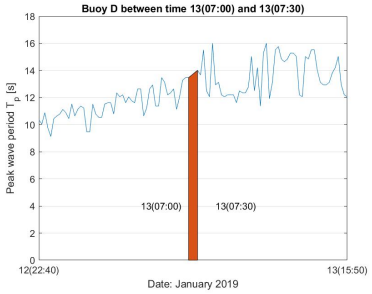

(d) T_p for 12 January between 07:00 - 07:30

Figure B.12: Buoy D

B.2.3 Mean wave period

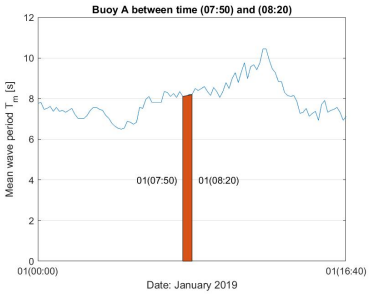

(a) T_m for 01 January between 07:50 - 08:20

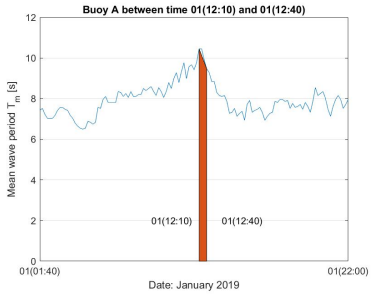

(b) T_m for 01 January between 12:10 - 12:40

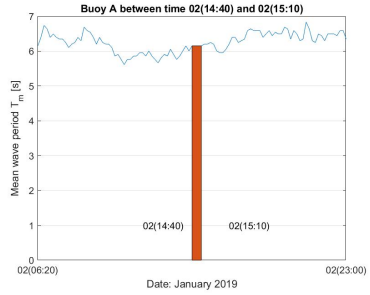

(c) T_m for 02 January between 14:40 - 15:10

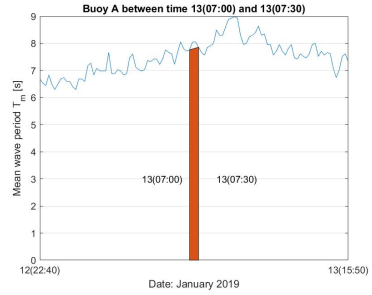

(d) T_m for 12 January between 07:00 - 07:30

Figure B.13: Buoy A

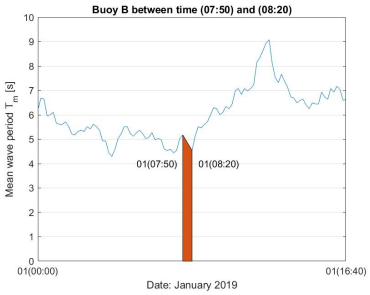

(a) T_m for 01 January between 07:50 - 08:20

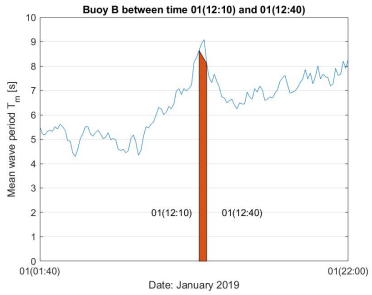

(b) T_m for 01 January between 12:10 - 12:40

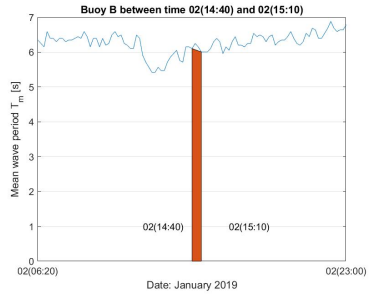

(c) T_m for 02 January between 14:40 - 15:10

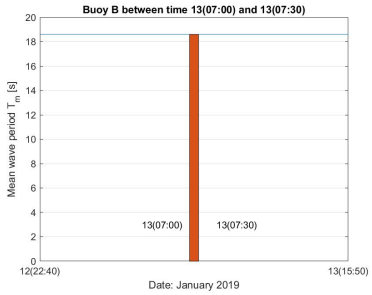

(d) T_m for 12 January between 07:00 - 07:30

Figure B.14: Buoy B

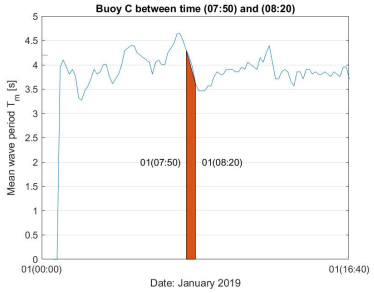

(a) T_m for 01 January between 07:50 - 08:20

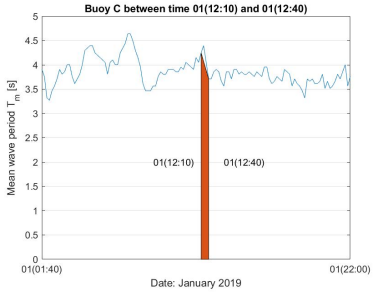

(b) T_m for 01 January between 12:10 - 12:40

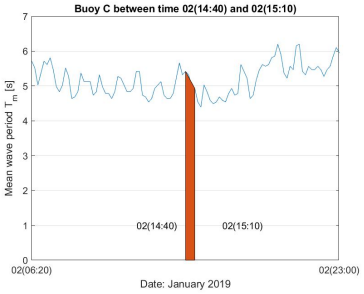

(c) T_m for 02 January between 14:40 - 15:10

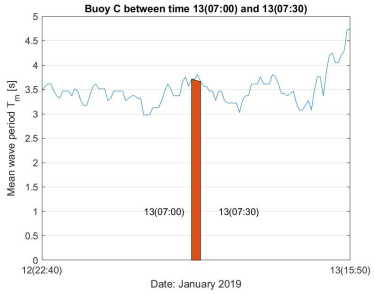

(d) T_m for 12 January between 07:00 - 07:30

Figure B.15: Buoy C

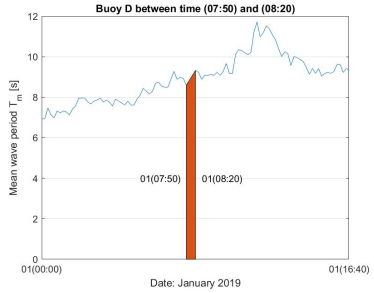

(a) T_m for 01 January between 07:50 - 08:20

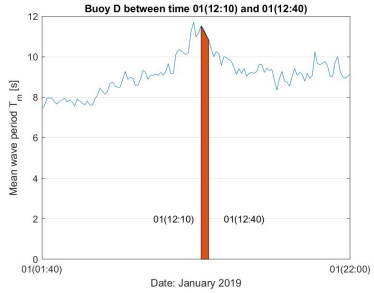

(b) T_m for 01 January between 12:10 - 12:40

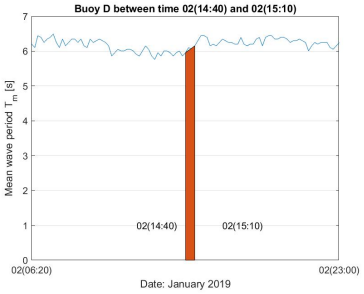

(c) T_m for 02 January between 14:40 - 15:10

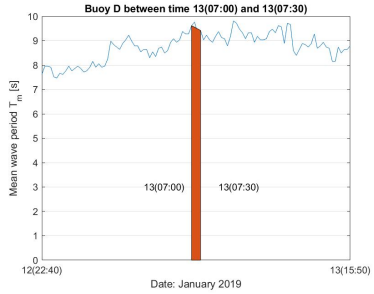

(d) T_m for 12 January between 07:00 - 07:30

Figure B.16: Buoy D

B.2.4 Mean wave direction

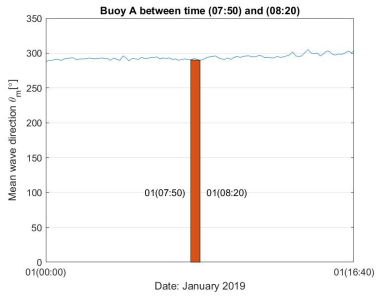

(a) θ_m for 01 January between 07:50 - 08:20

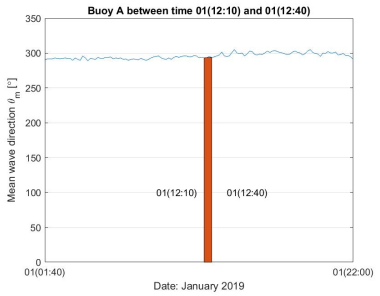

(b) θ_m for 01 January between 12:10 - 12:40

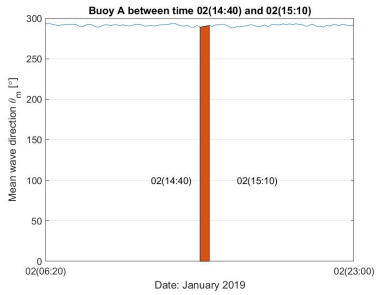

(c) θ_m for 02 January between 14:40 - 15:10

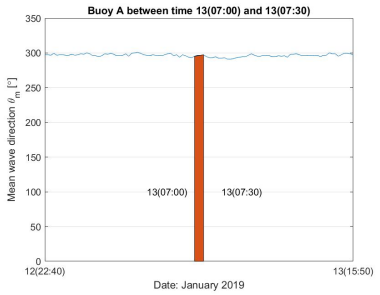

(d) θ_m for 12 January between 07:00 - 07:30

Figure B.17: Buoy A

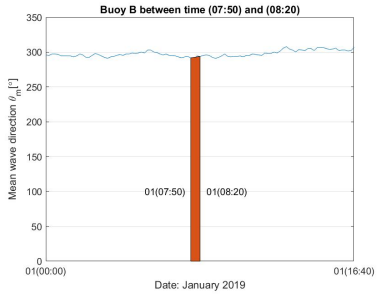

(a) θ_m for 01 January between 07:50 - 08:20

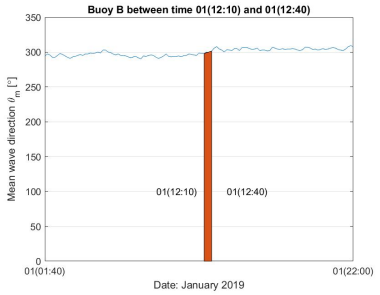

(b) θ_m for 01 January between 12:10 - 12:40

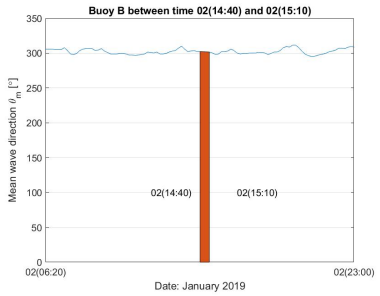

(c) θ_m for 02 January between 14:40 - 15:10

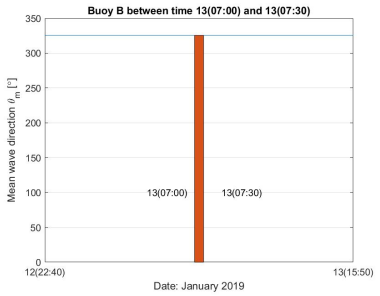

(d) θ_m for 12 January between 07:00 - 07:30

Figure B.18: Buoy B

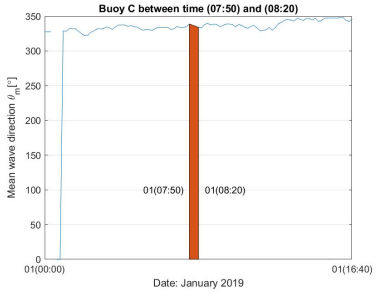

(a) θ_m for 01 January between 07:50 - 08:20

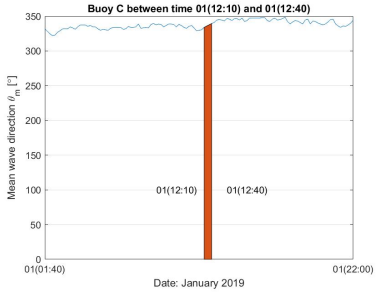

(b) θ_m for 01 January between 12:10 - 12:40

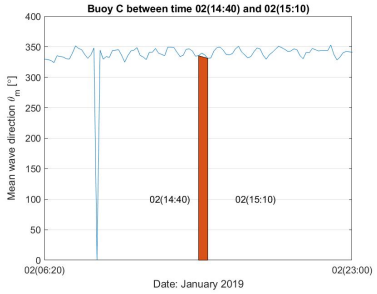

(c) θ_m for 02 January between 14:40 - 15:10

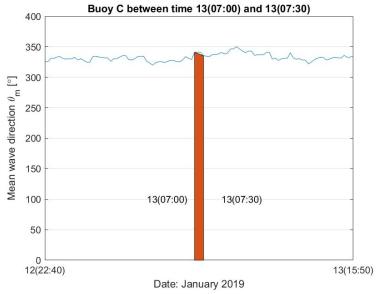

(d) θ_m for 12 January between 07:00 - 07:30

Figure B.19: Buoy C

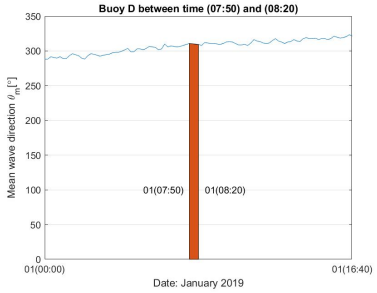

(a) θ_m for 01 January between 07:50 - 08:20

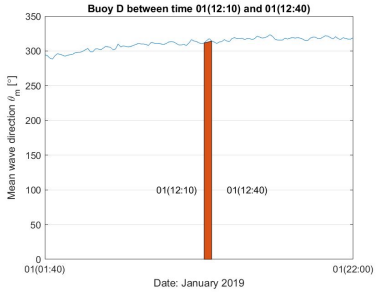

(b) θ_m for 01 January between 12:10 - 12:40

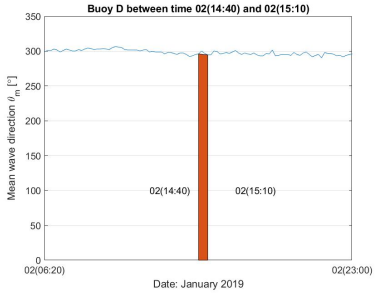

(c) θ_m for 02 January between 14:40 - 15:10

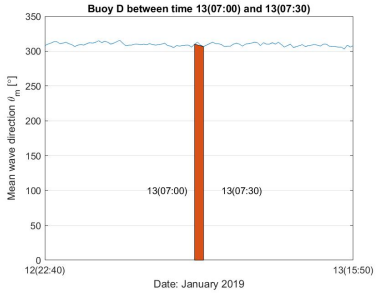

(d) θ_m for 12 January between 07:00 - 07:30

Figure B.20: Buoy D

B.2.5 Directional spreading

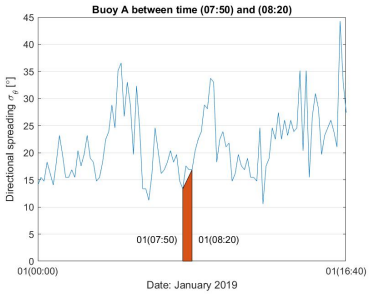

(a) σ_θ for 01 January between 07:50 - 08:20

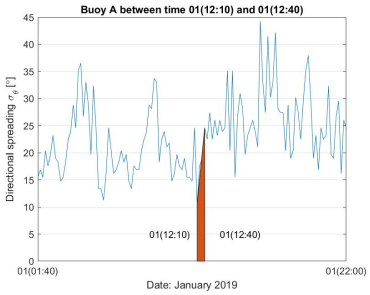

(b) σ_θ for 01 January between 12:10 - 12:40

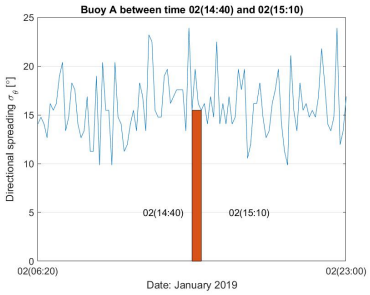

(c) σ_θ for 02 January between 14:40 - 15:10

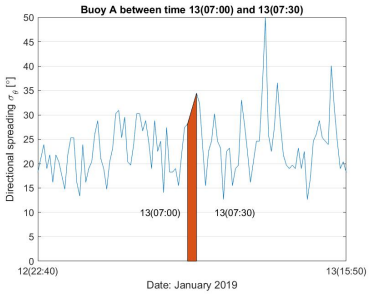

(d) σ_θ for 12 January between 07:00 - 07:30

Figure B.21: Buoy A

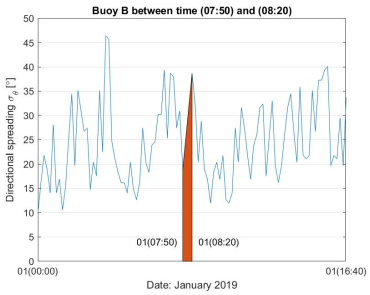

(a) σ_θ for 01 January between 07:50 - 08:20

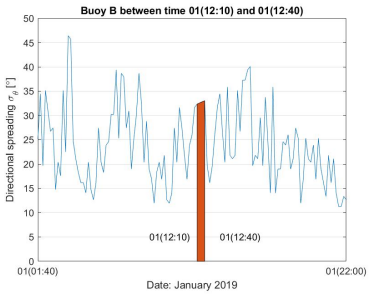

(b) σ_θ for 01 January between 12:10 - 12:40

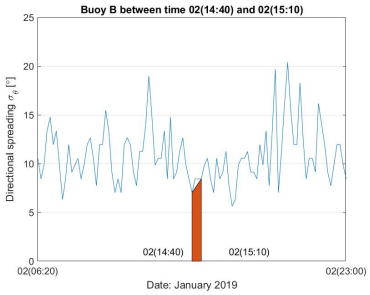

(c) σ_θ for 02 January between 14:40 - 15:10

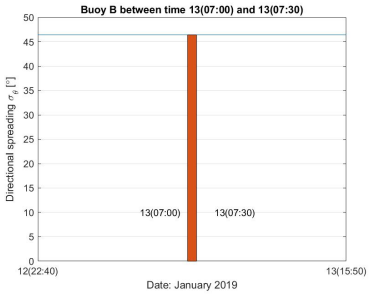

(d) σ_θ for 12 January between 07:00 - 07:30

Figure B.22: Buoy B

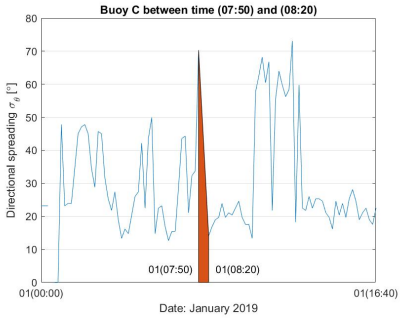

(a) σ_θ for 01 January between 07:50 - 08:20

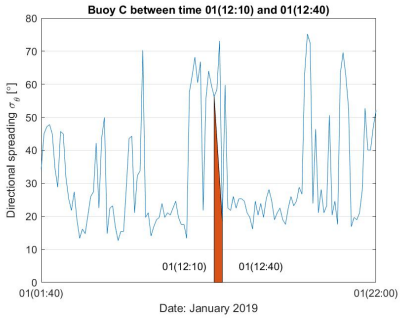

(b) σ_θ for 01 January between 12:10 - 12:40

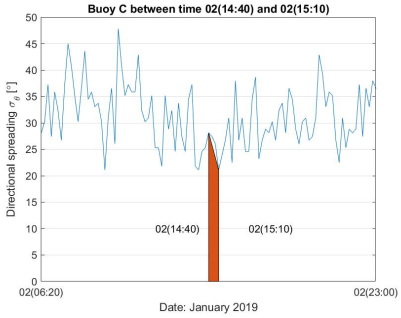

(c) σ_θ for 02 January between 14:40 - 15:10

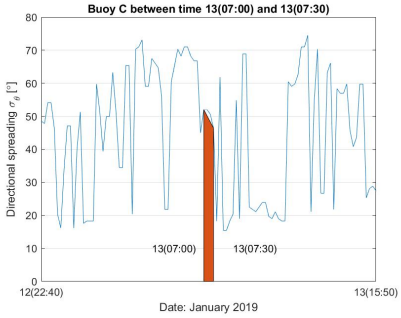

(d) σ_θ for 12 January between 07:00 - 07:30

Figure B.23: Buoy C

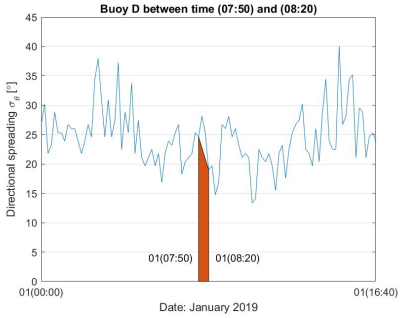

(a) σ_θ for 01 January between 07:50 - 08:20

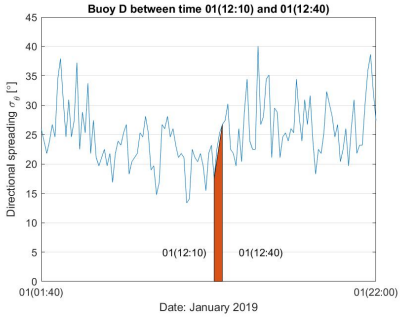

(b) σ_θ for 01 January between 12:10 - 12:40

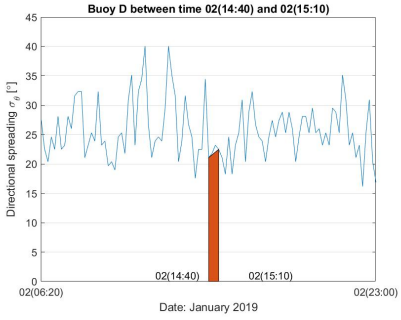

(c) σ_θ for 02 January between 14:40 - 15:10

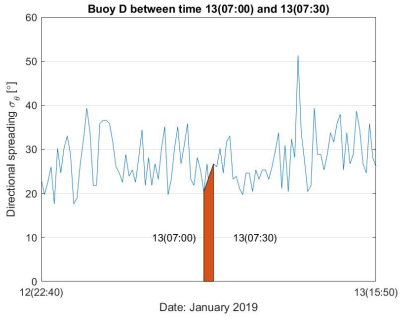

(d) σ_θ for 12 January between 07:00 - 07:30

Figure B.24: Buoy D

B.3 Wind data

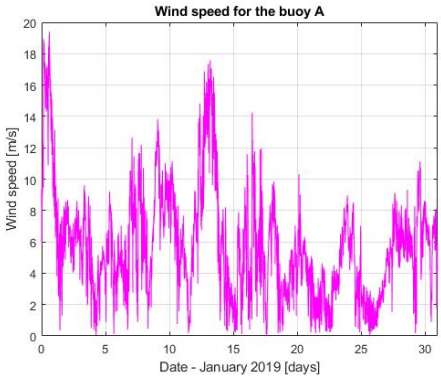

(a) Wind speed

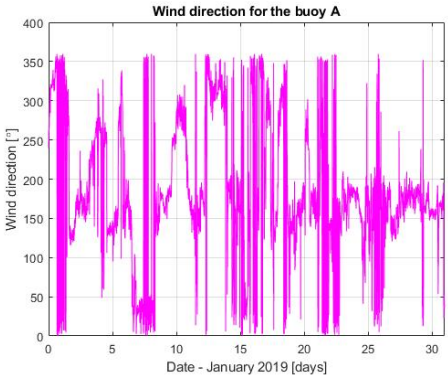

(b) Wind direction

Figure B.25: Buoy A - wind data

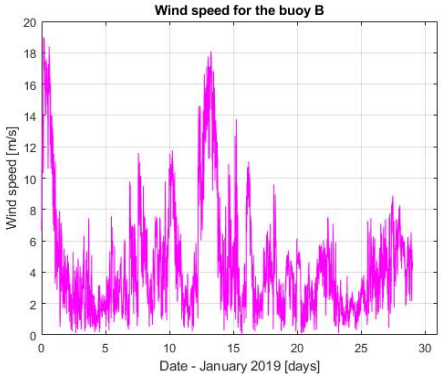

(a) Wind speed

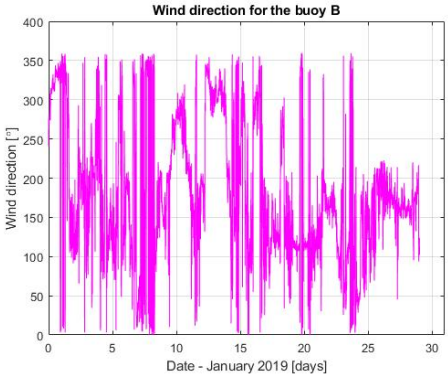

(b) Wind direction

Figure B.26: Buoy B - wind data

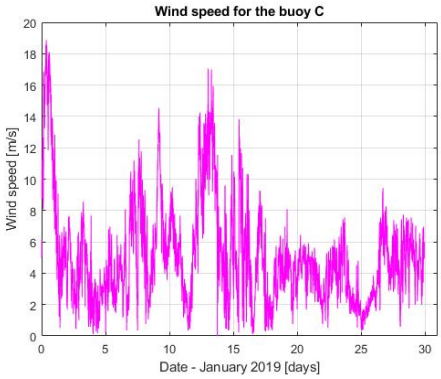

(a) Wind speed

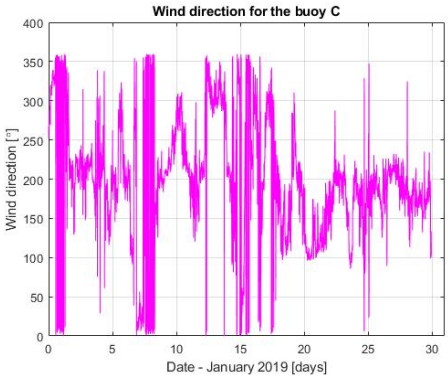

(b) Wind direction

Figure B.27: Buoy C - wind data

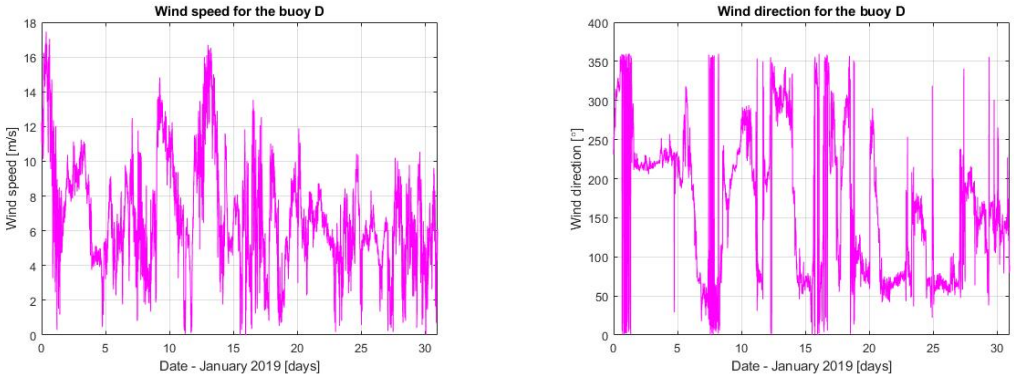

(a) Wind speed *(b) Wind direction*

Figure B.28: Buoy D - wind data

Bibliography

[1] Arun Kamath Weizhi Wang, Hans Bihs and Øivind Asgeir Arntsen. Large scale cfd modelling of wave propagation in sulafjord for the e39 project.

[2] Leo H. Holthuijsen. *Waves in oceanic and coastal waters*. Cambridge university press, Cambridge University Press The Edinburgh Building, Cambridge CB2 8RU, UK, 2007.

[3] Karl Henning Halse. Marin hydrodynamikk: Havmiljøbeskrivelse – bølger 1.

[4] University of Texas in Dallas. Oceanography - http://www.utdallas.edu/~mitterer/Oceanography/pdfs/OCEChapt09.pdf?fbclid=IwAR3oYm9WyTmOG2S4ddQwRzXZO7jIX49hROAkrrnzc9Ypi5mVQPXUMk2VX_A.

[5] College of liberal arts and science. Nearshore wave information - http://users.clas.ufl.edu/adamsp/Outgoing/GLY4734_Spring2014/S11_PropShoalRefrac.pptx.pdf.

[6] University of Hawaii. Oceanography - http://www.soest.hawaii.edu/oceanography/courses_html/OCN201/instructors/Carter/SP2016/waves2_2016_handout.pdf.

[7] Kyle Stock. Spilling, surging, plunging: The science of breaking waves - https://www.surfertoday.com/surfing/what-is-wave-refraction.

[8] physicstutorials.org. Water waves - http://www.physicstutorials.org/home/waves/water-waves?fbclid=IwAR2wOL91kGsdBv-MUvh6mvezDNepucQ49f8nyvuN5Vw07enEVCx6hk1P0N0.

[9] DNV-GL. Environmental conditions and environmental loads.

[10] Verbcatcher. Diffraction - https://commons.wikimedia.org/w/index.php?curid=68991367.

[11] Wikipedia. Diffraction - https://en.wikipedia.org/wiki/Diffraction.

[12] Mayilvahanan Alagan Chella. Breaking wave characteristics and breaking wave forces on slender cylinders.

[13] Klaus Hasselmann. On the spectral dissipation of ocean waves due to white capping*.

[14] Coastalwiki. Wave transformation - http://www.coastalwiki.org/wiki/Wave_transformation.

[15] Mayilvahanan Alagan Chella. Breaking wave characteristics and breaking wave forces on slender cylinders.

[16] Kyle Stock. The science of breaking waves - https://www.theinertia.com/surf.

[17] Surfertoday. The four types of breaking waves - https://www.surfertoday.com/surfing/the-four-types-of-breaking-waves.

[18] rlss poole lifeguard. Rookie lifeguard - http://www.rlss-poole.org.uk/wp-content/uploads/2013/10/1-Waves-Info.pdf.

[19] L.H. Holthuijsen N. Booij and R.C. Ris. A third-generation wave model for coastal regions.

[20] The SWAN team. Swan scientific and technical documentation.

[21] G. Ph Van Vledder T.J Zitman A.J. Van der Westhuysen G.S. Stelling, L.H Holthuijsen. Wave physics in a tidal inlet.

[22] Leo H. Holthuijsen. *Waves in oceanic and coastal waters*. Cambridge university press, Cambridge University Press The Edinburgh Building, Cambridge CB2 8RU, UK, 2007.

[23] Wikiwaves. Ocean-wave spectra - https://wikiwaves.org/Ocean-Wave_Spectra.

[24] Wikipedia. Wave setup - https://en.wikipedia.org/wiki/Wave_setup.

Wave modelling in coastal areas
IP305012

Candidate: 10009

A thesis presented for the degree of
Bachelor of Science

Department of Civil and Environmental Engineering
Norwegian University of Science and Technology (NTNU)
Ålesund, Norway
May 19, 2019

Contents

Chapter 1

General theory

1.1 Effects in shallow water

1.1.1 Shoaling

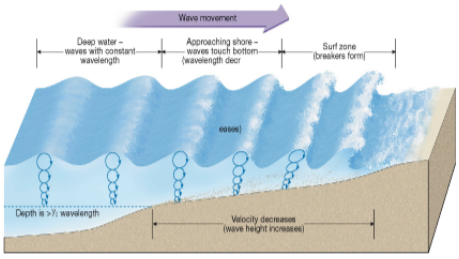

Figure 1.1: Changes that occur when a wave shoals (moves into shallow water).[1]

Wave shoaling is the effect by which sea surface waves entering shallower water change in wave height. This is caused due to the decrease in the group velocity.

We can consider a condition where the wave propagates along an even slope and perpendicularly towards the beach. The incoming wave energy needs to be conserved when it depart from the inlet. Since the group velocity (which is the energy transport velocity) is decreasing, the wave amplitude needs to compensate for these loses by increasing. This increase in the wave amplitude can be called as 'energy bunching' or shoaling.

What also can be mentioned is that shoaling waves will exhibit a reduction in wavelength while its frequency remains the same. This allows for the dispersion relationship for arbitrary depth to be retained, which simplifies a already complex field [2].

$$\omega^2 = gk\tanh(kd) \tag{1.1}$$

Where ω is the radial frequency, g is the gravitational acceleration, k is the wave number and d is the water depth.

1.1.2 Diffraction

Wave diffraction happens when a wave tries to bend around an obstacle like headland or breakwater into the shadow of these objects.

The intensity of diffraction dependant on the size of the aperture. The lower the aperture the higher the diffraction.

What happens it that the wave will try to fill the lee side of the obstacle by spreading its amplitude in a circular pattern towards areas with lower amplitude. The highest amplitude remains at the direction of the propagation, where it will steadily decrease [4] [2].

Figure 1.2: Circular waves generated by diffraction from the narrow entrance of a flooded coastal quarry [3].

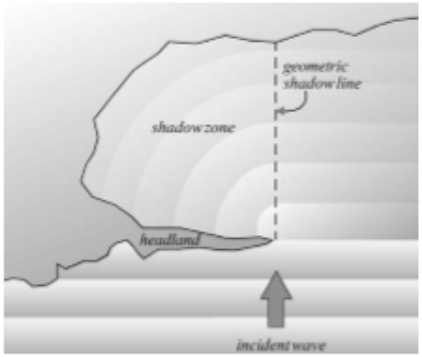

(a) Diffraction around a headland.

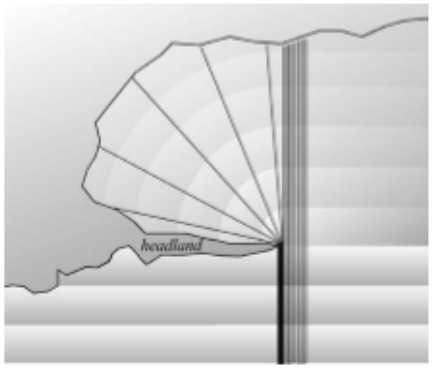

(b) Diffraction represented with wave rays.

Figure 1.3: Diffraction [2]

1.1.3 Wave Breaking

Wave breaking occurs when a wave becomes progressively steeper, until it reaches a critical point.
When that point is reached the wave front overturnes and eventually breaks. This is usually determined by the fact that the particle velocity u_x in the crest cannot be larger than the forward speed of the wave ($u_x \leq c_g$)[2].

Wave breaking in coastal regions is affected by multiple parameters (Wave amplitude, wave length, depth, etc.).

For deep waters, where the wave particle motion is unaffected by the depth, the wave breaks when the wave steepness (H_∞/λ_∞) becomes 0.141[1] [5].

The dominant dissipative mechanism for deep waters is due to white-capping [6]. This is not a strong dissipative mechanism, which means that the waves needs to be frequent for it to break in deep waters. This is characterized by the white foam in the sea.

We can consider an example.

[1] This is usually used as the upper breaking limit for deep water waves.

For deep water the dispersion relationship is defined as $\omega^2 = kg$. When we consider a low frequency wave of $f = 1/8Hz$ ($\omega = 2\pi \cdot f$), we can then calculate the wave height.

$$\omega^2 = kg \Rightarrow \lambda_\infty = \frac{2\pi g}{\omega^2} \approx 100.0m \tag{1.2}$$

By using the breaking criterion for deep water we get that the wave height needs to be 14.0 meters (wave amplitude 7.0 meters) in order to break. This is impossible to occur at deep waters.

For shallow waters the water particle motion is severely obscured by the water depth. This influence causes the wave to deform as it propagates into the decreasing water depth.

For a wave to break in shallow waters, the wave steepness needs also to exceed a specific steepness. For shallow waters although, it is more dynamic. The wave breaking limit is defined as, $\frac{H_b}{\lambda} = 0.142 \cdot \tanh\left(\frac{2\pi d}{\lambda}\right)$.

Where H_b is the wave height at breaking, λ is the wave length and d is the depth.

The dissipative mechanism for shallow water are mainly caused due to the depth variation and bottom friction, but also due to the same effects as in deep water, but enhanced [2]. Examples of shallow water breaking will be shown in later sections.

White-capping

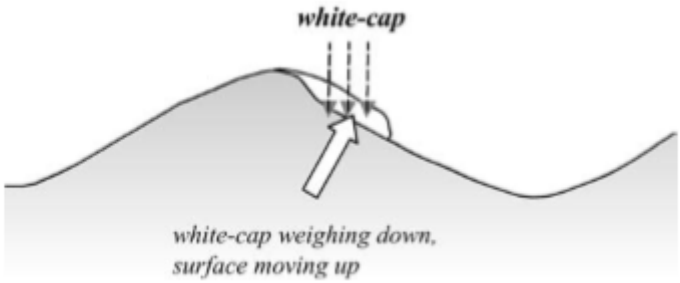

Figure 1.4: The white-cap as pressure pulse at the lee-wind side of the crest of a breaking wave [2].

Water waves are mainly wind generated. When the wind blows with a certain strength over a large fetch distance, large wind-waves will develop.

When the waves are small enough and the wind is strong, the waves will break due to white-capping. This phenomenon is very complicated, thus will not be well explained here.

White-capping is the white foam occurring at the surface of the wave crests. When the wind is strong enough, it blows away the water particles at the crest. This water mass falls down at the lee-wind side of the crest and slightly slowing it down, but stops further development (figure 1.4)[2].

Depth-induced breaking

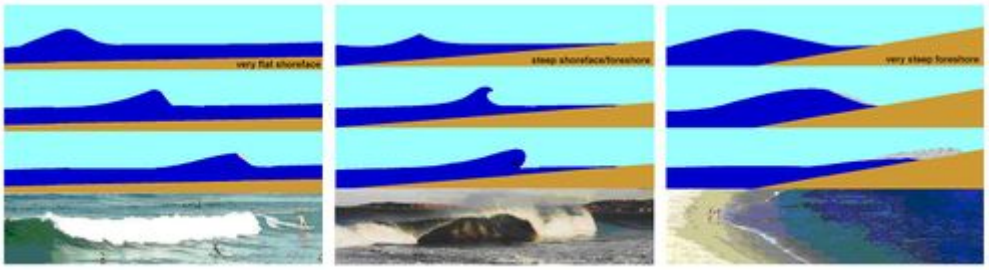

Figure 1.5: Depth-induced wave-breaking: spilling, plunging and surging [7]

Depth-induced breaking is the leading way that waves break in shallow water. Waves will eventually approach the shore, where the total remaining energy is dissipated at the shoaling zone or to land. This dissipation is dependent on the slope of the seabed and the steepness of the incoming wave.

At shallow waters, it has been documented four possible ways that a wave can break. It can break by spilling, plunging, surging and collapsing [8]. These breaker types can be identified based on the surf similarity parameter. Surf similarity parameter (Or Iribarren number) is defined like this $\xi_\infty = \frac{\tan\alpha}{\sqrt{H_\infty/\lambda_\infty}}$ or at the point of incipient breaking $\xi_{br} = \frac{\tan\alpha}{\sqrt{H_{br}/\lambda_\infty}}$, where ξ_∞ is the iribarren number for deep water, ξ_{br} is the iribarren number at breaking, α is the seabed angle, H_∞ is the wave height at the deep water, H_{br} is the wave height at breaking and λ_∞ is the wave length at the deep water.[2].

The iribarren values ranges for defining different types for depth-induced breaking can be seen on the next page.

spilling:	if $\xi_\infty < 0.5$	or $\xi_{br} < 0.4$
plunging:	if $0.5 < \xi_\infty < 3.3$	or $0.4 < \xi_{br} < 2.0$
collapsing or *surging*:	if $\xi_\infty > 3.3$	or $\xi_{br} > 2.0$

Figure 1.6: Surf similarity parameter ranges [2]

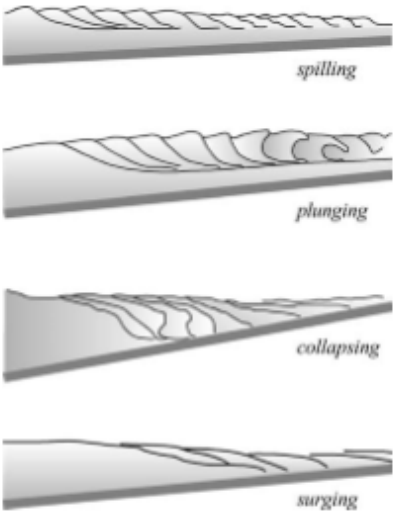

(a) The four main types of breaking waves (after Galvin, 1968). All intermediate states may appear on a real beach [2].

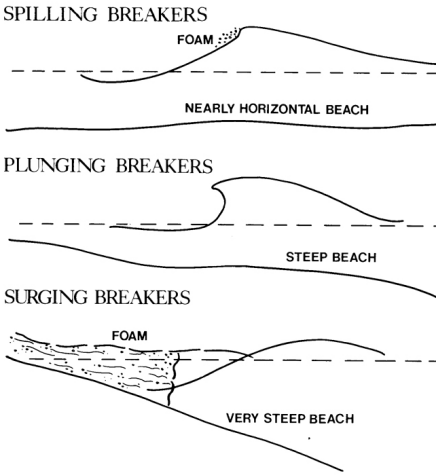

(b) Depth-induced wave-breaking: spilling, plunging and surging [9]

Figure 1.7: Wave breaking

- Spilling breakers happens when a wave propagates towards a beach with a very gentle slope, or when a wave is relatively steep and is propagating on a flat beach. As the wave approaches the shore, it slowly releases energy, and the crest gradually spills down its face until it is all whitewater.
- Plunging breakers occurs when an incoming wave propagates towards a steep seabed. It causes the wave to suddenly lose a lot of its speed, which results in a large increase in wave amplitude and a sudden collapse of wave crest.
- Surging breakers are produced when a wave approach a very steep seabed. These waves usually never becomes steep enough to break at the surf zone, but instead propagates towards the steep beach, dissipates a lot of its energy at a point and the rest surges forward.
- Collapsing breakage is a transition type between plunging and surging.

[10][11][12]

Chapter 2

Modelling of coastal waves

2.1 What is SWAN

SWAN is a third-generation wave model for obtaining realistic estimates of wave propagation in coastal areas from given wind, bottom and current conditions.

SWAN as any other third-generation wave model for ocean waters, models the processes of wind generation, white-capping, quadruplet wave-wave interactions and bottom friction dissipations.

Coastal regions experiences additional processes that needs to be included in order to model these areas. This requires for the adaptation of the spectral action balance equation to include effects like triad wave-wave interactions, depth-induced wave breaking, refraction and shoaling.

Third-generation oceanic wave models like WAM and WAVE-WATCH use an explicit method for numerical propagation. This makes it very computational expensive to use at domain scales lower that 20-30 km and water depths less than 20-30 m. This method cannot be used for coastal models, which demand more grid points for accuracy. This can be solved by using implicit propagation schemes (There is more to it, this is an rough explanation) [13].

Propagation processes that are represented in SWAN;

- Propagation through geographic space,
- Refraction due to spatial variations in bottom and current,
- Diffraction[1] - only approximations,
- Shoaling due to spatial variation in bottom and current,
- Blocking and reflections by opposing currents,
- Transmission through, blockage by or reflection against obstacles.

Generation and dissipation processes that are represented in SWAN;

- Generation by wind,
- Dissipation by whitecapping,
- Dissipation by depth-induced wave breaking,
- Dissipation by bottom friction,
- Wave-wave interactions in both deep and shallow water [14].

[1] Diffraction is modelled in a restrict sense. Spectral models are efficient partially because they neglect diffraction.

Source Term	Reference	SWAN Added	SWAN WAM 3	SWAN WAM 4
Linear wind growth	*Cavaleri and Malanotte-Rizzoli* [1981]	x		
Exponential wind growth	*Komen et al.* [1984]		xx	
	Janssen [1991a]			x
Whitecapping	*Komen et al.* [1984]		xx	
	Janssen [1991a] and *Komen et al.* [1994]			x
Quadruplet wave-wave interactions	*Hasselmann et al.* [1985]		xx	xx
Bottom friction	*Hasselmann et al.* [1973]		xx	xx
	Collins [1972]	x		
	Madsen et al. [1988]	x		
Depth-induced breaking	*Battjes and Janssen* [1978]	xx		
Triad wave-wave interactions	*Eldeberky* [1996]	xx		

Figure 2.1: Options of Third-generation source terms in SWAN [13].

2.1.1 Spectral action balance equation

All information about the sea surface is contained in the energy density $E(\sigma,\theta)$. Energy density describes the evolution of the wave spectrum over radian frequencies σ and propagation directions θ. Due to simplicity in wave propagation in the presence of ambient currents, the spectral action balance equation is used. The action balance equation is defined as $N(x,y,t;\sigma,\theta) = E(x,y,t;\sigma,\theta)/\sigma$ [2].

The full spectral action balance equation is;

$$\frac{\delta N(x,y,t;\sigma,\theta)}{\delta t} + \frac{\delta c_{g,x} N(x,y,t;\sigma,\theta)}{\delta x} + \frac{\delta c_{g,y} N(x,y,t;\sigma,\theta)}{\delta y} + \frac{\delta c_\theta N(x,y,t;\sigma,\theta)}{\delta \theta} + \frac{\delta c_\sigma N(x,y,t;\sigma,\theta)}{\delta \sigma} = \frac{S_{tot}(x,y,t;\sigma,\theta)}{\sigma}$$

The first term on the left-hand side represents the local rate of change of action density in time, the second and third term represent propagation of waves in geographic space (with propagation velocities $c_{g,x}$, $c_{g,y}$ for x- and y- space, respectively). The fourth term represents depth-induced and current-induced refraction (with propagation velocities c_θ in θ- space). The fifth term represents shifting of the relative frequencies due to variations in depth and currents (with propagation velocities c_σ in σ-space)[13].

The right hand side contains $S_{tot}(\sigma,\theta)$, which is the non-conservative source/sink term of energy density, that represents all physical processes which generate, dissipate, or redistribute wave energy at a point.

The right hand side equation $S_{tot}(\sigma,\theta)$ in shallow water is described by six processes.

$$S_{tot} = S_{in} + S_{nl3} + S_{nl4} + S_{ds,w} + S_{ds,b} + S_{ds,br} \tag{2.1}$$

These terms denote, respectively, wave growth by the wind, nonlinear transfer of wave energy through three-wave and four-wave interactions and wave decay due to white-capping, bottom friction and depth-induced wave breaking [14][15]. For more information regarding the formulations of these processes see "SWAN scientific and technical documentation" by SWAN team.

2.1.2 Boundary conditions

In SWAN the boundaries are either water or land. Land in SWAN is fully absorbing of the wave energy, while water requires further planning.

Often no wave conditions are known along boundaries, unless we give it one. SWAN assumes that no wave enters the area, but it can leave freely. This may involve potential errors that needs to be addressed while modelling.

The boundary conditions at the lateral boundary of the computational domain are completely unknown. These boundaries, if not taken into account can potentially influence the credibility of the results. For most situations it is recommended to create a domain that is sufficiently wide, so that it minimizes the erroneous effects of the lateral boundary (Recommended). What also can be done is to apply a incoming wave spectrum at a segment of the lateral boundary, if proper wave information are available. This is although very situations.

2.2 Wave spectrum

Waves in SWAN are described with the two-dimensional (frequency [f] and direction [θ]) wave action density spectrum $E(f,\theta)$. This is also the case for nonlinear processes at the surf zone.This makes it so that the waves cannot be fully described statistically. This is why it appears that the energy density increases at the surf zone.

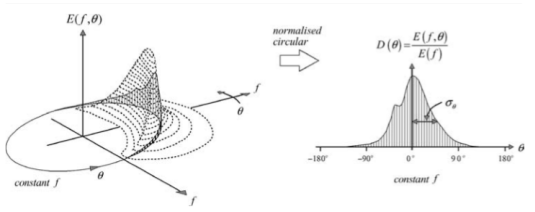

Figure 2.2: The 2D directional spectrum and the directional distribution [2].

The two-dimensional directional spectrum are described with the one-dimensional spectrum with introduced directional distribution $D(\theta)$. Together they define a 2D spectrum; $E(f,\theta) = E(f)D(\theta)$. It is essentially the cross-section through the two-dimensional spectrum at a given frequency, normalized such that its integral over the directions is unity. This integral is shown as follows;

$$\int_0^{2\pi} D(\theta)d\theta = \int_0^{2\pi} \frac{E(f,\theta)}{E(f)}d\theta = \frac{\int_0^{2\pi} E(f,\theta)d\theta}{E(f)} = \frac{E(f)}{E(f)} = 1 \tag{2.2}$$

The directional spreading of the waves can be defined as the (one-sided) directional width of $D(\theta)$, denoted as σ_θ, and thereafter the standard deviation of the directional distribution is defined as;

$$\sigma_\theta^2 = \left(\frac{180}{\pi}\right)^2 \int_0^{2\pi} \left[2\sin\left(\frac{1}{2}\theta\right)\right]^2 D(\theta)d\theta \tag{2.3}$$

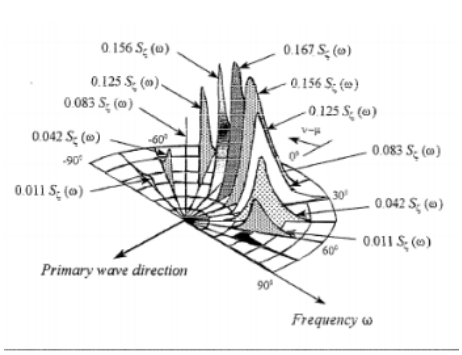

(a) Directional distribution[16]

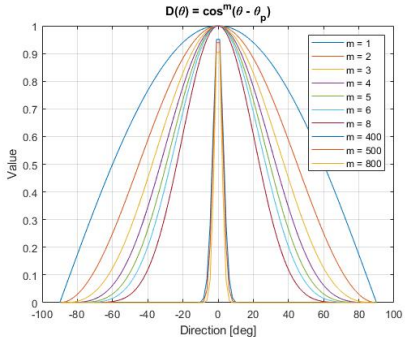

(b) SWAN's directional distribution $D(\theta) = cos^m(\theta - \theta_p)$

Figure 2.3

The directional width (σ_θ) of the directional distribution ($D(\theta)$) is called "DSPR" in SWAN, where it can be defined with the power m.

In SWAN the directional distribution of incident wave energy is given by;

$$D(\theta) = cos^m(\theta - \theta_p) \tag{2.4}$$

Where θ is the wave direction and θ_p is the peak wave direction. The above parameter "m" is related to the one-sided directional spreading of the waves (σ_θ) and the values are shown in table 2.1.

m	σ_θ (Deg)
1	37.5
2	31.5
3	27.6
4	24.9
5	22.9
6	21.2
8	18.8
400	2.9
500	2.56
800	2.0

Table 2.1: Directional spreading, for full table see SWAN User Manual p.106

The spectrum in SWAN is discretized with a constant directional resolution $\Delta\theta$ and a frequency resolution $\Delta f / f$ (logarithmic frequency distribution, see SWAN User Manual p.33). The discrete frequencies are defined between a fixed low-frequency cutoff (flow) and a fixed high-frequency cutoff (fhigh).

If the frequency resolution is too low, the wave spectrum will not represent the desired wave conditions.

We can consider a conditions where the desired significant wave height is 1.0 m and a peak frequency of 1/10 Hz. If the frequency distribution is low, we might end up with the closest calculated frequency, which is either higher or lower. This spans a

lower energy density. SWAN will thereafter start the simulation with a wave height that is lower than the one we wanted. This applies to every spectrum shape.

In SWAN we can input four "spectrum" shapes at boundaries, JONSWAP, Pierson and Moskowitz, Gaussian and a single frequency column (BIN). Where the Gaussian shape describes the surface elevation, which can be used to describe initial waves. As for BIN, we can initiate a regular wave. These shapes will be shown and explained later.

Before showing these spectral distributions we can consider a setup that will be used. The significant wave height H_s = 1.0 m, peak wave period T_p = 10 s, number of meshes in θ-space 180 (This gives a directional resolution of $\Delta\theta = \frac{360^\circ}{180} = 2^\circ$) and the spectral distribution Δf = 50 (This gives the number of frequencies of 51). These parameters will be used throughout the next sections.

BIN (Regular waves)

BIN is a command in SWAN that lets you create regular waves. SWAN locates the energy into one frequency column (bin). This frequency column will be the closest one to the peak wave period, where the width and therefore the accuracy is dependant on the spectral distribution Δf.

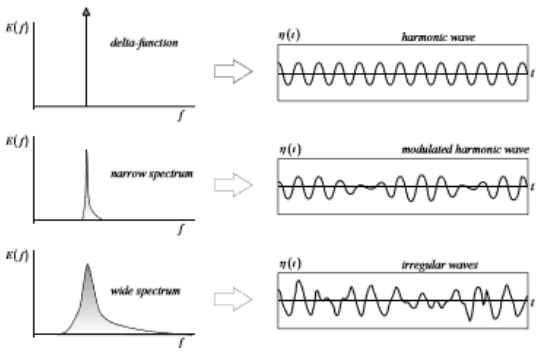

Figure 2.4: The (ir)regular character of the waves for three different widths of the spectrum[2].

To obtain the regular wave with the peak period of 10 s, we want to distribute the frequencies over a very narrow frequency range. For this case we can setup the lowest-frequency range [flow] to 0.09 Hz and the highest-frequency range [fhigh] to 0.11 Hz. This increases our likelihood of getting the frequency and the energy density we want. The result of this can be seen in figure 2.5.

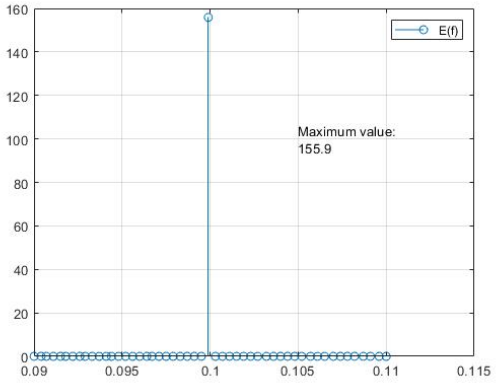

Figure 2.5: 1D frequency BIN in frequency domain [f]

For a simple regular wave in deep water, we can easily make a hand calculations of the significant wave height for a given one-dimensional spectral wave energy density $E(f)$.

This as to check if the simulated significant wave height will be the same as the input significant wave height.

The total energy density at a frequency is defined as;

$$E(f) = \int_0^{2\pi} E(f,\theta)d\theta = \int_0^{2\pi} E(f)D(\theta)d\theta \tag{2.5}$$

Furthermore the variance of the sea surface elevation $\underline{\overline{\eta}}^2$ can be defined as;

$$\underline{\overline{\eta}}^2 = \int_0^{+\infty} E(f)df \tag{2.6}$$

For a regular wave the variance of the sea surface elevation can be easily calculated by hand for a regular wave (see figure 2.6). That is because the variance will be equal to the sea surface elevation. So that $\underline{\overline{\eta}}$ can be simply written as η.

$$\underline{\overline{\eta}}^2 = \int_a^b E(f)df = E(f_m)(f_b - f_a) \Rightarrow \eta^2 = 155.9\frac{m^2}{Hz}\cdot(0.1003Hz - 0.0999Hz) = 0.06236m^2 \tag{2.7}$$

The variance of the sea surface elevation is also given by the zero-th moment of the energy density spectrum $m_0 = \underline{\overline{\eta}}^2$. This defines the significant wave height for deep water as;

$$H_s = 4\sqrt{m_0} = 4\sqrt{\underline{\overline{\eta}}^2} \Rightarrow 4\sqrt{\eta^2} = 4\sqrt{0.06236m^2} = 0.999m \approx 1.0m \tag{2.8}$$

The significant wave height was set up to be 1 meter, which is the value that we got.

Total energy of this one wave;

$$J_{tot} = \frac{1}{2}\rho_w g\underline{\overline{\eta}}^2 \Rightarrow \frac{1}{2}\rho_w g\eta^2 = \frac{1}{2}\cdot 1025\frac{kg}{m^3}\cdot 9.81\frac{m}{s^2}\cdot 0.06236m^2 = 313.52\frac{J}{m^2} \tag{2.9}$$

The point of these calculations is to show the consequences of choosing a wrong spectral distribution Δf and frequency ranges. The comparisons will be done with a narrow Gaussian shape a bit later.

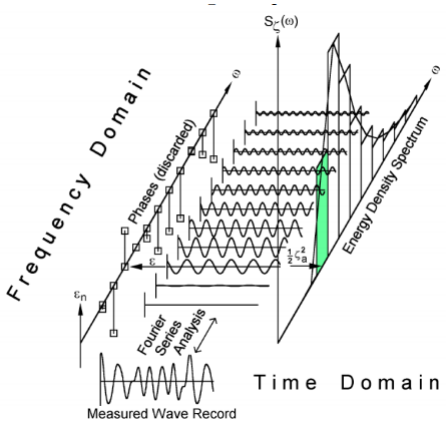

Figure 2.6: Energy density spectrum[16]

A 2D directional energy density spectrum $E(f,\theta)$ describes how the energy is spread out in the domain. The directional spectrum in figure 2.7a has been modelled with a high power "m" of 500, this gives a directional spreading σ_θ 2.56° (see table 2.1). This makes the energy density to be concentrated at one direction (the peak wave direction θ_p), which makes it long crested.

As for the figure 2.7b, the power "m" has been set to 3, which makes it short crested. This plot is very thin, that is because the waves are of only one frequency bin.

If we integrate the 2D directional energy density spectrum $E(f,\theta)$ over the directions θ we get the concentrated energy in a 1D energy density spectrum as shown in figure 2.5. This is the case for both long and short crested waves (shapes will differ).

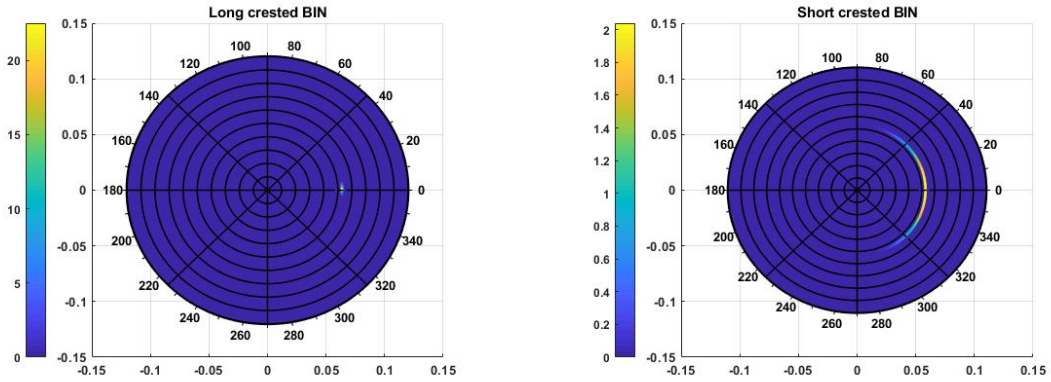

(a) Long crested frequency BIN. *(b) Short crested frequency BIN.*

Figure 2.7: A 2D directional wave spectrum for long and short crested frequency BIN in θ- and f-space.

GAUSS -shape (Sea-surface elevation)

In the linear approximation of ocean waves, the instantaneous sea-surface elevation is a Gaussian distribution. Assuming the mean to be zero, the Gaussian probability density function can be written as [17]:

$$p(\eta) = \frac{1}{(2\pi m_0)^{1/2}} exp\left(-\frac{\eta^2}{2m_0}\right) \tag{2.10}$$

Where η is the sea-surface elevation and m_0 is the zero-th moment of the energy density spectrum.

The width of the Gaussian-shape frequency spectrum is controlled by the standard deviation $\overline{\eta}$ (σ_{fr} in SWAN). The larger the number the more the frequencies will be spread out in its domain (larger amount of random waves). This difference can be seen in figure 2.8 for a 1D spectrum and in figure 2.9 for 2D spectrum.

By decreasing the standard deviation ($\overline{\eta}$) we make the Gaussian shape to be narrower, which when narrow enough can represent a regular wave. This can be seen in figure 2.8a.

For simplicity we consider the same significant wave height and the peak wave period as before.

The frequency range of the spectrum shown in figure 2.8a and figure 2.8b is [flow] = 0.03 Hz and [fhigh] = 0.2 Hz. This is acceptable for the case in figure 2.8b, but not for the case in figure 2.8a. The latter one when compared to the frequency bin as shown in figure 2.5, got the same spectral distribution ($\Delta f = 50$) over a larger range. It so happens that we missed the desired frequency because of this. The frequency used to calculate the energy density for a regular wave is always the closest one. In this case it is $f = 0.1010$ Hz instead of $f = 0.1$ Hz. This does not sound much, but when considered that this spectrum is still not narrow enough, we result in a significant wave height (H_s) of 0.9699 meters.

Gaussian distribution is symmetrical, figure 2.8c show that the lowest frequency cut out is too high to show the entire shape. In this case the the lowest frequency [flow] would need to be somewhere between -0.3 Hz, or the peak wave frequency (f_p) would need to be moved to higher frequency of around 0.3 Hz ($T_p = 7s$).

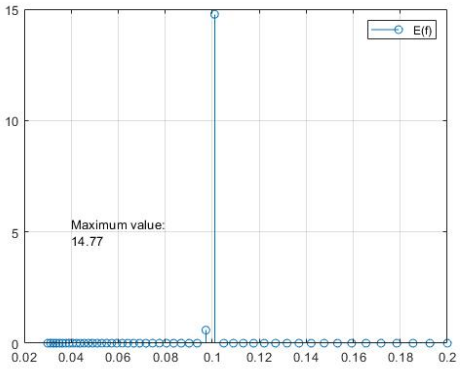

(a) 1D Gauss distribution for standard deviation $\underline{\overline{\eta}} = 0.001$.

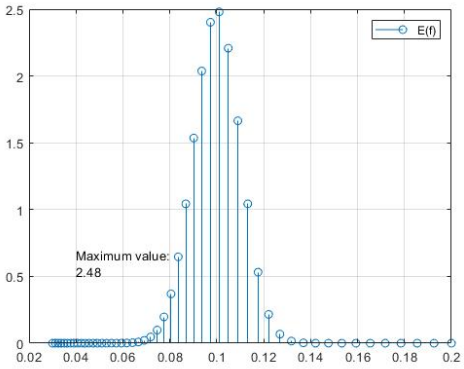

(b) 1D Gauss distribution for standard deviation $\underline{\overline{\eta}} = 0.01$.

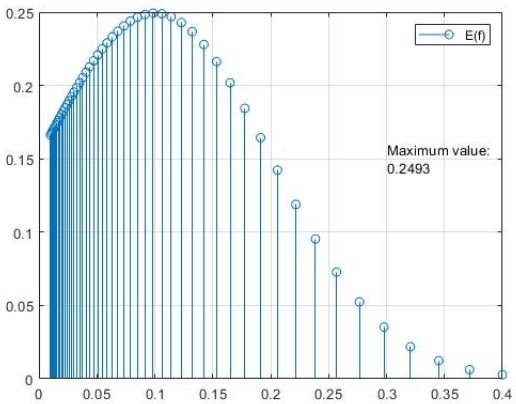

(c) 1D Gauss distribution for standard deviation $\underline{\overline{\eta}} = 0.1$.

Figure 2.8

The same set of calculations can be done for figure 2.8a as previously with BIN, but since the frequency range is much larger, we cannot expect the same result.

$$\underline{\overline{\eta}}^2 = \int_a^b E(f)df = E(f_m)(f_b - f_a) \Rightarrow \eta^2 = 14.77\frac{m^2}{Hz} \cdot (0.1049Hz - 0.1010Hz) = 0.0576m^2 \tag{2.11}$$

For the significant wave height;

$$H_s = 4\sqrt{m_0} = 4\sqrt{\underline{\overline{\eta}}^2} \Rightarrow 4\sqrt{\eta^2} = 4\sqrt{0.0576m^2} \approx 0.9600m \tag{2.12}$$

Values for the significant wave height obtained from SWAN are 0.9699 m.

Thereafter we can calculate the total energy J_{tot} of one harmonic wave;

$$J_{tot} = \frac{1}{2}\rho_w g\underline{\overline{\eta}}^2 \Rightarrow \frac{1}{2}\rho_w g\eta^2 = \frac{1}{2} \cdot 1025\frac{kg}{m^3} \cdot 9.81\frac{m}{s^2} \cdot 0.0576m^2 = 289.59\frac{J}{m^2} \tag{2.13}$$

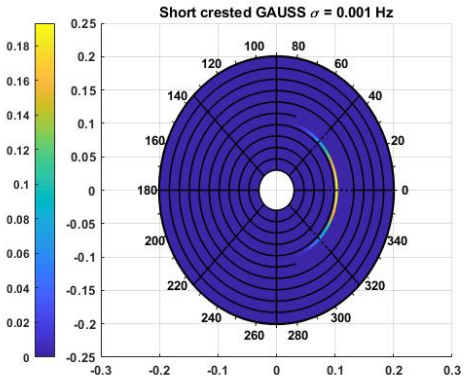

(a) Standard deviation $\underline{\overline{\eta}} = 0.001$.

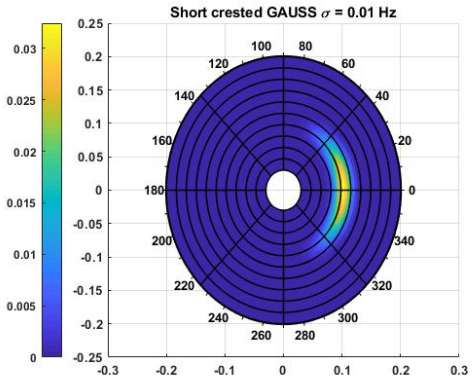

(b) Standard deviation $\underline{\overline{\eta}} = 0.01$.

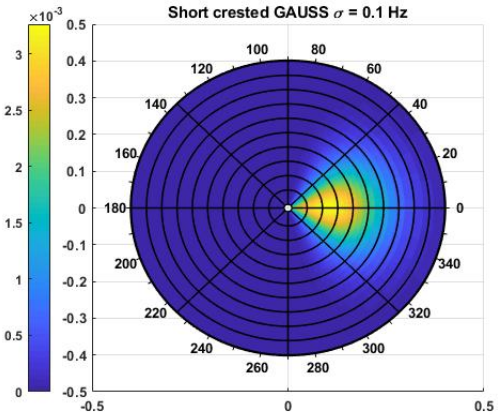

(c) Standard deviation $\underline{\overline{\eta}} = 0.1$.

Figure 2.9: 2D directional short crested GAUSS-shaped distribution.

In figures above we can clearly see how the wave energy is redistributed in f- and θ- space. Where figure 2.9c got its energy noticeable more redistributed over different frequencies than the other figures.

Pierson and Moskowitz

Pierson and Moskowitz is the second most used spectral shape behind JONSWAP, but it is also the simplest for defining the irregular ocean waves.

The assumption here is that if wind blew steadily for a long time over a large area, the wave would come into equilibrium with the wind. This is called a fully developed spectrum or sea, which occurs only in spacial cases [18].

In SWAN we can simulate sea behaviour by defining the waves at the boundary as a Pierson and Moskowitz spectrum.

The fully developed spectrum (Pierson and Moskowitz) is described as [17];

$$E_{PM}(f) = \frac{\alpha_{PM} g^2}{(2\pi)^4 f^5} exp\left(-\frac{5}{4}\left(\frac{f}{f_{PM}}\right)^{-4}\right) \tag{2.14}$$

Where α_{PM} is the energy scale value for PM and f_{PM} is the peak frequency value for PM (for more information see "Waves in oceanic and coastal waters" p. 155 by Leo H. Holthuijsen).

To show this spectrum shape we limited the frequency range to the lowest frequency [flow] 0.03 Hz and the highest frequency [fhigh] 0.2 Hz. When we look at the figure 2.10b we see that this range could have been moved a little bit towards the lower frequencies.

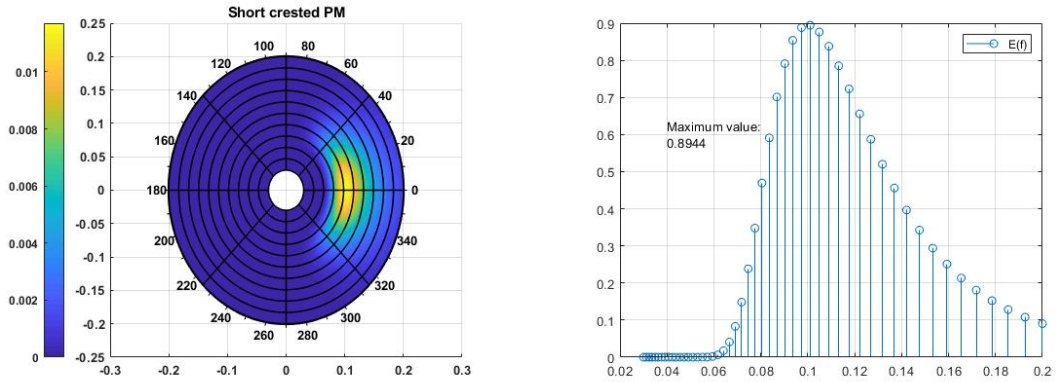

(a) 2D short crested directional PM spectrum. *(b) 1D short crested PM spectrum*

Figure 2.10: Pierson and Moskowitz spectrum done in SWAN.

The shape of a JONSWAP spectrum is based on Pierson and Moskowitz with added peak enhancement parameter (γ), which is a parameter that increases the peakedness of this spectrum. If this parameter is set to one ($\gamma = 1$), the JONSWAP shape will be the same as a Pierson and Moskowitz shape, this is shown in figure 2.12.

JONSWAP

JONSWAP (JOint North Sea WAve Project) is the most important wave spectrum for defining the irregular oceanic waves.

The spectra observed during the JONSWAP appeared to have a sharper peak than the Pierson and Moskowitz spectrum. To account for this in a parametrisation of the observations, the scientists of JONSWAP chose to sharpen the Pierson and Moskowitz spectrum (not its energy scale or frequency scale) and to enhance its peak with a peak-enhancement function $G(f)$:

$$G(f) = \gamma^{exp\left[-\frac{1}{2}\left(\frac{f/f_{PM}-1}{\sigma_j}\right)^2\right]} \tag{2.15}$$

Where γ is the peak-enhancement factor and σ_j is the pea-width parameter ($\sigma_j = \sigma_a$ for $f \leq f_p$ and $\sigma_j = \sigma_b$ for $f > f_p$)

This sharpens the spectrum peak, but has no effect on other parts of the spectrum. This idealised spectrum is called the JONSWAP spectrum. Its complete expression is [17];

$$E_{JONSWAP}(f) = \underbrace{\underbrace{\frac{\alpha_{PM} g^2}{(2\pi)^4 f^5} exp\left(-\frac{5}{4}\left(\frac{f}{f_{PM}}\right)^{-4}\right)}_{\text{Pierson and Moskowitz shape}} \gamma^{exp\left[-\frac{1}{2}\left(\frac{f/f_{PM}-1}{\sigma_j}\right)^2\right]}}_{\text{JONSWAP}} \tag{2.16}$$

Where α_{PM} is the energy scale value for PM and f_{PM} is the peak frequency value for PM (for more information about JONSWAP see "Waves in oceanic and coastal waters" p. 160 by Leo H. Holthuijsen).

In figures below we can see the effect that the peak-enhancement factor γ has on the shape of the JONSWAP spectrum. This yields both for the 1D and 2D spectrum.

Almost all models done in this rapport, are done with the JONSWAP spectrum with the peak-enhancement factor γ = 3.3 has been used. These figures have been used to determine the correct frequency range for Sulafjord wave models, where there are different peak frequencies.

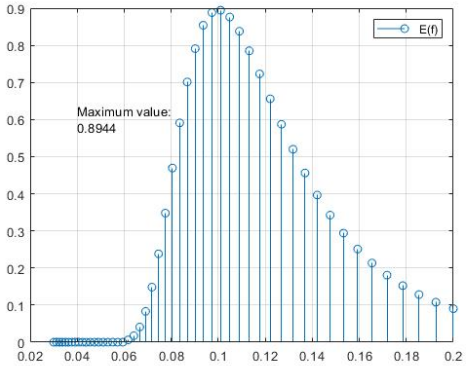

(a) peak-enhancement factor $\gamma = 1$

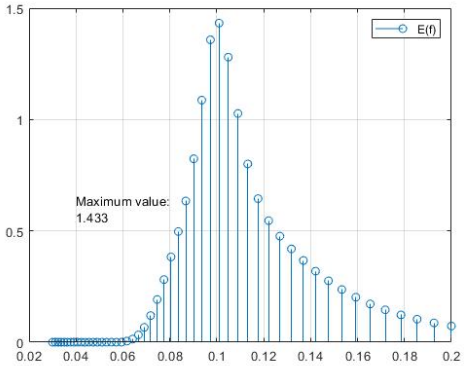

(b) peak-enhancement factor $\gamma = 2$

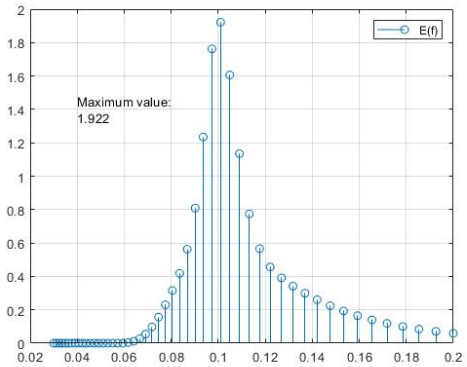

(c) peak-enhancement factor $\gamma = 3.3$

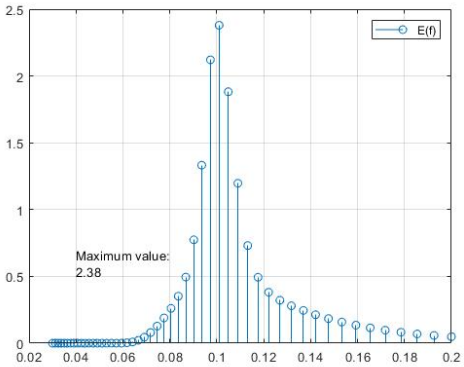

(d) peak-enhancement factor $\gamma = 5$

Figure 2.11: 1D short crested JONSWAP spectrum for the peak-enhancement factors $\gamma = 1$, $\gamma = 2$, $\gamma = 3.3$ and $\gamma = 5$

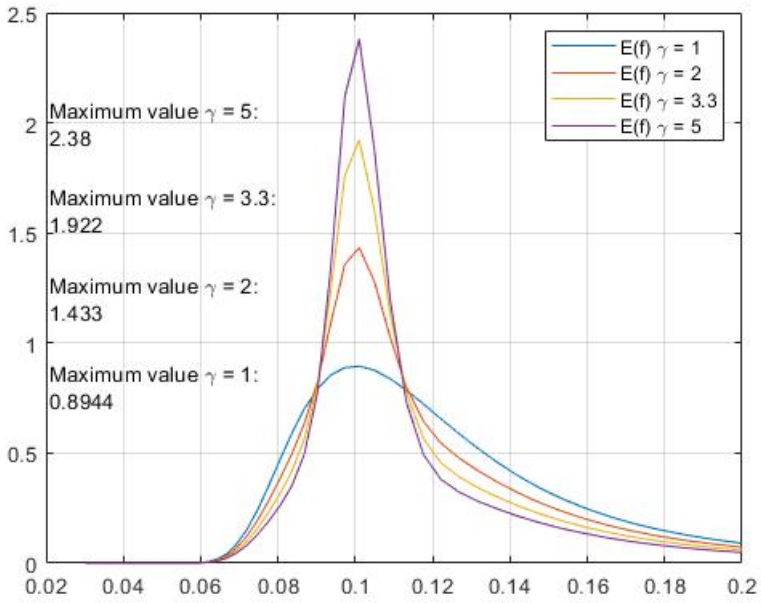

Figure 2.12: Multiple 1D plots of JONSWAP spectrum for the peak-enhancement factors $\gamma = 1$, $\gamma = 2$, $\gamma = 3.3$ and $\gamma = 5$

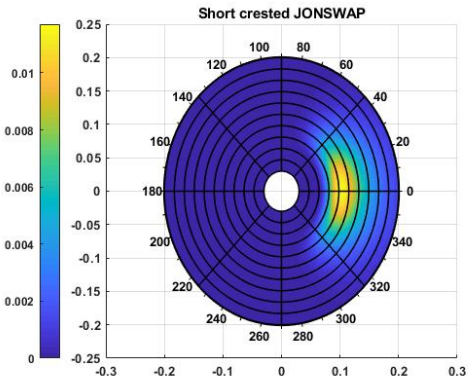

(a) peak-enhancement factor $\gamma = 1$

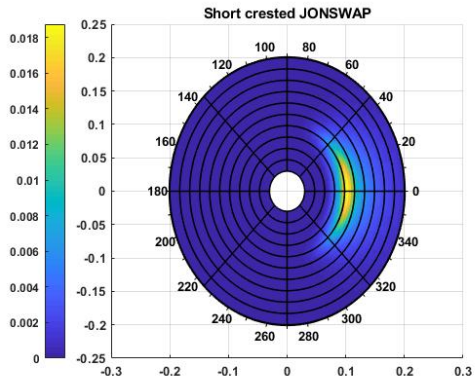

(b) peak-enhancement factor $\gamma = 2$

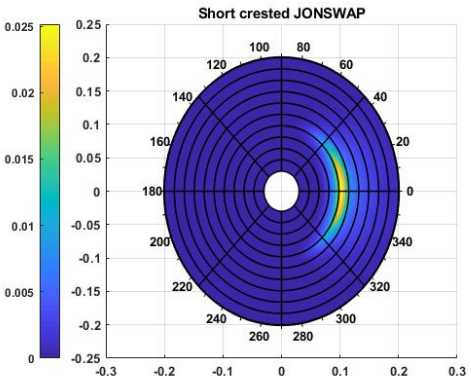

(c) peak-enhancement factor $\gamma = 3.3$

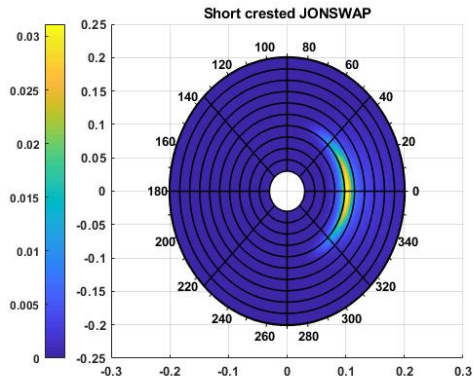

(d) peak-enhancement factor $\gamma = 5$

Figure 2.13: 2D directional short crested JONSWAP spectrum for the peak-enhancement factors $\gamma = 1$, $\gamma = 2$, $\gamma = 3.3$ *and* $\gamma = 5$

2.3 Wave models

2.3.1 Shoaling

As the wave propagates into shallower water, the phase speed approaches the group velocity and the wave becomes less and less dispersive.

Both the phase speed and the group velocity approach zero at the waterline. This has serious consequences for the applicability of the linear wave theory under such conditions, because it causes the wave amplitude to go to infinity (see below).

$$a_2 = \sqrt{\frac{c_{g,1}}{c_{g,2}}} a_1 \tag{2.17}$$

Where a is the wave amplitude and c_g is the group velocity.

The above energy balance shows that, as the group velocity approaches zero at the waterline, the wave amplitude theoretically goes to infinity. Obviously, the theory breaks down long before that. In addition, other processes such as refraction and wave breaking may well cause a totally different evolution of the waves over an arbitrary seabed topography.

Phase speed and group velocity;

$$c_p = \sqrt{\frac{g}{k}\tanh(kd)} \qquad c_g = \frac{1}{2}\left[1 + \frac{2kd}{\sinh(2kd)}\right]c_p \tag{2.18}$$

Where k is the wave number, d is the water depth and g is the gravitational acceleration.

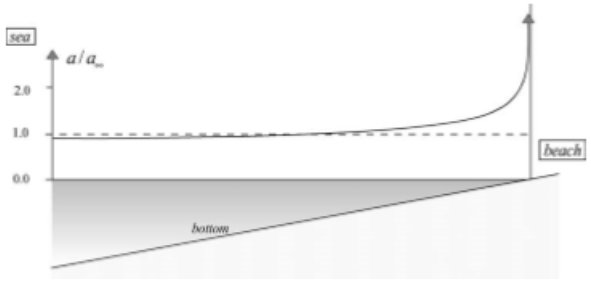

Figure 2.14: Wave amplitude evolution due to shoaling [2].

Shoaling wave model

We can present a simple model of shoaling in SWAN. For this we can consider a wave propagating perpendicularly towards the beach for two slopes, a small and a large slope. That way we can can show effects that occur on larger slopes, effects like wave setdown.

If we look at figure 2.18a, which shows the significant wave height for a large slope. We can notice a decline in the significant wave height at approx. 300 meters. This happens persistently when a wave propagates from relatively deep to shallow water, over a large slope, where the effect spikes (can also be observed later in figure 2.34a). This effect will be explained later.

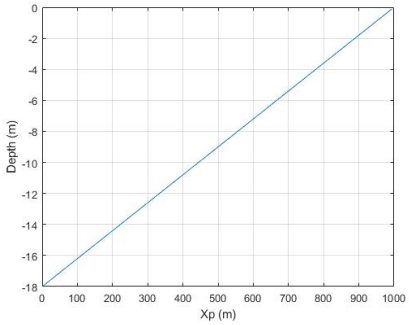

Figure 2.15: Depth = 18.0 m

It has been mentioned above that the phase speed and the group velocity will both eventually approach zero at the waterline. This caused for the wave amplitude to shoot up to infinity. In reality the wave will break before that happens.

In figure 2.18a and 2.17a we can notice that the wave amplitude does indeed go to infinity. To counteract this, we can introduce depth-induced breaking into this numerical model. This will make sure that the energy will dissipate accordingly when the wave propagates.

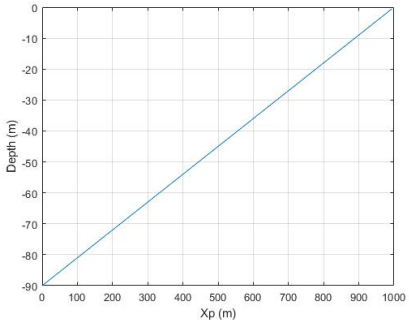

Figure 2.16: Depth = 90 m

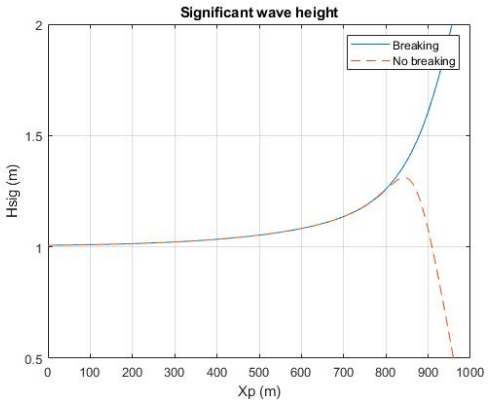

(a) Significant wave height at depth 18.0 meters.

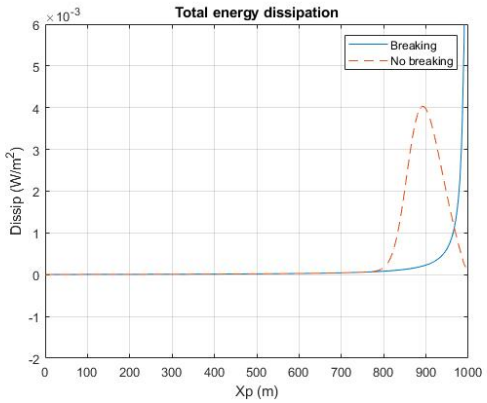

(b) Total energy dissipation at depth 18.0 meters (S_{tot})

Figure 2.17

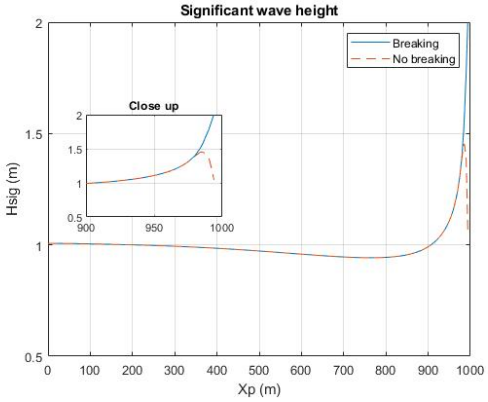

(a) Significant wave height at depth 90.0 meters.

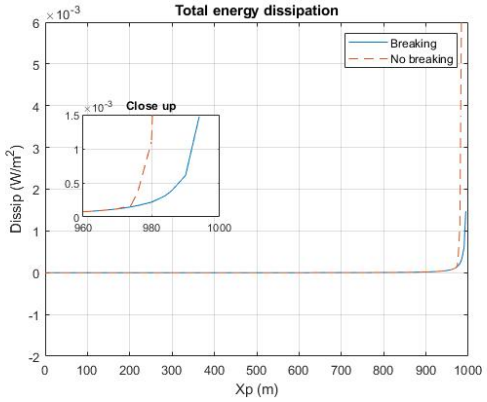

(b) Total energy dissipation at depth 90.0 meters (S_{tot})

Figure 2.18

Wave setup and setdown

In fluid dynamics, wave setup is the increase in mean water level due to the presence of breaking waves. Similarly, wave setdown is a wave-induced decrease of the mean water level before the waves break (during the shoaling process). For short, the whole phenomenon is often denoted as wave setup, including both increase and decrease of mean elevation. This setup is primarily present in and near the coastal surf zone [19].

There is a command in SWAN called "setup", which accounts for the wave-induced setup.

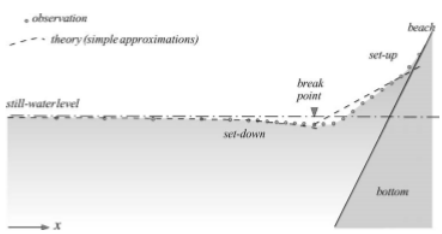

Figure 2.19: Step-up and step-down induced by waves approaching a very steep beach[2].

2.3.2 Diffraction

Diffraction in SWAN is very limited. Spectral action balance equation models usually neglects diffraction in order to be more computational friendly. The same goes for SWAN.

To accommodate diffraction in SWAN simulations, a phase-decoupled refraction-diffraction approximation is suggested. This allows for SWAN to still make simple diffraction approximations.

Nevertheless diffraction in SWAN should not be used when;

- An obstacle or coastline covers a significant part of the down-wave view.
- The distance to that obstacle or coastline is small (less than a few wave length).
- The reflection off that obstacle or coastline is coherent.
- The reflection coefficient is significant.

This implies that the SWAN diffraction approximation can be used in most situations near absorbing or reflecting coastlines of ocean, seas, bays, lagoons and fjords with an occasional obstacle such as islands, breakwaters, or headlands but NOT in harbour or in front of reflecting breakwaters or near wall-defined cliff walls. The SWAN results seem reasonable if the above conditions are met [14].

Diffraction model

To model diffraction in SWAN, we need to create a depth that involves absorbing breakwaters.

A command in SWAN called "obstacle" cannot be used since it models reflecting obstacles. This will usually yield no result after computation. What can be done instead is to model a land mass in the bottom file.

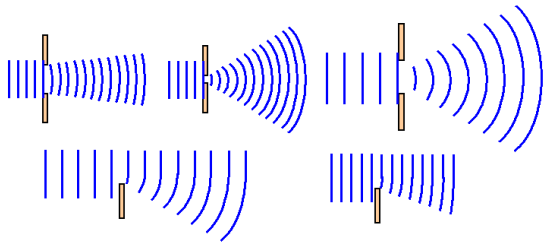

Figure 2.20: Simple cases that show diffraction

The boundaries in SWAN are either land or water. Land in SWAN does not generate waves and it fully absorbs wave energy (which is what we need for diffraction to work).

	Aperture $[m]$	$\Delta x[m]$	$\Delta y[m]$	$\lambda_p[m]$
Figure 2.21a	50	50	25	6.25
Figure 2.21b	150	50	25	6.25

Table 2.2

We assume a monochromatic[2] wave propagating from the west side of the domain. Its significant wave height (H_s) is 0.2 meters and peak wave period (T_p) is 2.0 sec.

Plots of diffraction done in SWAN can be seen on the next page.

[2] It's a wave with a single wavelength and frequency. Harmonic and long crested.

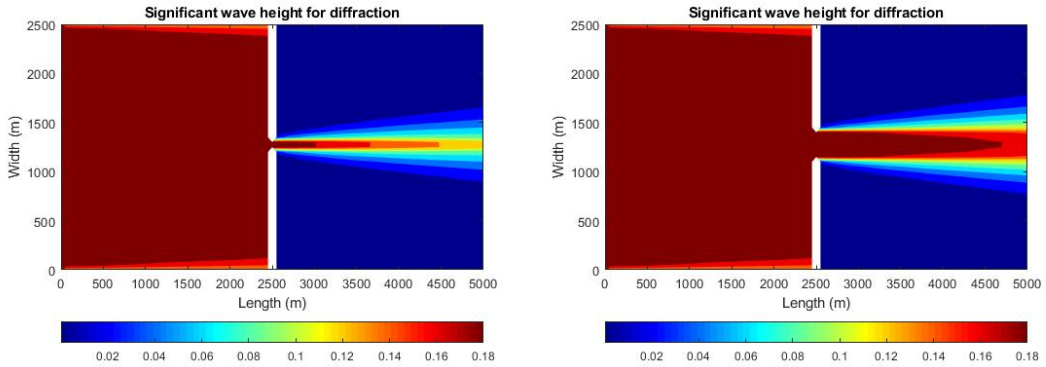

(a) *(b)*

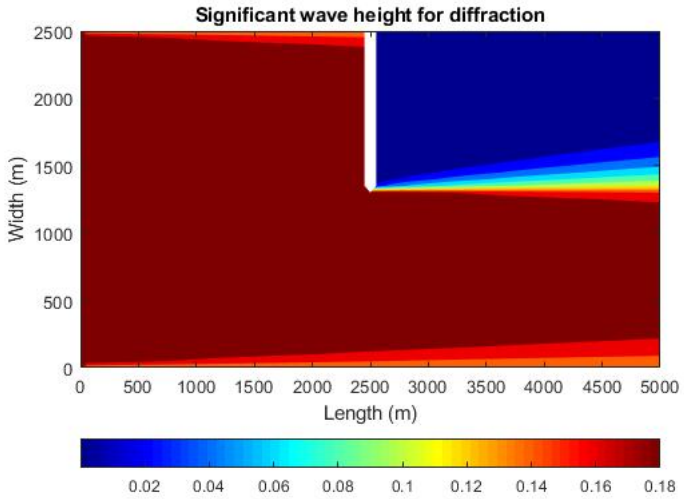

(c)

Figure 2.21

2.3.3 Depth-Induced breaking

Wave breaking is arguably the most important process that waves are subjected to. Unfortunately it is also one of the most difficult process to describe mathematically.

At shallow waters, the waves energy dissipate decisively due to the influence of the bottom depth. Depth can cause the wave to plunge when a certain wave steepness is reached, it can cause the wave to spill its energy to the sides (spilling) or also cause it to surge when the beach slope is large. The model of wave breaking in SWAN corresponds to the theory, where the slopes of the seabed will be gradually increased. in SWAN there is no clear way to identify what kind of breaking occurs. For this this section will include the iribarren number, which will help use understand what breaking should theoretically happen.

In this section we will use the iribarren number to determine the range of these different breakages (as mentioned in section 1.1.3). Thereafter model them accordingly to get spilling, plunging and surging breakage, and run a simulation with SWAN. The collapsing breaking will be ignored, since it happens between a plunging and surging breaking, with no clear definition of its own. This data might be proven useful further when looking at the results of Sulafjorden.

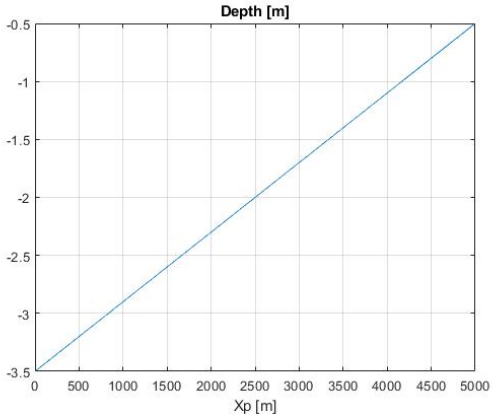

Figure 2.22: A depth used to simulate spilling breaking, with a slope of 3:5000.

Spilling breaking

Spilling breaking occurs when a wave propagates in shallow water along a flat, or a very small sloped seabed. A spilling breakage is defined when the iribarren number (the surf similarity parameter) is below 0.5 ($\xi_\infty < 0.5$).

The wave will gradually spill its energy over the distance traveled towards the shore, it will result in a steady decline in wave amplitude and wave length due to it slowing down, until it reaches land or it loses all of its energy while propagating.

We want to create a model to simulate that satisfies these conditions. For this purpose we decided to input a significant wave height as one meter (H_s = 1.0 meter), the peak wave period (T_p) as 10.0 seconds, directional width σ_θ = 27.6° and a JONSWAP-shaped frequency spectrum with a peak enhancement parameter γ = 3.3.

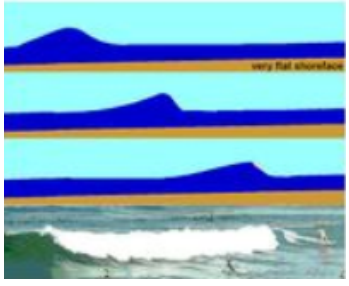

Figure 2.23: Spilling breaking

As the wave propagates, the energy is supposed to spill gradually to the base or to the sides. This will cause a continuous decline in the significant wave height, this can be seen in figure 2.24a.

This dissipation is mainly caused due to surf effect (figure 2.24b.), but also due to the bottom friction and the triad wave-wave interactions.

The calculation of iribarren number;

$$\xi_\infty = \frac{\tan\alpha}{\sqrt{H_\infty/\lambda_\infty}} = \frac{3/5000}{\sqrt{1.0m/156.0m}} = 7.5\cdot 10^{-3} \tag{2.19}$$

The iribarren number shown in 2.19 is much lower than the limit number where the spilling should occur ($7.5 * 10^{-3} << 0.5$). The parameters can be changed to a slope of 0.04 ($\alpha = 2.0°$), which gives a depth of approx. 200 meters. These values can be used next time when simulating spilling.

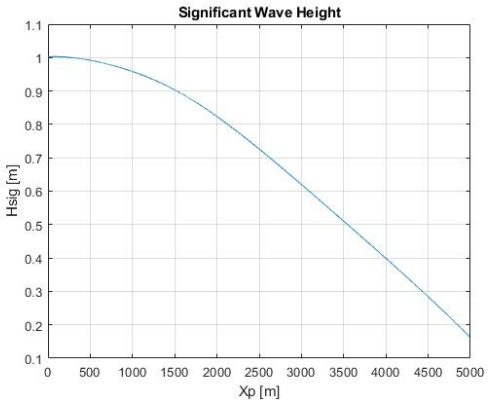

(a) Significant wave height. for spilling breaking (H_s)

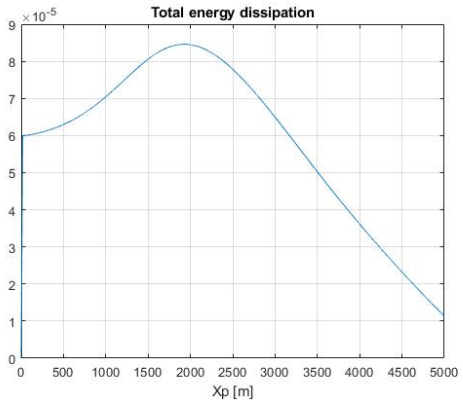

(b) Total energy dissipation (S_{tot})

Figure 2.24

A spilling breaking cannot reach a steepness $\left(\frac{H_s}{\lambda_a}\right)$ ratio that will cause it to break by plunging. To validate this model we need to determine the wave steepness, and compare it to the breaking criterion $H_b/\lambda_a = 0.142. * \tanh(kd)$. Where H_b is the maximum wave height, λ_a is the average wave length, k is the wave number and d is the water depth. The steepness values from SWAN are calculated by taking a ration between the significant wave height over the average wave length at each point.

The plots of these values can be seen in figure 2.25.

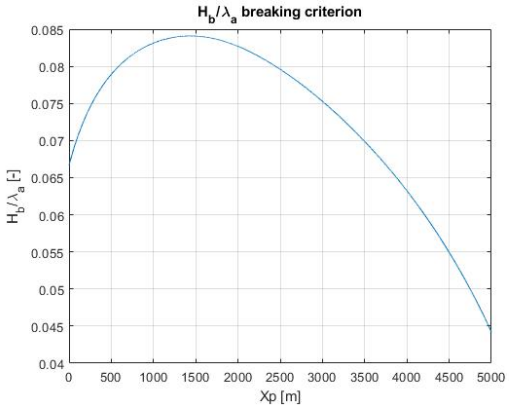

(a) Breaking criterion. Steepness at which the wave should break.

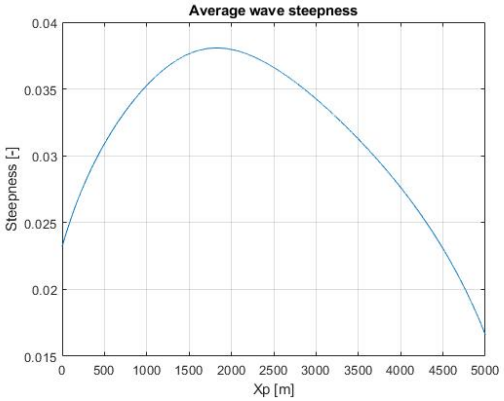

(b) Average wave steepness. Calculated from SWAN.

Figure 2.25: Steepness limit and steepness value

The occurring effects are expected to happen, which satisfies the general theory behind spilling breaking. To our understanding SWAN gave satisfactional results based on the theoretical input. This comes from a conclusion that the wave steepness does not exceed the breaking criterion, the significant wave height and the energy dissipation gradually decreases, which is what we expected.

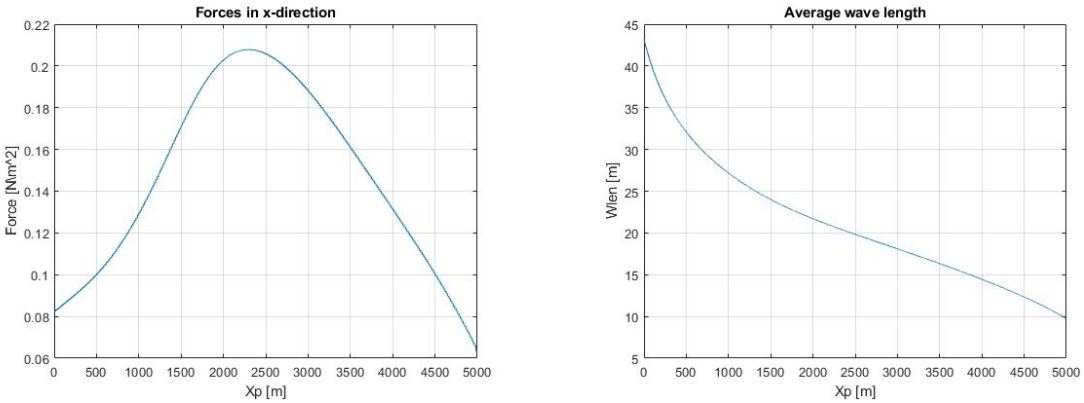

(a) Forces *(b) Average wave length.*

Figure 2.26: Forces in x-direction and average wave length

Plunging breaking

A wave plunges when the front face become vertical, where it eventually falls into the base of the wave. This happens when the wave approaches a moderately steep seabed. Where, eventually at a point the wave becomes too steep and breaks.

A plunging breaking is defined when the iribarren number is between 0.5 and 3.3 ($0.5 < \xi_\infty < 3.3$).

To verify the effects of plunging breaking in SWAN we can consider the same wave parameters as mentioned previously.

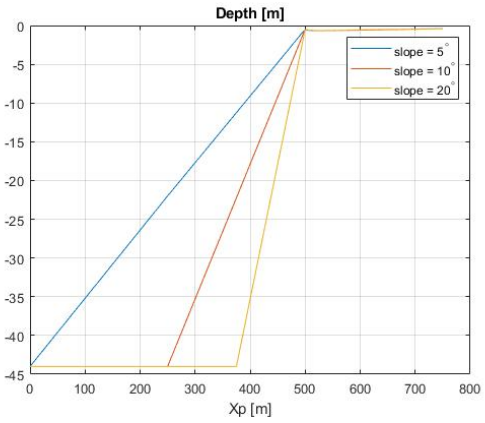

Figure 2.27: A depth used to simulate and compare plunging breaking of different slopes. Slopes used are 11:125, 22:125 and 44:125.

To better show this effect we can consider a wave propagating towards a bottom angle of 5°, 10° and 20°.

We can also compare them by making the slopes end at the same point, and give them the same maximum depth.

Seabed angle (α)	Slope	Iribarren number (ξ_∞)
5°	11:125	1.1
10°	22:125	2.2
20°	44:125	4.4

Table 2.3: Iribarren number for these three slopes.

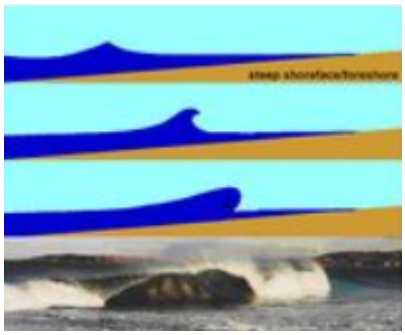

Figure 2.28: Plunging breaking

Table 2.3 gives the values of iribarren number at each slope.

We can notice that the iribarren number for the slope of $\alpha = 20°$ is way above the limit. This indicates that the breaking should be either a surging or a collapsing. The thing that is certain is that it will have many similarities to the surging breaking shown next.

Before proceeding to show the results, we can make some assumption as to how the waves will behave.

When we look at the depths shown in figure 2.27 we can conclude that the significant wave height will start increasing at the lowest slope first, this will cause a gradual surf dissipation at first. As for the higher slopes the energy dissipation will be more sudden and the wave amplitude will steepen faster. These results can be observed in figure 2.30.

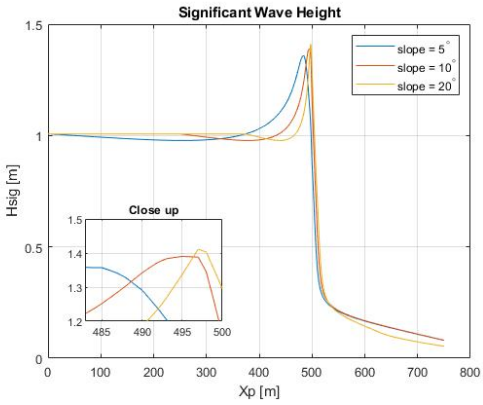

(a) Significant wave height, for plunging breaking.

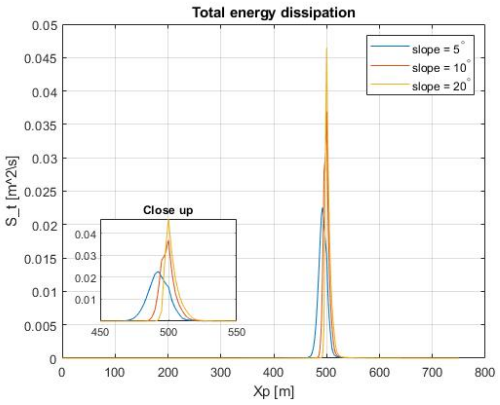

(b) Close up of the total energy dissipation.

Figure 2.29

A plot of wave steepness generated from SWAN can be seen on figure 2.30b. We can notice that at the point of discontinuity (500 meters), the steepness is way above the breaking limit. If we look closer at these figures 2.30, we can also notice that few meters before the discontinuity, the steepness of these cases are equal to the limit shown in figure 2.30a. This matches the significant wave height shown in figure 2.29a quite well.

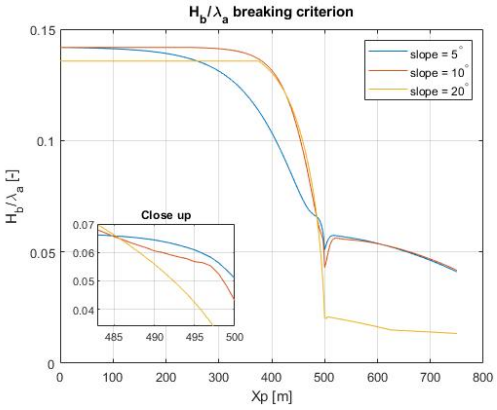

(a) Steepness at which the wave should break. Breaking limit.

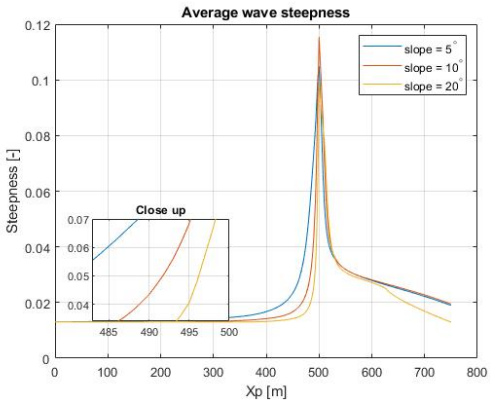

(b) Average wave steepness, computed from SWAN.

Figure 2.30: Steepness limit and steepness value

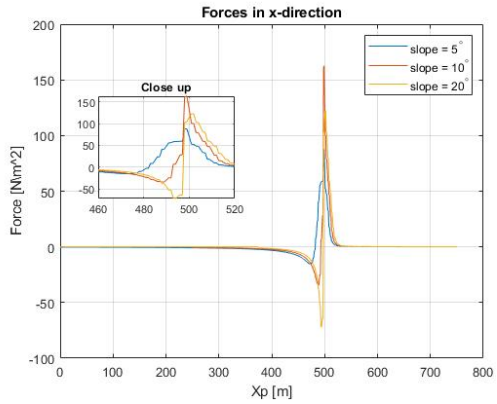

(a) Wave-induced force per unit surface area

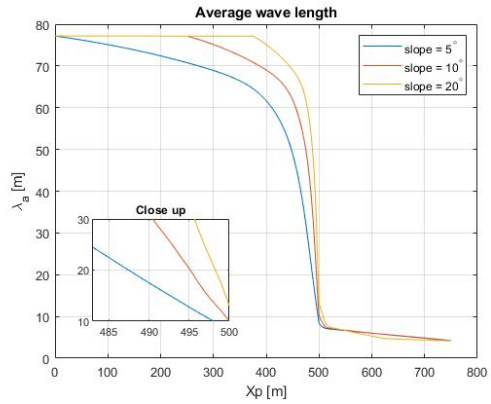

(b) Average wave length

Figure 2.31: Wave-induced force and average wave length

When a wave breaks it turns its wave energy into a turbulent energy. For larger slopes this energy will spike around one location. This may cause severe structural damage. In SWAN we can plot the wave induced forces. Forces for plunging breaking can be seen in figure 2.31.

As mentioned before, we cannot determine what kind of breaking will occur. What we can conclude is that the waves break at around the maximum wave height as they are supposed to.

What also happened is that the largest slope does not look that much different from the other two, but it does hold a lot of similarities to a surging breakage. The wave steepness for this case do exceed the breaking criterion. This do seem like a collapsing breaking. The wave height and the setdown effect did spike more for this slope.

Surging breaking

A surging breaking occurs when a wave approaches a relatively steep seabed. These waves do not break, instead they surge up and down the slope with most of its energy being reflected. Surging wave breaking is defined at iribarren number larger than 3.3 ($\xi_\infty > 3.3$).

To recreate this process in SWAN, we assume a large slope of 200:250, this gives a angle of approx. 40°. The significant wave height and peak period still remains as 1.0 meters and 10 seconds.

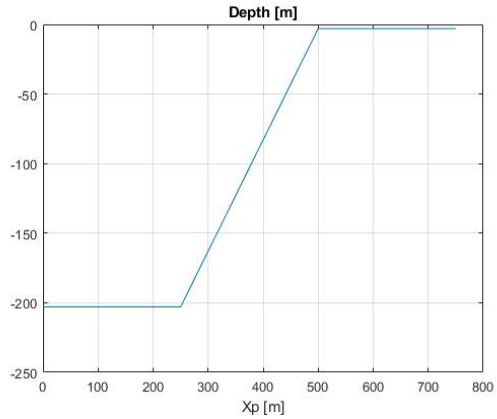

Figure 2.32: A depth used to simulate surging breaking at slope 200:250.

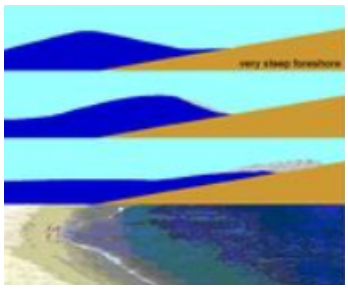

Figure 2.33: Surging breaking

The calculation of iribarren number;

$$\xi_\infty = \frac{\tan\alpha}{\sqrt{H_\infty/\lambda_\infty}} = \frac{200/250}{\sqrt{1.0m/156.0m}} = 10 \qquad (2.20)$$

In equation 2.20 we can notice that the iribarren number for this slope is way above the definition value (10 >> 3.3). The slope can be significantly reduced, this will cause for the results to be similar to the previous case in plunging (seabed angle α = 20°). To be within the limits, we could have change the parameters to a bottom slope of 0.2642, seabed angle α = 14.8°, which gives a depth = 66m and a domain length of 250 m. Regardless, the value of 10 can be still used as an example.

As the wave propagates towards the shore, the wave will quickly steepen and cause a large portion of its energy to dissipate fast. This is because of the seabed slope being large, which causes a fast transition between depth contours. The rest of the energy will dissipate later while it propagates further into land. This can be seen in figure 2.34b.

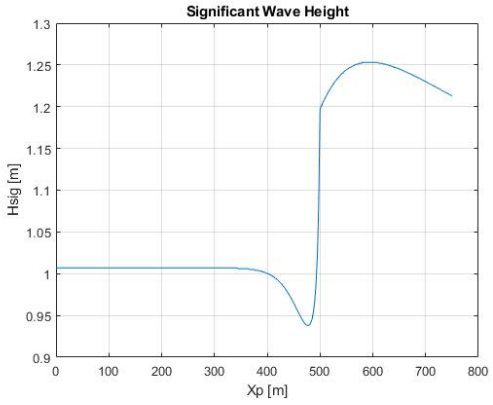

(a) Significant wave height for a surging breakage.

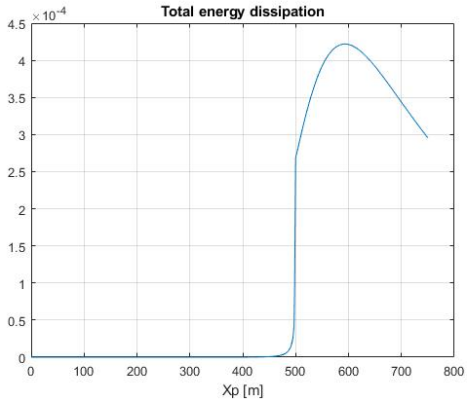

(b) Total energy dissipation

Figure 2.34

It has been mentioned before that a surging breakage is not supposed to break. To check if that is true in this case, we need to plot a figure that shows the steepness of the wave and the wave breaking criterion, exactly like before. The results can be seen in figure 2.35.

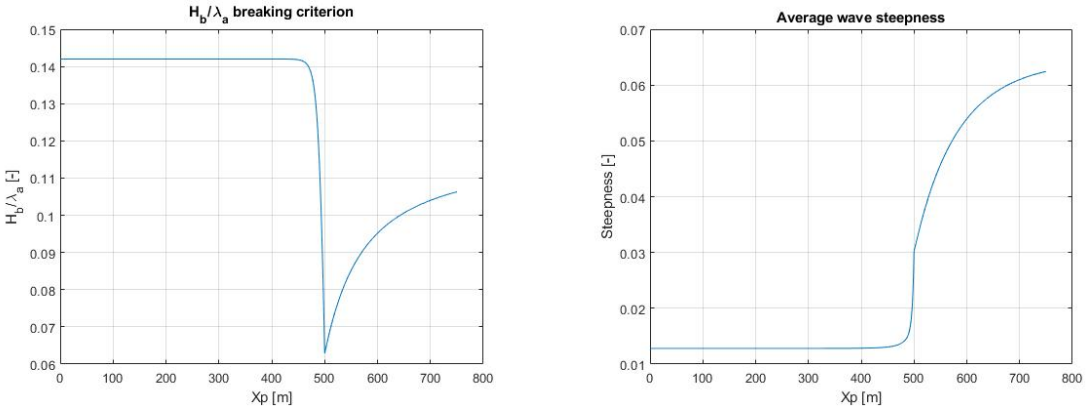

(a) Breaking criterion *(b) Average steepness of the wave*

Figure 2.35: Breaking criterion and the average steepness with close up windows

There are few things that can be concluded from running this model. The first is that the wave does not seem to break like the waves shown in plunging section.

A surging breaking is supposed to be reflecting and when we look at the figure 2.36b we can see that there is a much larger force reflection than in the previous cases. This seems to satisfy the theory.

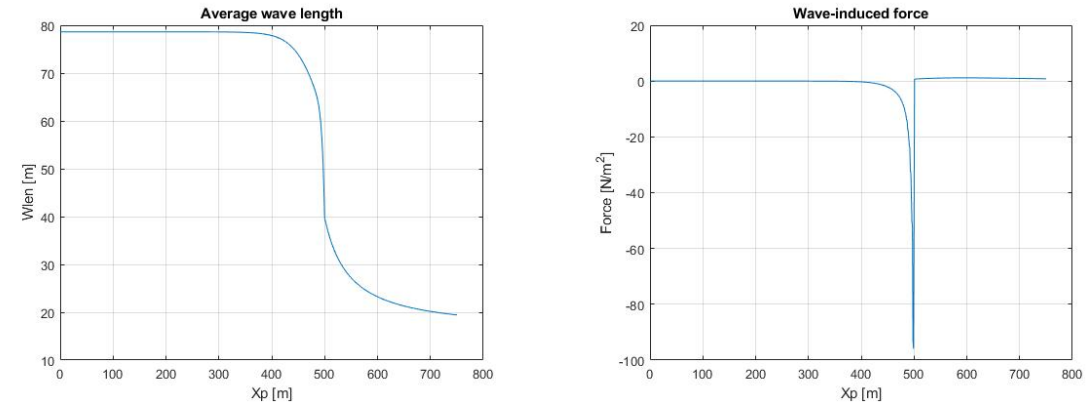

(a) Average wave length *(b) Forces in x-direction*

Figure 2.36

Bibliography

[1] College of liberal arts and science. Nearshore wave information - http://users.clas.ufl.edu/adamsp/Outgoing/GLY4734_Spring2014/S11_PropShoalRefrac.pptx.pdf.

[2] Leo H. Holthuijsen. *Waves in oceanic and coastal waters*. Cambridge university press, Cambridge University Press The Edinburgh Building, Cambridge CB2 8RU, UK, 2007.

[3] Verbcatcher. Diffraction - https://commons.wikimedia.org/w/index.php?curid=68991367.

[4] Wikipedia. Diffraction - https://en.wikipedia.org/wiki/Diffraction.

[5] Mayilvahanan Alagan Chella. Breaking wave characteristics and breaking wave forces on slender cylinders.

[6] Klaus Hasselmann. On the spectral dissipation of ocean waves due to white capping*.

[7] Coastalwiki. Wave transformation - http://www.coastalwiki.org/wiki/Wave_transformation.

[8] Mayilvahanan Alagan Chella. Breaking wave characteristics and breaking wave forces on slender cylinders.

[9] Kyle Stock. The science of breaking waves - https://www.theinertia.com/surf.

[10] Surfertoday. The four types of breaking waves - https://www.surfertoday.com/surfing/the-four-types-of-breaking-waves.

[11] rlss poole lifeguard. Rookie lifeguard - http://www.rlss-poole.org.uk/wp-content/uploads/2013/10/1-Waves-Info.pdf.

[12] DNV-GL. Environmental conditions and environmental loads.

[13] L.H. Holthuijsen N. Booij and R.C. Ris. A third-generation wave model for coastal regions.

[14] The SWAN team. Swan scientific and technical documentation.

[15] G. Ph Van Vledder T.J Zitman A.J. Van der Westhuysen G.S. Stelling, L.H Holthuijsen. Wave physics in a tidal inlet.

[16] Karl Henning Halse. Marin hydrodynamikk: Havmiljøbeskrivelse – bølger 1.

[17] Leo H. Holthuijsen. *Waves in oceanic and coastal waters*. Cambridge university press, Cambridge University Press The Edinburgh Building, Cambridge CB2 8RU, UK, 2007.

[18] Wikiwaves. Ocean-wave spectra - https://wikiwaves.org/Ocean-Wave_Spectra.

[19] Wikipedia. Wave setup - https://en.wikipedia.org/wiki/Wave_setup.

Wave modelling in coastal areas
IP305012

Candidate: 10020

A thesis presented for the degree of
Bachelor of Science

Department of Civil and Environmental Engineering
Norwegian University of Science and Technology (NTNU)
Ålesund, Norway
May 19, 2019

Contents

Chapter 1

General theory

1.1 Wave theory

The first step in describing ocean waves is to consider the vertical motion of the sea surface at one horizontal position, for instance along a vertical pole at sea as addressed in the previous chapter. The ocean waves then manifest themselves as a surface moving up and down in time at that one location.

It is normal to classify ocean waves by their wavelength or period and "disturbing force", the force that originally created the waves. This information alone will tell a lot about how the wave will behave out on the ocean and how it will propagate towards land. Short wind generated waves will normally be easy to notice and predict, while longer waves like tsunamis can be hard to notice at first because of their long wavelength but can suddenly build up to really huge waves once they hit shallow water near shore.

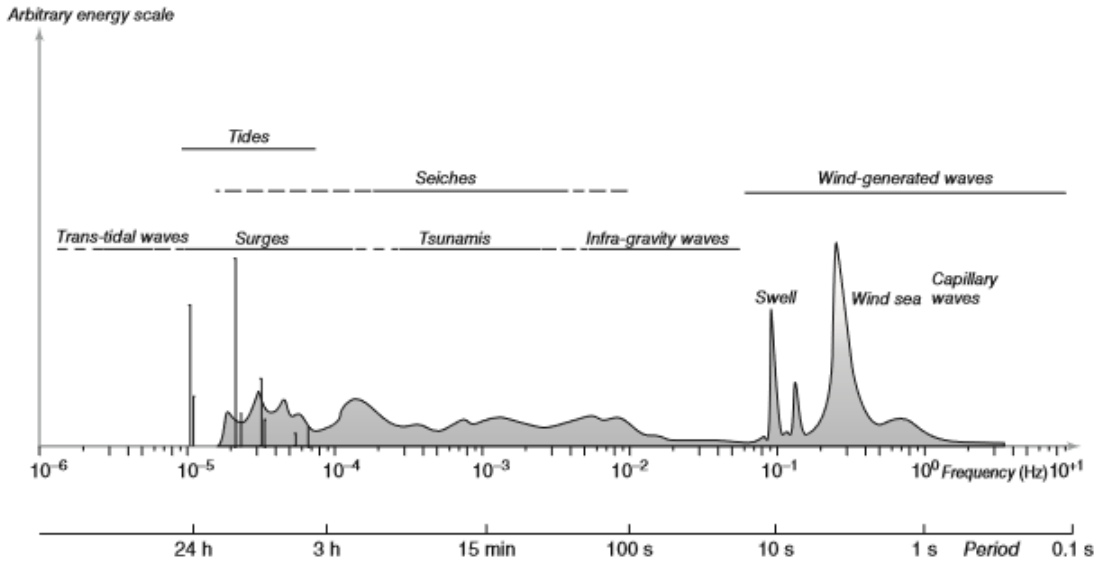

Figure 1.1: The frequencies and period of the vertical motions of the ocean surface [1]

With the definition of wave as "vertical motions of the ocean surface", the longest waves are trans-tidal waves and tides generated by low-frequency fluctuations in the Earth's crust, the rotation of the earth and the gravitational attraction of the moon and

the sun. Their wavelength can vary from a few hundred kilometers to half the circumference of the earth, with periods ranging from few hours to little more than a day at the most.

Next is waves generated by sudden changes to the seafloor, like earthquakes, landslides and volcanic eruptions under water. These are therefor called seismic sea wave or tsunamis. Like mentioned earlier tsunamis can be really dangerous and hard to predict. They normally have a period around 15-20 minutes and corresponding wavelength of about 200km.

Seiches waves are standing waves generated in enclosed or partially enclosed bodies of water like harbor, lakes, but can also happen at sea like the Adriatic Sea where the sea is partially enclosed by Italy. Seiches is often the result of distant waves, storm surges, seismic activity or change in atmospheric pressure that makes the body of water oscillate back and forth within the basin. Wavelength vary as a function of the basin size as the frequency is equal to the resonance frequency of the basin in which they occur. Seiches can be really hard to notice because of their really long wavelengths, and with periods up to several hours they are often mistaken for tides.

"Wind generated waves" can be split into 3 different groups, Capillary Waves, Wind waves and Swell. They are all generated by the effect of wind over water transferring wind energy into the water. The smallest of these waves are called Capillary waves with periods shorter than ¼ of a second which gives a wavelength of about 10 centimeters. Unlike wind waves and swells that are restored to equilibrium by gravity the restoring force of the smaller capillary waves are mainly the surface tension.

Wind generated waves with a period longer than 1/4 of a second, but shorter than 30 seconds are called wind sea/wind waves. These waves are irregular and short crested while they are in the wind affected area called the "fetch", where they are being generated by local winds.

In deep water, longer waves travel faster than shorter waves and leave the generating area faster. Once out of the wind affected zone these waves take on a regular and long-crested appearance and are called "swells". [1]. Swells travel huge distances and are unlike "Wind Sea" hardly affected by local winds.

"Infra Gravity waves" are generated when swells and shorter periods wind waves mix together and are most noticeable in shallow water where they can build up to huge and irregular waves.

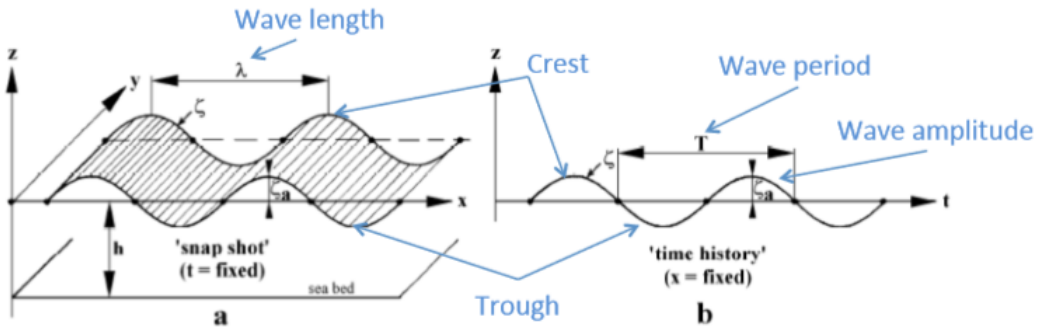

Figure 1.2: Linear ocean surface wave [2]

- Wave crest: Highest point of a wave.
- Wave trough: Lowest point of a wave.
- Wave height [H]: Distance between the through and the crest.
- Wave length [λ]: Distance between one crest and the next.
- Wave period [T]: The time required for the wave to travel one wave length.
- Wave frequency [f]: Number of waves over one unit time. Labeled as $f = 1/T$.
- Phase velocity: The propagation velocity of the wave form. Labeled as $c_p = \frac{\lambda}{T}$ for infinite depth.
- Group velocity: The velocity of multiple waves combined. Which is also the speed of the energy transfer.
- Significant wave height [H_s]: The mean of the highest one-third of waves in the wave record.

1.2 Shallow water vs. deep water

It is considered deep water if the depth is bigger than 1/2 the wavelength. In deep water the waves are not affected by the bottom and are normally only affected by winds and currents etc. As soon the depth is less than 1/2 wavelength it is called intermediate depth and the waves starts to "feel" the bottom.

The wave speed C and wavelength L decreases while wave height increases. When the depth is less than 1/20 of the wavelength it is called shallow water. In shallow waters the wavelength and wave speed is depth-dependent and decreases utterly while the period does not change. This results in increased wave height and eventually breaking of wave if the wave becomes too steep.

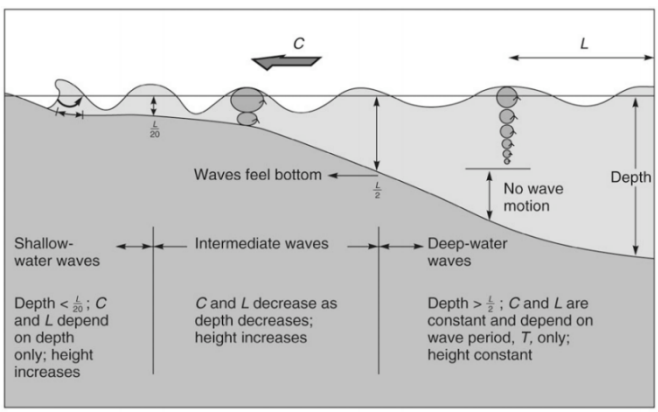

Figure 1.3: The influence of the depth on the particle motion [3]

Process	Oceanic waters	Coastal waters		
		Shelf seas	Nearshore	Harbour
Wind generation	•••	•••	•	○
Quadruplet wave–wave interactions	•••	•••	•	○
White-capping	•••	•••	•	○
Bottom friction	○	••	••	○
Current refraction / energy bunching	○/•	•	••	○
Bottom refraction / shoaling	○	••	•••	••
Breaking (depth-induced; surf)	○	•	•••	○
Triad wave–wave interactions	○	○	••	•
Reflection	○	○	•/••	•••
Diffraction	○	○	•	•••

••• = dominant, •• = significant but not dominant, • = of minor importance, ○ = negligible.

Figure 1.4: The relative importance of the various processes affecting the evolution of waves in oceanic and coastal waters (after Battjes, 1994)[1]

1.3 Effects in shallow water

1.3.1 Refraction

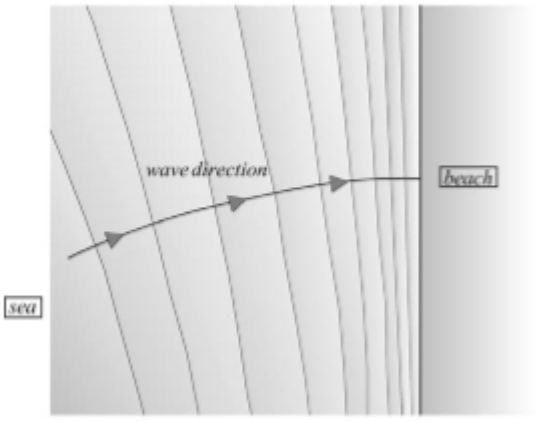

Figure 1.5: Refraction [1]

When waves propagate towards a shore at an angle they tend to bend and become aligned parallel with the shoreline. This effect is called refraction and is caused by the fact that the waves propagate more slowly in shallow water than in deep water. In a given time interval, the crest moves over a larger distance in deeper water than it does in shallower water (see figure 1.6) [1].

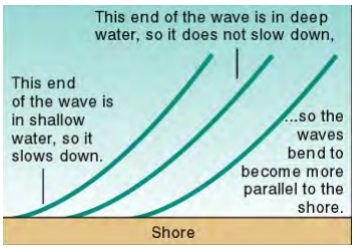

Figure 1.6: The change of wave [4]

As mentioned in the chapter about wave theory, once we are in shallow water the wave speed is dependent of the water depth. The result is that the waves bend towards the region with shallower water, i.e., towards the coast. This is a universal characteristic of waves: a wave always turns towards the region with lower propagation speed [1].

Normally the coastline is not straight and regular, but vary in both depth contours and outline, like bays, headlands and beaches.

Below, figure 1.7 showing wave refraction around headlands.

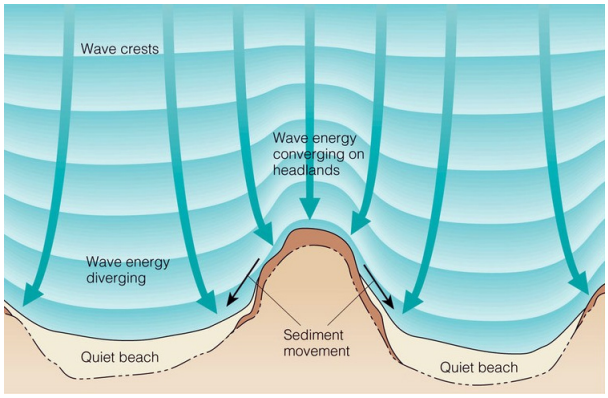

Figure 1.7: Refraction around headlands [5]

An interesting phenomenon happens when waves propagate towards a irregular coastline with headlands, as in figure 1.7. The waves will then converge on the headland, focusing the wave energy in a smaller area creating a bigger wave at this location. This is called Concave refraction.

The opposite happens when the wave propagates towards a larger, shallow water area like bays and such, see figure 1.7. Here the we get a defocusing of the waves, and the wave energy diverges, making a quite zone since the energy gets spread out over a larger area. This is called Convex refraction [6].

Wave refraction can also be caused by currents, which can reduce or increase parts of waves phase speed.

Wave refraction can also have a small impact on the amplitude of the wave [7].

Chapter 2

Modelling of coastal waves

2.1 Wave models

2.1.1 Refraction

When waves propagate towards land at an angel the wave crest will be turned towards the land and get aligned parallel with the depth contours, as mentioned is section 1.3.1. This is due to the change is Phase speed [c_p] along the wave crest.

The part of the wave in shallower water will move slower than parts of the wave in deeper water, which will have a bending effect of the wave crest turning it towards the shallower depth. When the waves enter shallow water the phase speed [c_p] becomes a function of water depth instead of wavelength as in deep water.

The equation of the phase speed at a arbitrary depth is;

$$c_p = \sqrt{\frac{g}{k} \cdot \tanh kd} \tag{2.1}$$

This equation can be further simplified to an equation for deep water ($\tanh kd \Rightarrow 1$) and shallow water ($\tanh kd \Rightarrow 0$).

$$c_{pD} = \sqrt{\frac{g}{k}} \qquad\qquad c_{pS} = \sqrt{g \cdot d} \tag{2.2}$$

Where c_{pD} is the phase speed for the deep water, c_{pS} is the phase speed for the shallow water, k is the wave number, d is the water depth and g is the gravitational acceleration.

For simpler cases where the depth contours are parallel the change of wave direction can be calculated by a simplified use of Snel's law.

$$\frac{\sin\theta}{c_p} = \text{Constant} \tag{2.3}$$

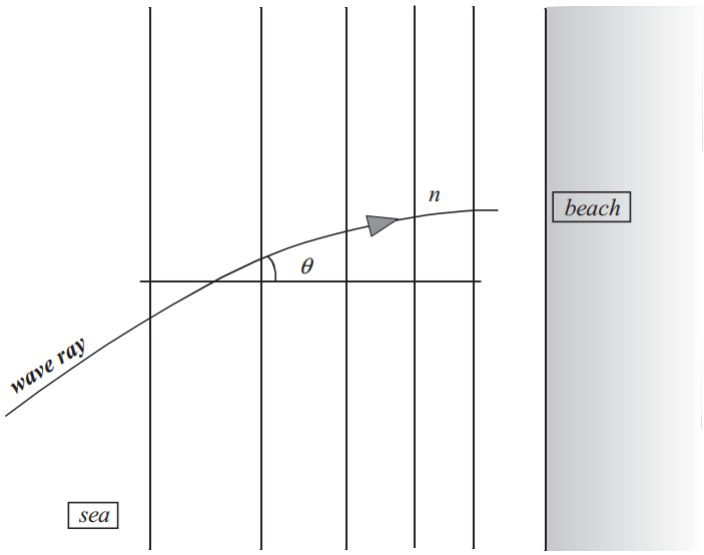

Figure 2.1: The angle θ in Snel's Law is taken between the wave ray and the normal to the straight and parallel depth contours[1].

Refraction wave model

To show the effect of refraction in SWAN a simple wave model was created. We modeled a simple wave propagating towards a beach, with parallel depth contours, at an angel of 30 degrees with respect to the width . The wave initial wave height was set to 1m and other inputs like wind and currents was ignored for this simulation.

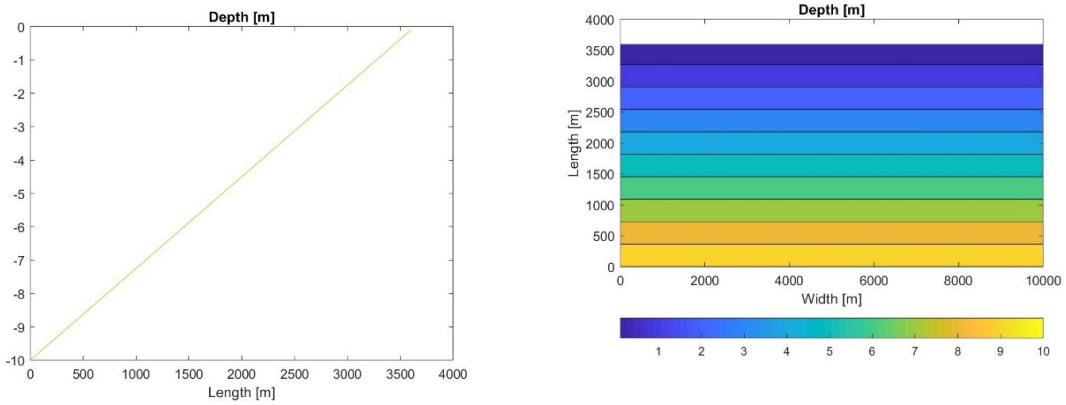

(a) One dimensional depth

(b) Two dimensional depth

Figure 2.2

The case we are running is a cutout from a considered long straight beach, with parallel depth contours going out in the water. Therefor we also included a segmented wave boundary on half of the east side in addition to the wave boundary on the whole of south side to get more realistic results.

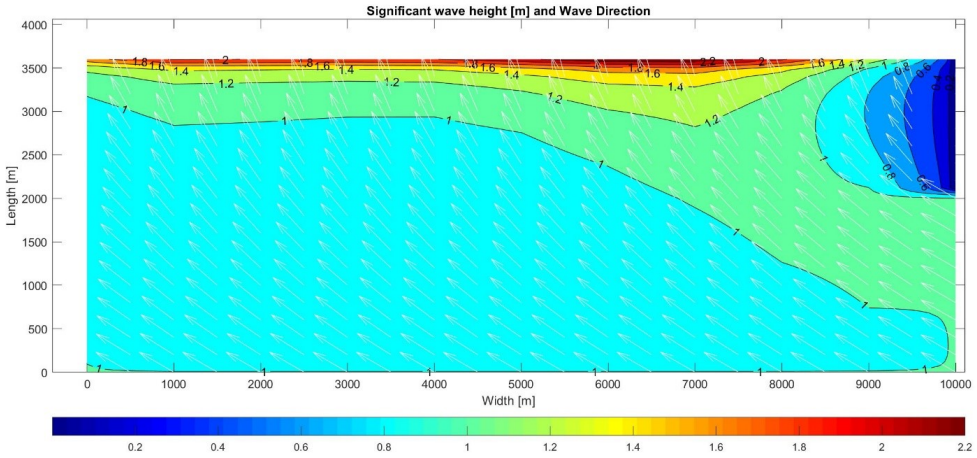

Figure 2.3: Resulting significant wave height with arrow showing the wave direction at $\theta_m = 30°$

As explained by the theory, we can clearly see the waves initially propagating at an angel of 30 degrees change direction towards the beach as they propagate along the width of the beach.

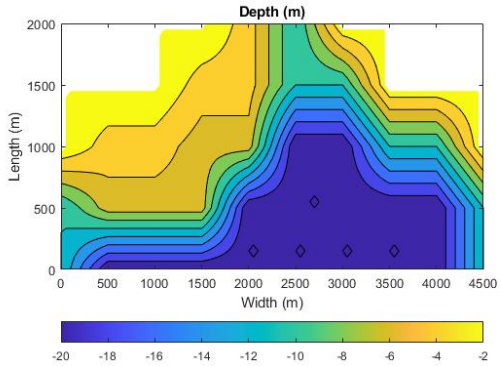

(a) A more complex depth

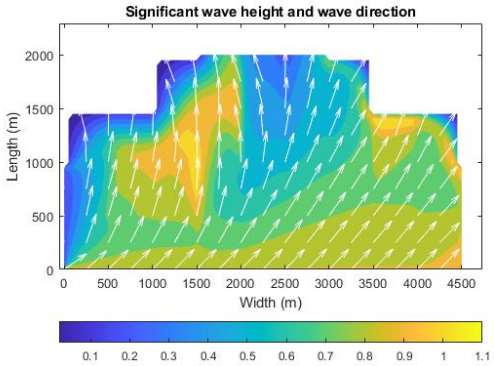

(b) Resulting significant wave height with arrow showing the wave direction at $\theta_m = 30°$

Figure 2.4

Bibliography

[1] Leo H. Holthuijsen. *Waves in oceanic and coastal waters*. Cambridge university press, Cambridge University Press The Edinburgh Building, Cambridge CB2 8RU, UK, 2007.

[2] Karl Henning Halse. Marin hydrodynamikk: Havmiljøbeskrivelse – bølger 1.

[3] University of Texas in Dallas. Oceanography - http://www.utdallas.edu/~mitterer/Oceanography/pdfs/OCEChapt09.pdf?fbclid=IwAR3oYm9WyTmOG2S4ddQwRzXZO7jIX49hROAkrrnzc9Ypi5mVQPXUMk2VX_A.

[4] University of Hawaii. Oceanography - http://www.soest.hawaii.edu/oceanography/courses_html/OCN201/instructors/Carter/SP2016/waves2_2016_handout.pdf.

[5] Kyle Stock. Spilling, surging, plunging: The science of breaking waves - https://www.surfertoday.com/surfing/what-is-wave-refraction.

[6] physicstutorials.org. Water waves - http://www.physicstutorials.org/home/waves/water-waves?fbclid=IwAR2wOL91kGsdBv-MUvh6mvezDNepucQ49f8nyvuN5Vw07enEVCx6hk1P0N0.

[7] DNV-GL. Environmental conditions and environmental loads.